WAVELENGTH COMPENSATION IN FUSED FIBER COUPLERS

By

Zhi G. Wang

Dissertation submitted to the Faculty of the Virginia Polytechnic Institute and State University in partial fulfillment of the requirements for the degree of

Doctorate of Philosophy

in

Electrical Engineering

APPROVED:

Dr. Richard O. Claus, Chairman

Dr. Kent A. Murphy

Dr. Anbo Wang

Dr. Ira Jacobs

Dr. Ting-C. Poon

Dr. Seshu B. Desu

February, 1996

Virginia Tech, Blacksburg, Virginia

Key words: Fiber Optic Coupler, Wavelength-Flattened, WDM, Fiber Communication

WAVELENGTH COMPENSATION IN FUSED FIBER COUPLERS

By

Zhi G. Wang

Dr. Richard O. Claus, Chairman

Electrical Engineering

(ABSTRACT)

The performance of fused fiber couplers is wavelength dependent. Wavelength spectral compensation is a technique to decrease the effect of the wavelength dependence, which is an essential task for many applications in fiber optic communication systems. Fiber devices such as wavelength-flattened couplers (WFCs) can be fabricated using wavelength spectral compensation methods. In this dissertation, wavelength spectral compensation techniques in fused biconical taper (FBT) couplers including both multimode and single-mode fiber couplers are studied in detail. In multimode fiber coupler operation, a novel theoretical model based on frustrated total internal reflection (FTIR) has been developed to effectively describe the power coupling and loss mechanism. Experimental results support the theoretical predictions. In single-mode fiber couplers, the conventional technique of fabricating WFCs is discussed. An alternative analytical model has been developed based upon coupled mode theory, which provides a relatively simple and mathematically sound explanation to the

wavelength spectral compensation. Aiming to simplify WFC fabrication, a new way of constructing WFCs is proposed and demonstrated by connecting regular single-mode fiber couplers, some of which serve as wavelength spectral compensators. WFCs of various structures including 2x2, 1x3, $1x2^N$, and 4x4 have been developed, and the experimental data agree with theoretical predictions of performance. Potential applications and future research directions in wavelength spectral compensation are also presented.

Abstract

Acknowledgments

This dissertation is literally the summary of my past six years of research experience in the Fiber & Electro-Optics Research Center in the Bradley Electrical Engineering department at Virginia Tech. I could not have accomplished this work without the help of many extraordinary individuals I have encountered at Virginia Tech. Among them, first I would like to recognize Dr. Richard O. Claus, my academic advisor, for providing me with the opportunity and support to do research in the fiber optics group. In addition to academics, he has taught me many other invaluable lessons that one should know in order to succeed in high-tech research environments, including how to develop research proposals, how to manage technical projects, and the importance of self-confidence. Secondly, I would like to acknowledge the other members of my committee. I was very fortunate to have Dr. Kent A. Murphy as a key technical advisor to teach me the principle as well as practical fabrication techniques of fiber optic couplers and sensors in an easy-to-understand and no-nonsense manner. I wish to thank Dr. Anbo Wang for introducing me to the field of fiber optic sensors and the physics behind their applications, particularly in intensity-based sensing systems. I wish to thank Dr. Ira Jacobs for teaching me fiber optic communications and for providing me over the years with up-to-date information and valuable comments about the future direction of fiber optics technology from the communication systems standpoint. I would also like to thank Dr. Ting-C. Poon and Dr. Seshu B. Desu for serving as my committee members; from both I have received much

of encouragement and inspiration as well as technical comments and suggestions about the research work.

My acknowledgments extend to all other members of the Fiber & Electro-Optics Research Center and Fiber and Sensor Technologies, Inc. families. Particularly, I wish to thank Mr. Michael F. Gunther for his patience and encouragement in teaching me how to fabricate fused fiber couplers. His wisdom in handling practical matters and his "get-thing-done-now" attitude have always inspired me. I would also like to thank Mr. Richard Crotts for sharing his experience in coupler fabrication with me in an effort to improve the quality of fiber coupler products.

Right from the beginning of my higher education career in the States eleven years ago, I have been constantly blessed and supported both financially and morally by my relatives in Baton Rouge, Louisiana. Among them, my great grand father, S.G. Chow, was responsible for bringing me to the States for higher education. He passed away five years ago. I wish he had lived to see that I am going to fulfill part of his dream -- getting a Ph.D. degree. For the past eleven years, my great grand mother, Y.F. Shih Chow, and great aunt, B.L. Chow Lam, have always been giving me their care and love whenever I had a rough time, which makes me feel that Baton Rouge, Louisiana, is my hometown. Finally, I would like to recognize my parents H.S. and M.Q. Wang, and my two lovely sisters H.M. and Y.Z. Wang for being spiritually with me all the time. My experience is

their experience. Although they live in China, they have always believed in me and reminded me that "today is better than yesterday, and tomorrow will be even brighter."

Contents

1. Introduction

Optical fiber is an electromagnetic guiding medium made of glass, plastic or other materials. Light signals can propagate inside conventional glass optical fibers for a long distance with very low transmission loss compared to that of other traditional communication media such as copper wire. The unique feature of fiber optic communication systems is that they have a much wider bandwidth, potentially up to tens of Tb/s, due to the enormous carrier frequency range of optical signals. For more than twenty years, generations of fiber optic communication systems have been developed and subsequently deployed. First, they were implemented for long-haul communication links such as coast-to-coast and across-ocean systems. Later, short-haul communication systems using fiber optic technology have gradually gained their momentum. The major reason is that fiber optic communication systems offer larger bandwidth and hence larger information rate capability than copper-based systems. Examples of short-distance communication systems include local area networks (LANs) for intercity, interbuilding, and interoffice applications. It will be essential in the future to employ fiber-based (high bandwidth) systems which permit broadband and multimedia services such as voice, image, facsimile, videoconferencing, high-definition television (HDTV), and many others.

One of the key components in any fiber optic communication system is the fiber coupler, the prime subject of this dissertation. In this chapter, from the physics and component

standpoint, typical fiber optic communication systems are studied, and key physical elements are identified. The basic structure of the fiber amplifier is also analyzed, as it is evident that fiber amplifiers will be indispensable components in the future generation of communication systems. The objective here is to identify the important roles fiber couplers will play in these communication systems and thus suggest the importance of this dissertation topic. Various types of fiber couplers are briefly discussed in order to understand their functionality and construction. Finally, the fused biconical taper (FBT) coupler is introduced, which opens the door for further discussion and study of this and related types of couplers. The organization of the rest of this dissertation is also presented at the end of this chapter.

1.1 Fiber optic communication systems

Long-haul systems

A simplified physical layout of a long-haul point-to-point fiber optic communication system is shown in Figure 1-1.

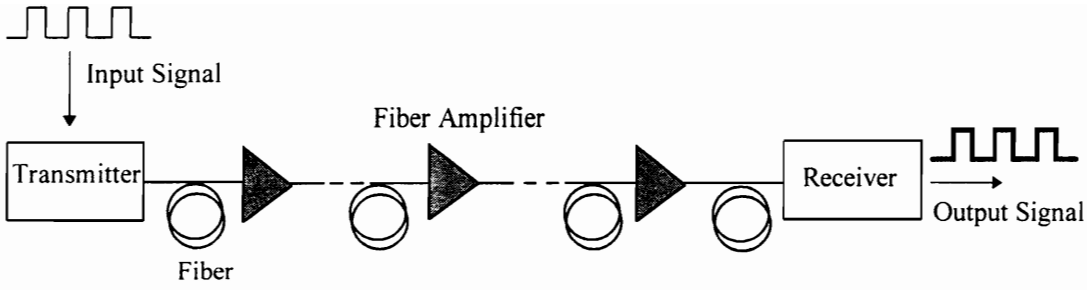

Figure 1-1. Long-haul fiber optic communication system.

An electrical signal in digital form modulates the transmitter, typically a laser diode which generates an optical signal, and this modulated optical waveform propagates along the low loss fiber to a distant destination (the receiver). Between the transmitter and receiver, a series of in-line fiber amplifiers are used to boost the signal power level. The separation between two adjacent amplifiers is about 60 km - 100 km, which is much larger than the separation of electronic repeaters in copper-wire based transmission systems. The operation wavelength would likely be around 1.3 μm or 1.55 μm. More details about these systems will now be given.

A typical example of this long-haul communication system is long-distance telephone trunk lines (backbones). Single-mode fiber should be deployed to minimize modal dispersion for long distance transmission. Fiber optic couplers (not shown in Figure 1-1) are often used as tap-off devices such that signals at different stages could be monitored. Fiber amplifiers are important components in this implementation and a detailed discussion will be presented in the next section.

Local area networks

In data communication, local area networks are often deployed to connect computers and their peripherals together. Typical structures are shown in Figure 1-2.

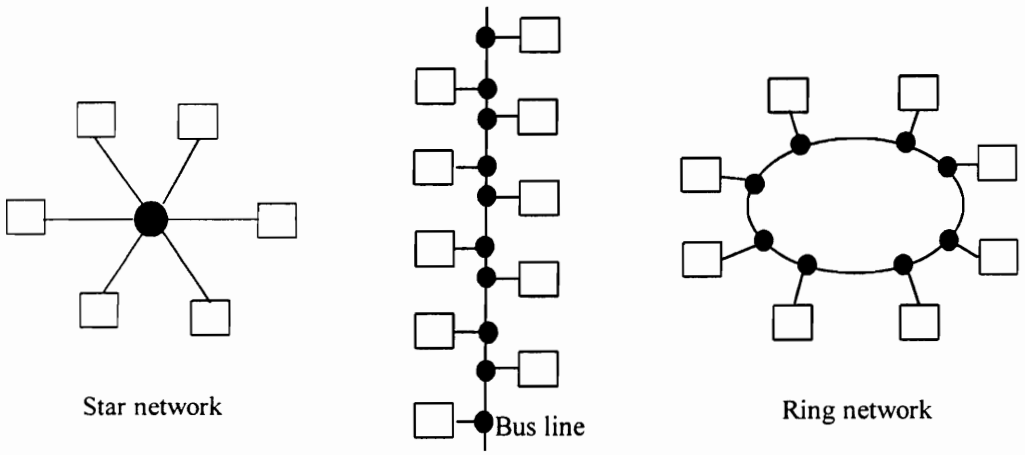

Figure 1-2. LAN architectures.

Each of the small rectangular squares represents a transmitter/receiver unit. Information is transmitted from one terminal to other terminals, or is received from any of the terminals. Notice that at each node (where more than one fiber comes into one point) there is a fiber coupler. In the star network, a star fiber coupler is needed. In the bus line and ring networks, many 2x2 fiber couplers are needed. Depending on specific applications, some fiber LANs are multimode-fiber-based systems, where inexpensive LEDs and electrical circuitry are used . If laser diodes and single-mode fiber are employed in LANs, fiber amplifiers (not shown in Figure 1-2) could be employed rather

than electronic amplifiers and circuits to compensate for power loss due to a large number of users in the network.

Transmission wavelengths

After several decades of research and development, it has been established that there are three primary spectral regions within which optical signal have minimum attenuation in fiber glass material and practical and relatively low-loss components are available. Figure 1-3 shows the attenuation of conventional single-mode glass-on-glass optical fiber versus wavelength [1].

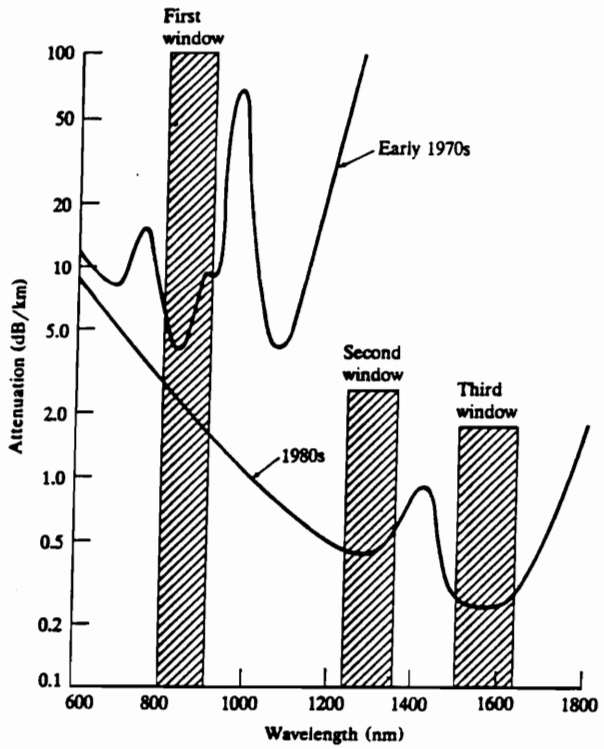

Figure 1-3. Optical fiber attenuation as a function of wavelength.

The three wavelength regions are often referred to as the first widow (800 nm - 900 nm), the second window (around 1300 nm), and the third window (around 1550 nm), respectively. The first window systems employ LEDs, silicon photodetectors, and simple electronics. It can be used for short distance applications. The bit rate can be up to approximately 100 Mb/s, and first window systems typically offer options for the least expensive implementation. The second window systems (1300 nm) exhibit much lower attenuation than first window systems. Hence, larger networks can be implemented. Although both multimode and single fiber systems can be operated at this wavelength, single-mode systems have much larger bandwidth than multimode systems, partly because 1300 nm is within the region of relatively low dispersion [2-3]. Operating rates of much greater than 1 Gb/s have been achieved. The 1550 nm window systems are most efficient in terms of fiber loss because the inherent attenuation loss of the fiber medium is a minimum. Another major advantage of such third-window systems is that current fiber optic amplifiers work most effectively for single-mode systems operating at 1550 nm than for other wavelength windows. Although 1550 nm systems typically suffer from more signal distortion due to fiber dispersion, use of special fibers can overcome this drawback. This latest generation system has the future potential to offer extremely high-capacity, long-span terrestrial and undersea transmissions.

Wavelength Division Multiplexing (WDM) systems

To take the advantage of the large bandwidth that optical fiber has to offer, many signals modulated by different sources of different wavelengths can be coupled into one fiber, and at the receiving end these signals can be separated by wavelength into different output ports. This system configuration is called *wavelength-division multiplexing* (WDM) (or *frequency-division multiplexing* - FDM). Figure 1-4 shows a simplified WDM system.

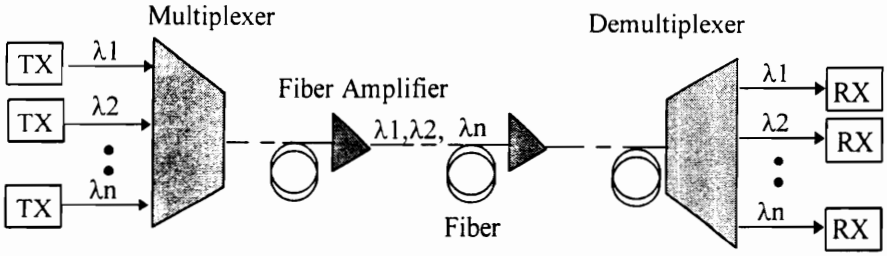

Figure 1-4. Wavelength-division multiplexing communication system.

The total information capacity of this WDM system is N times the capacity of a single channel, where N is the number wavelength channels. The multiplexing and demultiplexing units are normally passive specialized fiber couplers - namely WDMs. Wavelengths could be chosen from any of the three windows mentioned previously, although the most common wavelengths are around 1300 nm or 1550 nm. High-density WDM systems of up to 16 channels operating in the range between 1530 nm - 1560 nm have been implemented [4].

To increase network information capacity, WDM techniques could be used for both long-haul and short-haul communication systems such as the structures shown in Figures 1-1 and 1-2. One example is a tree structure presented in Figure 1-5.

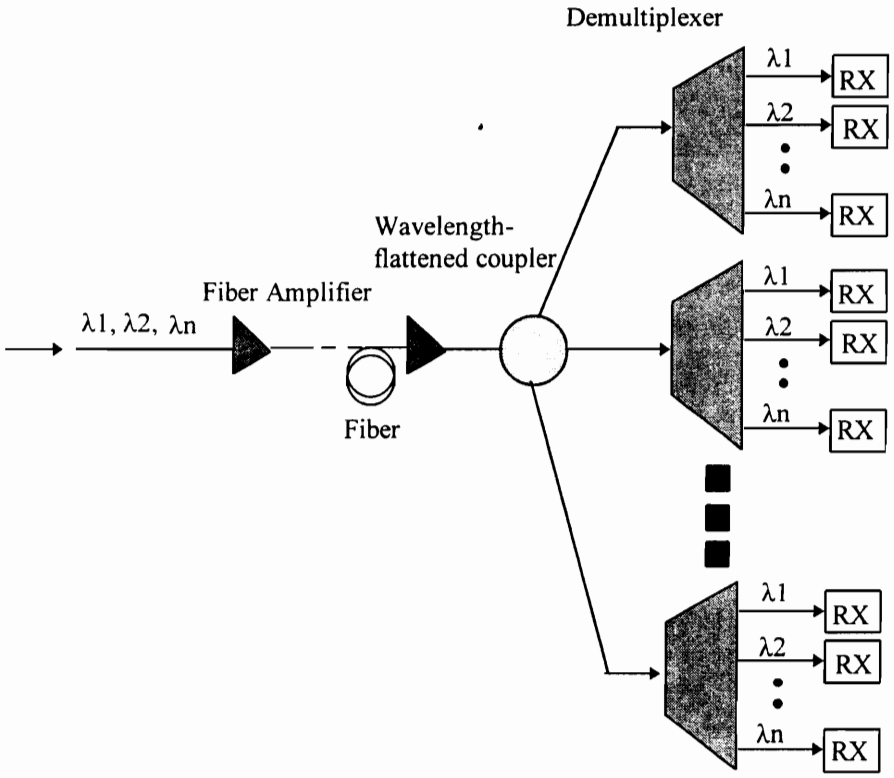

Figure 1-5. A tree structure WDM system.

In this system, the multiplexed signal is first divided evenly into many branches, and each of these branches is then demultiplexed by wavelength into many channels. The fiber coupler that splits the signal evenly, with insensitivity to wavelength, is referred to as a wavelength-flattened coupler (WFC). Potential applications of this tree structure are in future cable television industry, where many new services such as video telephony may

be provided. The wavelength multiplexed signals coming from the master head end could be separated by the tree WFC to many head end/hub units (demultiplexers). It is worth mentioning that wavelength-division multiplexing can be deployed in multimode fiber based systems as well as single-mode systems, thus creating a similar demand for multimode WFCs.

1.2 Fiber amplifiers

As mentioned previously, an optical fiber amplifier is an essential component in fiber optic communication systems. Its function is to boost optical signal power by as much as more than 1000 times (30 dB), hence the number of signal regenerators can be minimized or in some cases eliminated. There are many types of fiber amplifiers including semiconductor laser amplifiers, Raman amplifiers, and Erbium-doped fiber amplifiers (EDFAs). Among these fiber amplifiers, Erbium-doped fiber amplifiers operating at 1550 nm provide enormous potential for future communication systems, and they have already been commercially deployed. In this section, the basic structure of the EDFA is presented, specifically to identify the important roles that fiber couplers play. Figure 1-6 shows a simplified EDFA .

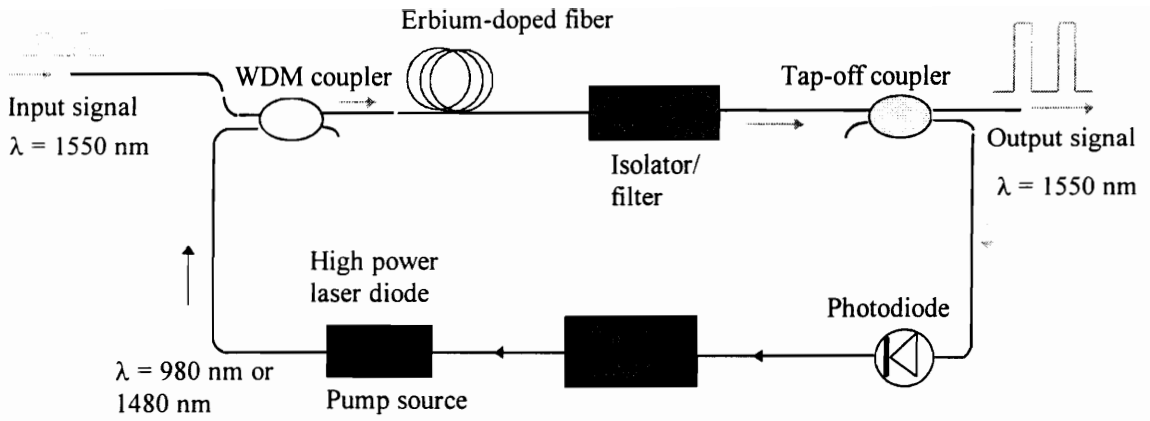

Figure 1-6. Erbium-doped fiber amplifier.

The weakened input signal (1550 nm) combines with the high power pump signal light (980 nm or 1480 nm) at the WDM coupler, where both inputs are efficiently coupled to one output port connected to the Erbium-doped fiber. The 1550 nm signal is amplified inside the Erbium-doped fiber and propagates through the isolator/filter unit. At the output of the EDFA, a tap-off fiber coupler is used such that most of amplified power propagates down the fiber while a small portion of the output power is fed into the photodiode. This feed-back signal serves as an output power level indicator to the pumping source such that the pumping power level can be adjusted in order to stabilize the output. Fiber couplers (both the WDM and tap-off couplers) function as the combiner and splitter of optical signals in the EDFA.

1.3 Fiber couplers

Fiber optic couplers are passive devices that split one incoming optical signal into many fiber outputs or vice versa - they combine many input optical signals into one fiber output. Figure 1-7 shows the general functionality of a fiber coupler.

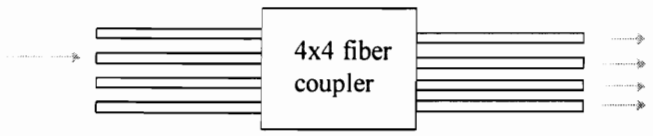

Figure 1-7. A 4x4 fiber coupler.

This 4x4 fiber coupler (star) has four input and four output ports. In most cases, it is symmetric, i.e. optical power is divided evenly among the output ports no matter which input port is excited, and the coupler operates the same way in either direction. Depending on the way a fiber coupler is designed and fabricated, there are many different types of fiber couplers such as regular (standard) couplers, wavelength-division multiplexing (WDM) couplers, wavelength-flattened couplers (WFCs), and several others. It may be helpful to give a brief description about these major types of couplers in order to distinguish them from one another.

Regular (standard) couplers are devices that split/combine optical power. For single-mode fiber, they operate at one particular wavelength. WDMs split input signals having different wavelengths or carrier frequencies into different output channels by wavelength,

or they combine many different wavelength channels into one output port. Wavelength-flattened couplers (WFCs) work like the standard couplers except they are insensitive to wavelength. Detailed discussion about these devices is given in later chapters. The widespread applications of these couplers can be found in both single-mode and multimode fiber systems.

Referring back to Figure 1-7, to implement the function that the central square performs requires physical mechanism such that optical signals in the fibers can be split or combined in a pre-determined manner. The following figures show some of the possible implementations of such physical mechanisms.

Mixing rod [5]

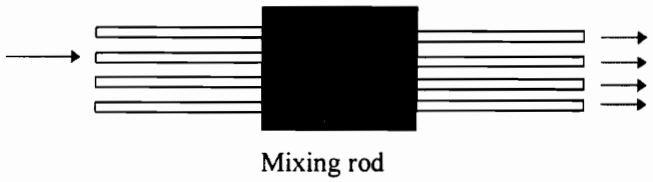

Figure 1-8. A 4x4 star using mixing rod.

Figure 1-8 shows the operation of a mixing rod. The central interaction region consists of a rod waveguide such that light is thoroughly mixed and evenly distributed onto output ports. This configuration works well especially for multimode fibers.

Fused biconical taper[6]

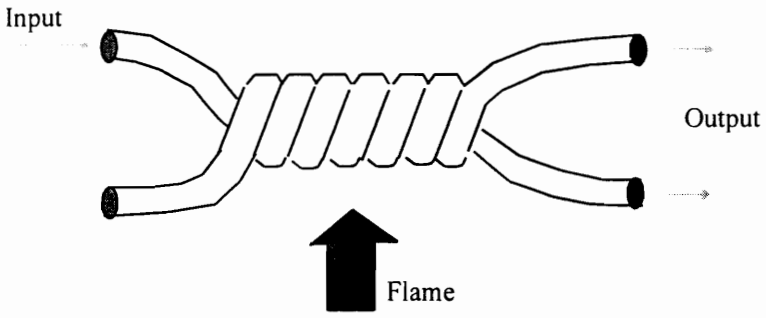

Figure 1-9. Fused biconical taper coupler.

In Figure 1-9, two fibers are twisted together and fused using a high temperature heating source (flame). After much processing as described in detail in subsequent chapters, light can be coupled in a carefully controlled way from one fiber to another. This fused biconical taper (FBT) method is perhaps the most common technique for fabricating couplers for both single-mode and multimode fibers.

Polished fiber [7]

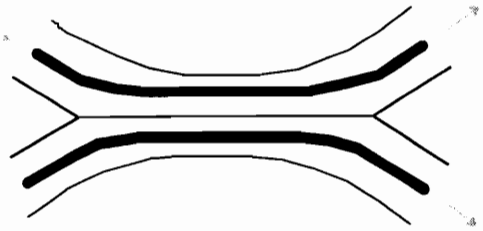

Figure 1-10. 2x2 polished fiber coupler.

In Figure 1-10, one section of each fiber is polished sideways, and then the pair of polished fibers is attached with index-matching fluid between them. Optical power can be transferred from the primary fiber to the secondary fiber due to the evanescent field phenomenon when the fiber cores are very close to the polished surface and to each other. Both single-mode and multimode fiber couplers can be constructed this way. Fiber WDMs, wavelength and power tuning devices can also be realized employing the polished fiber method.

GRIN lens [8]

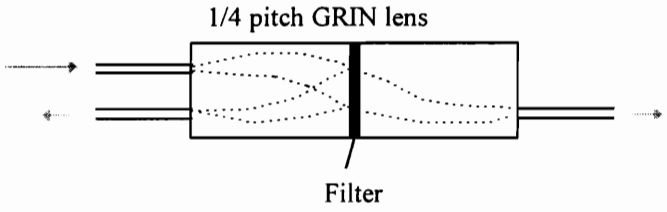

Figure 1-11. 1x2 fiber coupler with GRIN lens.

In Figure 1-11, two 1/4 pitch GRIN (Graded-Index) lenses are attached back-to-back with a filter or partially reflected/transmitted mirror between them. A portion of the input light is transmitted through the filter and coupled into the output port at the other end, and another portion of the input light is reflected back at the middle and coupled into the other fiber. WDMs can be easily constructed using this type of structure. This technique is especially efficient for the fabrication of multimode WDM fiber couplers.

GRIN lens with grating [9]

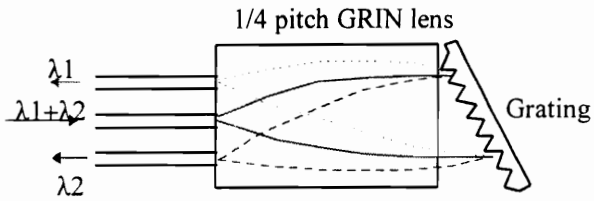

Figure 1-12. Fiber coupler using GRIN with a grating.

As shown in Figure 1-12, one 1/4 pitch GRIN lens is attached to a surface diffraction grating. Incoming input signals are decomposed (by wavelength) into two light signals, which are then coupled separately into two different channels. This technique is suitable for high-density WDM couplers.

Integraded optics [10]

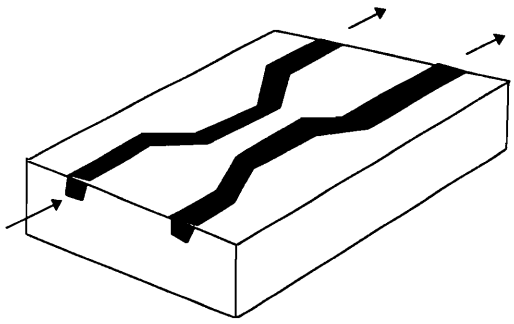

Figure 1-13. Integrated optics fiber coupler.

Shown in Figure 1-13 is a 2x2 coupler waveguide fabricated in a dielectric block. Fiber modulators and switches can be effectively made using integrated optical device techniques. This method is also suitable for mass-production of components in the future although cost and coupling performance limit their current use.

Depending on specific applications, different ways of fabricating fiber couplers have certain advantages and drawbacks compared with other methods. Cost is also an important factor. To date, the fused biconical taper (FBT) method is perhaps the most common technique for the fabrication of fiber couplers.

The objective of this dissertation is to consider new methods for the synthesis and use of fused biconical taper couplers. Particularly, as we have seen in an early part of this chapter, wavelength-flattened or insensitive couplers are essential in wavelength-division multiplexing (WDM) communication systems and methods for their implementation still

require development. Wavelength spectral compensation methods are necessary in order to fabricate wavelength-flattened devices. Several novel techniques are developed to effectively construct this device. Theoretical models are developed, and experimental implementations have been performed with the results that support the theoretical analysis.

The rest of this dissertation is organized as follows. Chapter 2 provides an overview of the fused biconical taper (FBT) process. This information serves as a foundation for the rest of the chapters. Chapter 3 deals with multimode fiber couplers, primarily power coupling principles and power loss mechanisms. A novel model based on frustrated total internal reflection (FTIR) is developed to explain the power coupling in multimode waveguides. The wavelength dependence of coupler performance is also studied. In Chapter 4, the traditional technique of fabricating single-mode fiber wavelength-flattened couplers is discussed. A new theoretical model based on coupled mode equations is developed aiming to simulate the wavelength compensation effect. Chapter 5 presents a novel and systematic way of constructing single-mode fiber wavelength-flattened couplers (WFCs) using regular (standard) fiber couplers. Starting with simple structures, 2x2 and 1x3 WFCs are studied in great detail. A theoretical model is developed to effectively simulate not only simple couplers but also complicated structures, which includes the coherence issue in connection with stability of coupler performance. The extension of the concept of using regular fiber couplers to construct complicated wavelength-flattened couplers (WFCs) is covered in Chapter 6. Devices such as 1x4,

1x8, and 4x4 WFCs are developed. Finally, Chapter 7 outlines the conclusions of this work in particular methods for wavelength spectral compensation in fused biconical taper couplers. Implications of the research and its future potential in practical fiber coupler based components are also discussed.

2. Fused biconical taper (FBT) couplers

Fiber couplers are essential passive components in fiber optic communication systems, including their use in fiber amplifiers. We also realize that fused biconical taper (FBT) fiber couplers are perhaps the most popular devices among many types of fiber couplers. In Section 1.3 of Chapter 1, the FBT coupler is briefly introduced. Since the core subject of this dissertation is fused biconical taper couplers, a detailed description of FBT couplers is necessary prior to in-depth studies concerning these couplers. In this chapter, the typical fabrication process for the construction of FBT couplers is presented along with a discussion of their unique features. Major system applications of FBT couplers are presented, including the operations of WDMs, wavelength-flattened couplers (WFCs), and polarization-maintaining couplers (PMCs). For convenience in future discussion, some key definitions and terminology regarding FBT couplers are given at the end of this chapter.

2.1 FBT coupler fabrication process

The fused biconical taper (FBT) method is a technique for fabricating fiber optic couplers which involves fusing and tapering fibers together. As an example, a 2x2 FBT coupler fabrication process is shown in Figure 2-1.

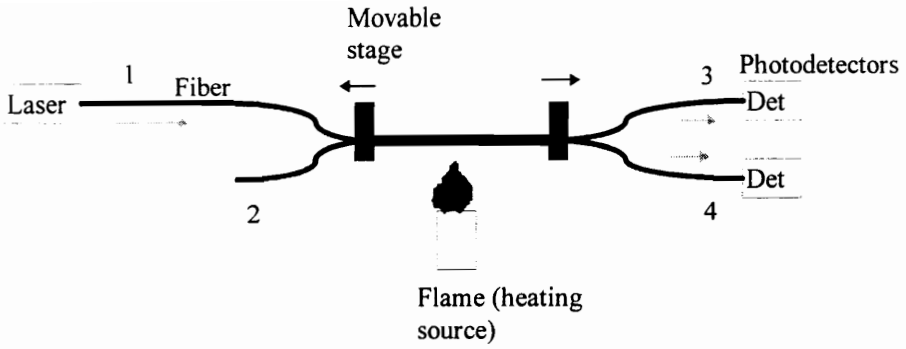

Figure 2-1 FBT fabrication station.

First, two fibers described by ports #1-#3 and ports #2-#4, are placed side by side, and sections of these fibers in the middle are then put together so they contact firmly with each other between the two movable blocks. This forms a region where the fibers are fixed onto the fabrication stage (two blocks). Secondly, heat is applied in order to soften the fiber glass in this middle region, and at the same time the fibers are stretched by moving the translation stages in opposite directions. The combined two-fiber section in the heated area becomes thinner and thinner as it is stretched, and the separation between the two fiber cores decreases. At a certain point during this process, optical power originally in leg#3 starts coupling to leg#4. Finally the process of fusing and stretching is stopped when the desired power levels in both ports #3 and #4 are reached.

The reason that optical power in one fiber can be coupled into another is because the taper region becomes very thin, and two fiber cores get very closed. Due to the

interference between modes in the guides defined by the two core regions, the power level in one fiber changes, even though the sum of power of all the output ports is constant. For single-mode fiber couplers, power varies periodically in one output fiber between maximum and minimum values. For multimode fiber couplers, this effect is dramatically reduced because a large number of modes interfere among themselves, and on the average modal interference effects cancel out with one another. More about the power coupling in multimode and single-mode fiber couplers will be given in later chapters. From the fabrication standpoint, it is vital to have a stable light source, constant and uniform moving motor speed, good photodetectors and power meters, and precise control of the heating source.

A large percent of the fiber optic couplers used in fiber optic communication systems are fused-biconical taper (FBT) couplers. The major reasons for its popularity include :

(1) Simplicity in fabrication

FBT couplers are relatively simple in structure and straightforward to manufacture compared with other types of fiber couplers such as polished fiber couplers and GRIN lens-based couplers.

(2) Stability and reliability in performance

Because of its simple structure, packaged FBT couplers are reliable for long-term use, resisting variations in performance due to various environmental disturbances including temperature, humidity, and vibration.

(3) Compatibility with fibers

FBT couplers are made by starting with communication fibers, hence only a minimum number of fiber-to-fiber connections or splices are required when they are installed in systems. Such is not the case for other kinds of fiber couplers such as integrated optics couplers, where the difficult task of low-loss fiber-to-waveguide (rectangular) connection is required.

(4) Versatility in applications

Various kinds of fiber couplers may be fabricated employing fused-biconical taper techniques. These devices include WDMs, wavelength-flattened couplers (WFCs), and polarization maintaining couplers (PMCs).

(5) Low cost

The simplicity and straightforwardness in fabricating FBT couplers lead to cost-

effectiveness because components can be fabricated in less time than that needed to fabricate couplers by other methods such as the polished fiber technique.

2.2 Major types of FBT couplers

Using the coupler station shown in Figure 2-1, many types of useful fiber couplers can be made. Among them, regular (standard) couplers, WDMs, WFCs, and polarization maintaining couplers are the most common. These fiber devices are all single-mode fiber based couplers but may have multimode counterparts.

Regular (standard) couplers

The structure in the interaction taper region of a regular 2x2 coupler is shown in Figure 2-2.

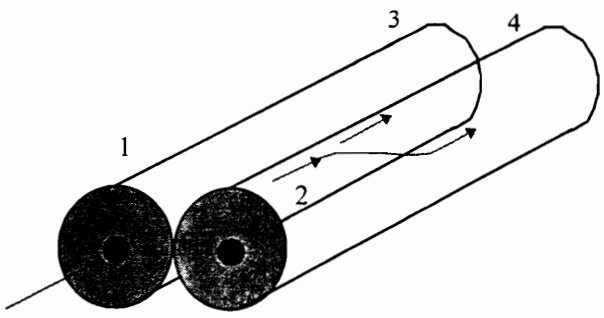

Figure 2-2. The interaction region in a regular 2x2 single-mode fiber couplers.

In this case, a light signal is launched into port #1. As the two fiber cores get close due to fusing and stretching, part of the optical signal in the first fiber will be coupled into the second fiber due to modal field coupling. The tapering process can be stopped when the desired output power distribution is obtained. Standard single-mode fiber couplers operate only at one particular wavelength, i.e. the output power distribution will be different if the wavelength is changed. High quality FBT couplers can be made under precise control of the tapering process and the stopping point.

WDMs

Normal fused biconical taper WDMs may be fabricated using a structure similar to that shown in Figure 2-2. The difference in fabrication is the precise control of the tapering process and the stopping point [11]. In particular, multiplexing and demultiplexing of two closely separated wavelengths requires greater degree of accurate control and monitoring than is needed for simple signal splitting or recombining. Hence, the taper length is usually longer and more time and effort are needed to fabricate a WDM than a standard coupler.

Wavelength-flattened couplers (WFCs)

The taper-section structure of a conventional 2x2 wavelength-flattened coupler is illustrated in Figure 2-3.

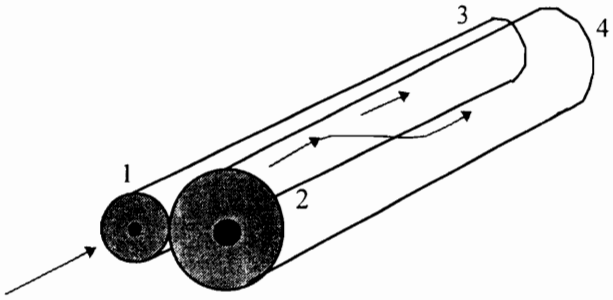

Figure 2-3. The conventional WFC structure.

Here, the two fibers are dissimilar, although both operate in the single-mode regime at the transmission wavelength [12]. Unlike the case of using two identical fibers, optical power in the primary fiber, here shown as the fiber between ports 1 and 3, can not be completely coupled into the secondary fiber due to phase mismatch, which in effect compensates for the wavelength response. The output power distribution of the WFC is insensitive to wavelength variation within a certain wavelength range. Detailed analysis of this coupler is presented in Chapter 4.

Polarization maintaining couplers (PMC)

Polarization maintaining couplers (PMCs) split/combine incoming linearly polarized light to produce output signals that maintain as linear polarization. PMCs are useful components in constructing fiber isolators, polarization controllers, and devices which are

used in polarization related sensing applications. Fabrication of PMCs requires special polarization maintaining fibers such as elliptical core single-mode fiber. Using the set-up shown in Figure 2-1, fused biconical taper-based polarization maintaining couplers can be fabricated. The coupling region waveguide layout is shown in Figure 2-4.

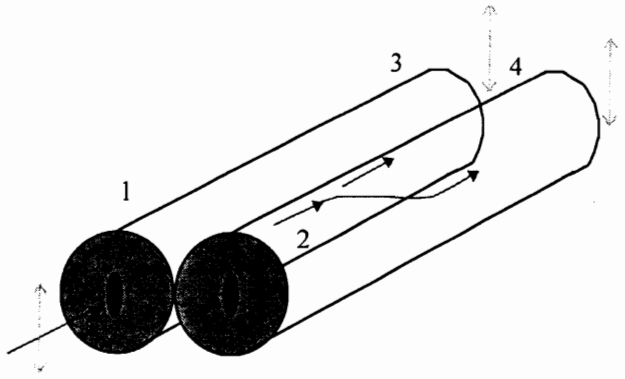

Figure 2-4. Polarization maintaining coupler using elliptical core fibers.

The key in fabricating polarization maintaining couplers is the alignment and stability of the polarization axes (major or minor axis for elliptical core fiber) of both fibers during the tapering process [13]. When a linearly polarized light signal is launched parallel to this axis, the coupler output signals are also linearly polarized.

2.3 Key definitions

Several key definitions concerning fiber couplers are introduced in an effort to help in

explaining various coupler operations in the rest of this dissertation. A packaged 2x2 fiber coupler is shown in Figure 2-5.

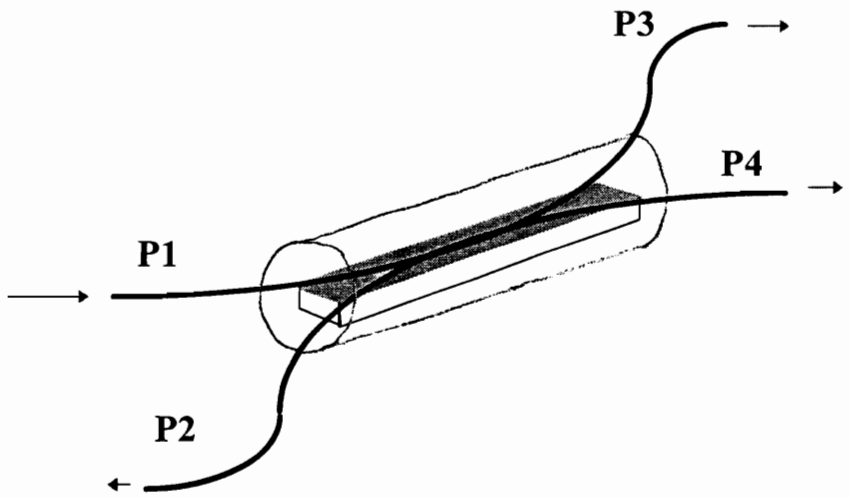

Figure 2-5. Packaged 2x2 fused coupler.

We assume powers P_1, P_2 , P_3 , and P_4 correspond, respectively, to the power in the coupler legs (ports) #1, #2, #3, and #4 designated in Figure 2-1. Light is launched into leg #1; this is the power P_1. We introduce the following definitions.

$$\textit{Output power ratio} = \frac{P_3}{P_3 + P_4} : \frac{P_4}{P_3 + P_4} \tag{2.0a}$$

$$\textit{Insertion loss} \text{ for leg\#3 (dB)} = -10 Log_{10}\left(\frac{P_3}{P_1}\right). \tag{2.0b}$$

$$Excess\ loss\ (\text{dB}) = -10Log_{10}\left(\frac{P_3 + P_4}{P_1}\right). \tag{2.0c}$$

$$Back\ reflection\ (\text{dB}) = -10Log_{10}\left(\frac{P_2}{P_1}\right). \tag{2.0d}$$

Note that the optical power in one fiber port is often compared with the optical power at the input power (P_1), and a logarithm (base 10) function is applied and then multiplied by 10 to obtain a value in dB.

3. Multimode fiber couplers

The subject of study in this chapter is multimode fiber couplers. Specifically, multimode fiber coupler power coupling and loss mechanisms are investigated in detail. Based on frustrated total internal reflection (FTIR), novel theoretical models of multimode waveguide power coupling and power loss are developed. Experimental studies of the external index dependence of coupler throughput power and its distribution have been conducted. The results support the theoretical analysis. Practical significance of this research work is also discussed.

3.1 Multimode fibers

Multimode optical fibers are referred to as those optical fibers which support many propagation modes. This is a relative term comparing their operation to that of single-mode fibers, which support only one guided mode. The core diameters of multimode fibers are much larger than the operating wavelength. Several common multimode fibers used in communication systems have core/cladding (in μm) ratios of 50/125, 62.5/125, and 100/140. For step-index profile fibers, the total number propagation modes can be approximated by [14]

$$M = \frac{1}{2}V^2, \qquad (3.1)$$

where

$$V = \frac{2\pi a}{\lambda} * \sqrt{n_{core}^{\ 2} - n_{clad}^{\ 2}}, \qquad (3.2)$$

here 'a' is the radius of the fiber core, λ is the wavelength, and n_{core} and n_{clad} are the refractive indices of the core and cladding, respectively. A related parameter, the NA (numerical aperture) is defined by

$$NA = \sqrt{n_{core}^{\ 2} - n_{clad}^{\ 2}}. \qquad (3.3)$$

Most of the multimode fibers in communication systems can support hundreds or thousands of modes. For example, for a step index profile fiber with 62.5/125, NA = 0.20 and λ = 1300 nm, we estimate the total number of modes using Equations (3.1) and (3.2) as M = 456. Notice that the propagation mode number is sensitive to wavelength as indicated in Equation (3.2). For the same fiber, if we use laser light with 1550 nm, the total number of modes becomes M = 321. More about the wavelength dependence is discussed in the next few sections.

Multimode fiber communication systems may be used to support local area networks including fiber distributed data interface (FDDI) systems. Low cost LEDs are often used as transmitting sources, and PIN diodes serve as detectors in such systems. The modulation and demodulation electronics are also relatively inexpensive compared to the cost of ultra high-speed single-mode fiber based systems.

3.2 Power coupling

We investigate next a 2x2 multimode fiber coupler to demonstrate the basic principle of power coupling. Other multimode fiber couplers could also be analyzed based on similar formulation. Figure 3-1 shows the 2x2 multimode coupler geometry.

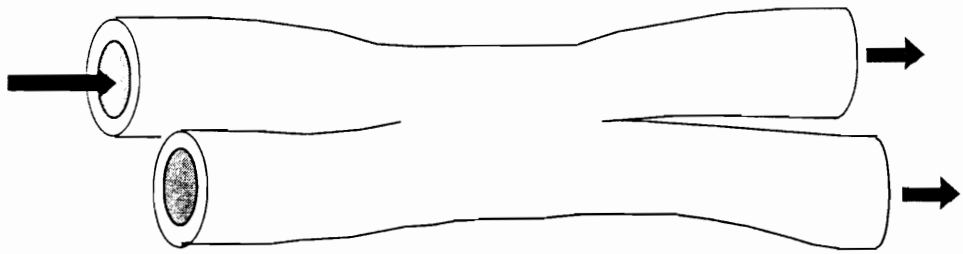

Figure 3-1. The geometry of a 2x2 multimode coupler.

Optical power is initially launched into the primary fiber. As the two fibers get closer and closer during the fusing and tapering process, a portion of the power will be coupled into the secondary fiber. If the tapering process continues, more and more power will be coupled to the secondary fiber. Eventually, both fibers will have the same amount of power, provided these two fibers are identical (symmetric coupler). If the two fibers are not the same, i.e. one has smaller core diameter than the other (asymmetric coupler), the final power levels in both fibers will not be the same.

Theoretical analysis - symmetric multimode coupler

Since a multimode fiber supports a large number of modes, the power in the fiber is the sum of the power carried by each mode [15]. Strictly speaking, the power coupling between the two fibers should be analyzed by studying mode-to-mode power coupling between these fibers. It would be a laborious task to do this modal analysis because there are so many modes involved, as indicated in Equations (3.1) and (3.2). Analysis concerning power coupling between two multimode fibers has been performed using a ray optics model in the past [16-17]. These models rely chiefly on the recapture of the cladding mode power in the up-taper region of the coupler, which may not be the only reason for power coupling, as observed experimentally [18].

We develop a new ray optics model in solving the power coupling between two multimode fibers based on frustrated total internal reflection (FTIR). For simplicity and to give an order of magnitude estimation of power coupling, we analyze the coupler in terms of a rectangular waveguide, so skew rays are ignored, and assume there is no loss in the coupler. Figure 3-2 shows a symmetric coupler geometry, in which the thin middle layer of thickness d is the cladding material sandwiched by the two core regions and the surrounding material is also cladding.

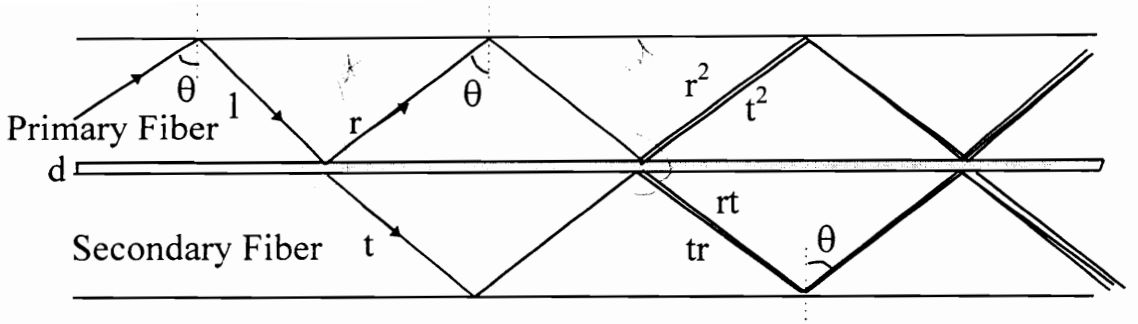

Figure 3-2. The waveguide structure of a symmetric 2x2 multimode coupler.

A portion of the power of one ray in the primary fiber could penetrate into the secondary fiber due to frustrated total internal reflection, provided the cladding layer thickness between the two cores is very small, on the order of a few wavelengths [19]. Assuming a broadband light source is used, all modes (rays) are equally excited in the primary fiber. For clarity, only one ray is considered. Quantitatively, if a light beam of unit amplitude is launched, then at the first crossover in the middle layer, we have

$$r + t = 1, \tag{3.4}$$

where r and t are the reflection and transmission coefficients (power amplitude), respectively. The incident angle θ satisfies total internal reflection condition. After the first splitting, two rays propagate along the taper length. At the second crossover, totally four rays are generated. This process would continue on and on down the fiber coupling

region. The total number of rays eventually becomes 2^m, where m is the number of crossovers at the middle layer. Figure 3-3 illustrates the power splitting mechanism.

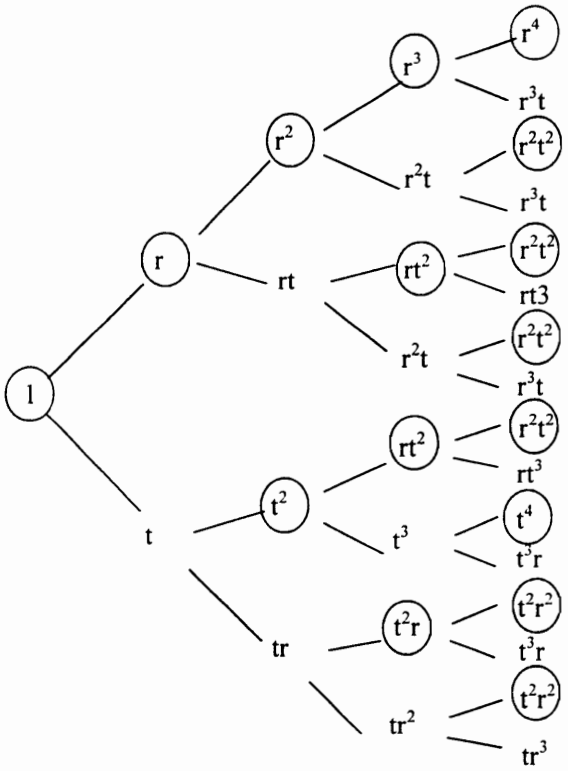

Figure 3-3. Amplitudes of split power terms in both primary and secondary fibers.

Here amplitudes of only five stages are presented. In each stage, one beam is divided into two beams corresponding to the reflection and penetration beams, respectively. The terms encircled in Figure 3-3 are the intensities of the components in the primary fiber,

and the rest are power amplitudes in the secondary fiber. Table 1 shows the amplitude terms of the power in both fibers for the first few crossovers.

Table 1. Power amplitude terms in a 2x2 symmetrical coupler

Number of crossovers	Power in the primary fiber	Power in the secondary fiber	Total power
0	1	0	1
1	r	t	$r + t = 1$
2	$r^2 + t^2$	2rt	$(r + t)^2 = 1$
3	$r^3 + 3rt^2$	$3r^2t + t^3$	$(r + t)^3 = 1$

Notice that due to the conservation of energy, the sum of the primary and secondary power is $(r+t)^m = 1$, where m is the number of crossovers (stages) at the middle layer given by

$$m = \frac{L}{2D\tan(\theta)}, \tag{3.5}$$

here L is the total taper length and D is the tapered fiber core diameter.

Field amplitude coefficients

For a long taper length, m is large, and the amplitude coefficients could be calculated through computer simulation. The basic routine for a symmetric coupler is

$$A_{p,new} = r * A_p + t * A_s \ , \qquad (3.6)$$

and

$$A_{s,new} = t * A_p + r * A_s , , \qquad (3.7)$$

where A_p and A_s are the current amplitude terms in the primary and secondary fibers, respectively. $A_{p,new}$ and $A_{s,new}$ are the next stage amplitude coefficients in the primary and secondary fibers, respectively. The r and t are the usual refection and transmission coefficients. The new amplitudes would become the current amplitudes for the next stage, and hence

$$A_p <= A_{p,new}, \text{ and } A_s <= A_{s,new}, . \qquad (3.8)$$

The initial conditions are :

$$A_p = 1, \text{ and } A_s = 0. \qquad (3.9)$$

Equations (3.6) - (3.9) represent a symmetric 2x2 multimode fiber coupler power coupling algorithm, because there is a symmetric static light beam intersection pattern. For a given initial launching angle (beam), the subsequent crossover points at the middle

layer are the same for all split beams. Later in this chapter, we will see that a different static pattern (asymmetric) is established for an asymmetric fiber coupler.

The transmission coefficient (t) can be obtained using [19]

$$t = 1 - \left| \frac{Z_2^{\,2} - Z_1^{\,2}}{Z_1^{\,2} + Z_2^{\,2} + 2iZ_1Z_2 \cot(k_{2z}d)} \right|^2 . \qquad (3.10)$$

Here, the key variable is d, the middle cladding layer thickness, and the rest of the variables are given below:

$$Z_1 = \frac{1}{n_{core} * \cos(\theta)}, \qquad (3.11)$$

$$Z_2 = \frac{1}{n_{clad} * \cos(\theta')}, \qquad (3.12)$$

for the component whose polarization direction is perpendicular to the plane of incidence, and

$$Z_1 = \frac{\cos(\theta)}{n_{core}}, \qquad (3.13)$$

$$Z_2 = \frac{\cos(\theta')}{n_{clad}}, \tag{3.14}$$

for the component whose polarization direction is parallel to the plane of incidence. Also

$$k_{2z} = \frac{2\pi}{\lambda} * \cos(\theta'), \tag{3.15}$$

where λ is the wavelength. θ' is the refractive angle in the cladding region. Since all rays bounded in the core region undergo total internal reflection at the core/clad boundary, the angle θ' is a complex angle given by

$$\cos(\theta') = i * \left(\frac{n_{core}^{\ 2}}{n_{clad}^{\ 2}} \sin^2(\theta) - 1 \right)^{\frac{1}{2}}. \tag{3.16}$$

The range of the incident angle θ is

$$\sin^{-1}\left(\frac{n_{clad}}{n_{core}}\right) \le \theta \le \frac{\pi}{2}. \tag{3.17}$$

Coupler taper model

In order to use Equation (3.10) along with Equations (3.6) - (3.9), we need a model to simulate how the fibers are deformed in the tapering process. For first order approximation, we use a three-layer waveguide shown in Figure 3-4.

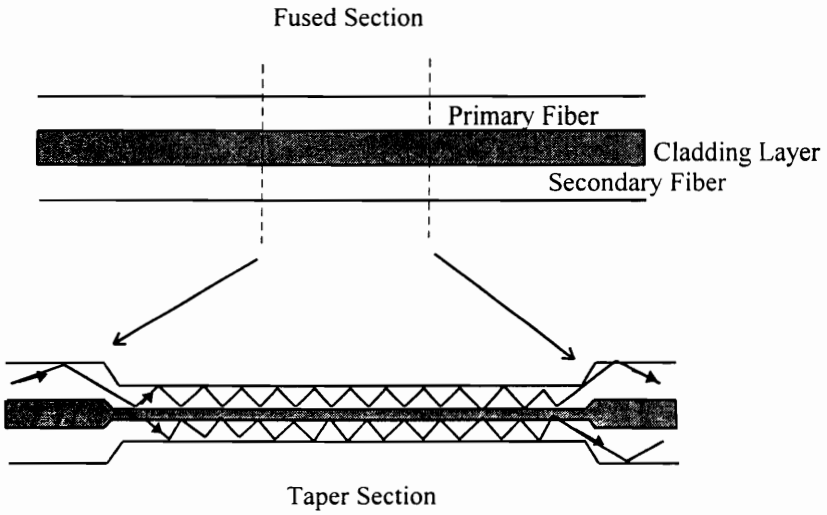

Figure 3-4. The 2x2 multimode fiber coupler taper section waveguide.

By the law of conservation of mass, the middle cladding layer thickness can be written as

$$d = \frac{D_0 * L_0}{L}, \tag{3.18}$$

where D_0 and L_0 are the original cladding thickness and length of fused section, respectively, and L is the taper length. In the numerical simulation, we assume n_{core}= 1.458, n_{clad}= 1.429 (NA= 0.29), and λ= 633 nm. The fiber is 100/140 and the length of

the fused section is 10 mm. The simulation result is shown in Figure 3-5, where thirty rays have been assumed to be initially excited in the range given in Eq.(3.17). The Matlab model programs used are listed in Appendix A.

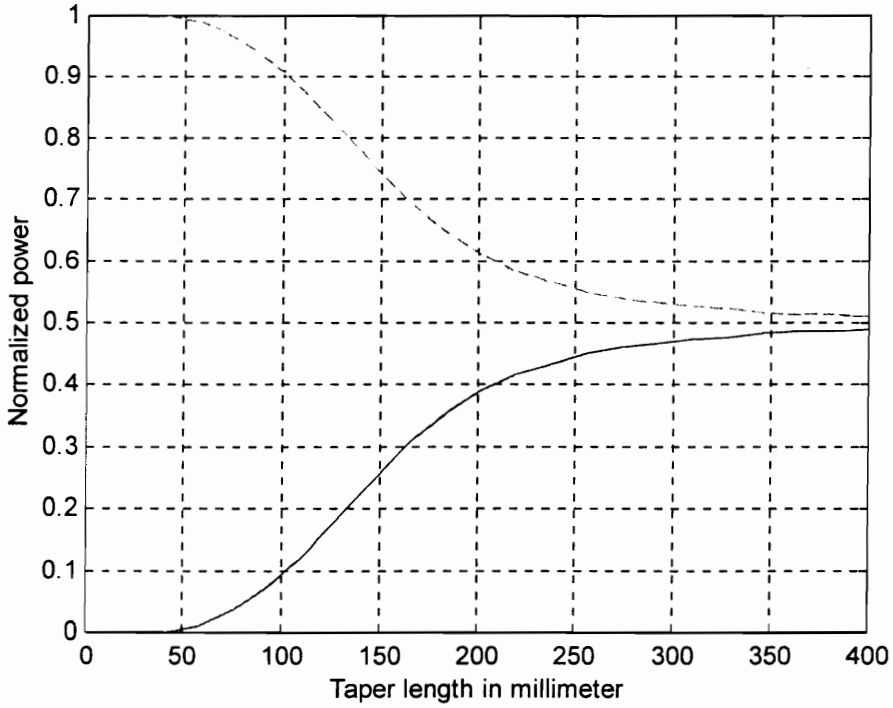

Figure 3-5. Simulation result of a symmetric coupler.

The top and bottom curves correspond to the power in the primary and secondary fibers, respectively. In reality, a shorter coupling length is needed to reach the final power splitting ratio because d decreases much faster due to the tension between the two fibers and to the fiber deformation in the tapering process. As observed, the final splitting ratio

for a 2x2 multimode fiber coupler is 50/50. This result agrees with the well-known prediction based on the statistical argument [20].

In the computer simulation, more than fifty rays have been used, and the result is almost the same as Figure 3-5. Since a high number of modes (rays) are involved in the modal coupling, on the average there would be no significant difference if the exact number of guided modes changes. Hence, practically, performance of multimode fiber couplers is independent of small changes in operation wavelength.

Asymmetric multimode couplers

The power coupling in an asymmetric multimode coupler could also be simulated using this model. The only difference is the static ray pattern. Figure 3-6 illustrates the static pattern with the primary fiber core twice the size of the secondary fiber core.

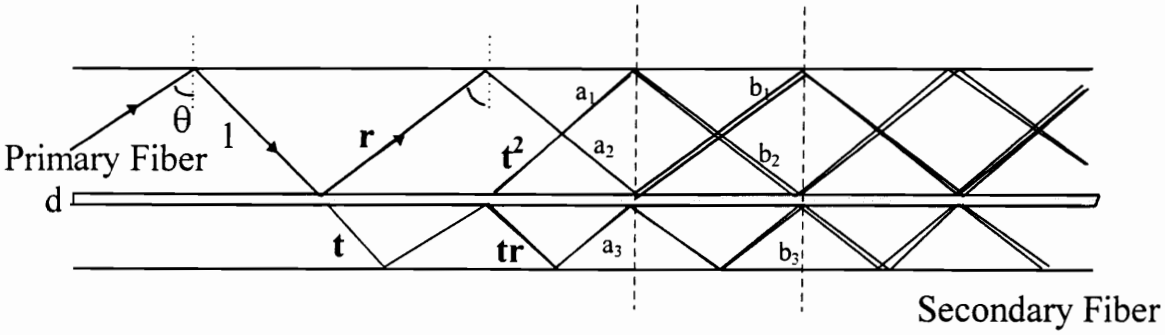

Figure 3-6. Asymmetric static ray pattern.

The power in both fibers can be represented by the coefficients a_1, a_2, and a_3, in which

$$\text{Power in Primary} = a_1 + a_2, \tag{3.19}$$

$$\text{Power in Secondary} = a_3. \tag{3.20}$$

These coefficients (a's) after passing through the middle layer many times can be derived by relating them to the next state coefficients b's, as indicated between the two vertical dashed lines in Figure 3-6.

$$b_1 = a_2*r + a_3*t, \tag{3.21}$$

$$b_2 = a_1, \text{ and} \tag{3.22}$$

$$b_3 = a_2*t + a_3*r. \tag{3.23}$$

The initial values are

$$a_1 = t^2, a_2 = r, \text{ and } a_3 = tr. \tag{3.24}$$

This routine could continue for the next crossover point by a simple transformation, namely

$$a_1 <= b_1, a_2 <= b_2, \text{ and } a_3 <= b_3. \tag{3.25}$$

Using Equation (3.4), we can easily verify that if

$$a_1 + a_2 + a_3 = 1, \tag{3.26}$$

then

$$b_1 + b_2 + b_3 = 1. \tag{3.27}$$

This corresponds analytically to an expression of the conservation of energy. The amplitude coefficients are given in Table 2.

Table 2. Power amplitude terms in a 2x2 asymmetrical coupler

Number of crossovers	Power in the primary fiber	Power in the secondary fiber	Total power
0	1	0	1
1	r	t	$r + t = 1$
2	$r + t^2$	rt	$(r + t) = 1$
3	$t^2 + r^2 + rt^2$	$rt + r^2t$	$(r + t)^2 = 1$

In the corresponding computer simulation, we assume 100/140 and 50/125 to be the primary and secondary fibers, respectively. The width of the heated area is 10 mm. The number of crossover points for a given taper length (L) is double that of Equation (3.5), in which D is the primary fiber core diameter. The simulation result is shown in Figure 3-7 [the computer program is listed in Appendix B].

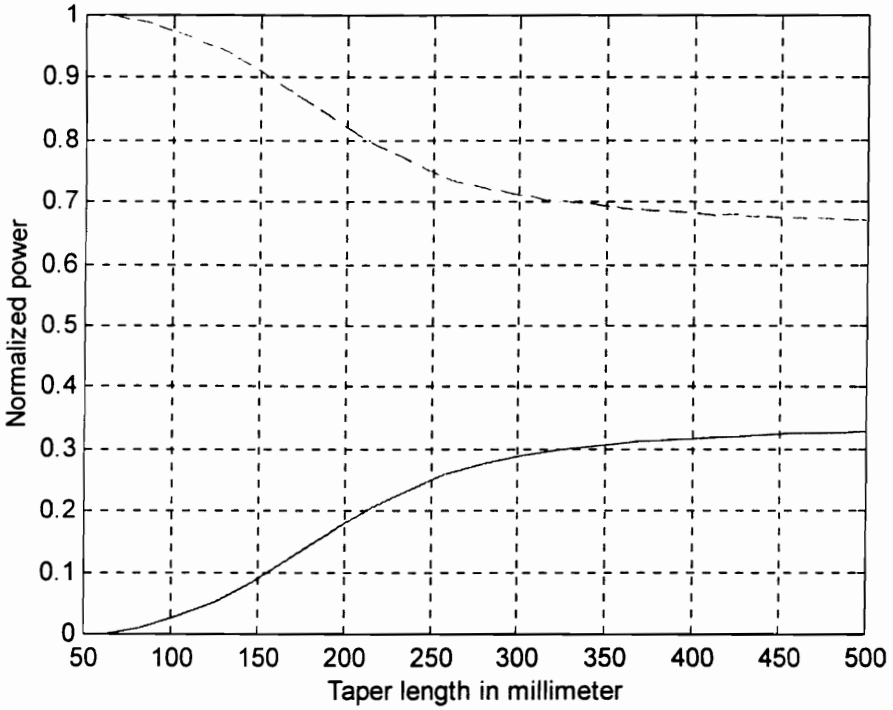

Figure 3-7. Power coupling in the asymmetric coupler.

The top and bottom curves correspond to the power in the primary and secondary fibers, respectively. Notice that the percentage power coupled from the primary fiber to the secondary fiber is not 50%, but proportional to a percentage relative to its fiber core diameter with respect to the total core width. In this case, the final power percentage in the secondary fiber is 50/(100+50) = 33%. This value would be different if another set of fibers having different widths are used, because a different static ray crossing pattern would be established. Similar to the symmetric coupler, the power coupling of asymmetric multimode fiber couplers is relatively insensitive to small changes in wavelength.

3.3 Loss mechanism

Power loss mechanisms in multimode fiber couplers is an important phenomenon not only in helping us to understand the physics but also in designing low-loss and high-quality couplers. In particular, we would like to study the dependence of coupler performance on the index of refraction surrounding the taper region.

Tapered multimode fiber waveguide

The loss mechanism of a multimode coupler is similar to that of a tapered multimode fiber, which supports a large number of modes. For a particular guided mode, the effective index satisfies

$$n_{clad} < \beta_i/k < n_{core} \qquad (3.28)$$

where β_i is the propagation constant and $k = 2\pi/\lambda$. The modes whose effective indices are close to n_{clad} are the higher order modes in reference to the lower order modes whose effective indices are close to n_{core}. The electric fields of the higher order modes extend more into the fiber cladding region than the fields of the lower order modes [21]. In the tapering process, the effective index of a higher order mode approaches n_{clad}, and when they are equal, this mode becomes cut-off and radiated, contributing to loss.

Unlike a single mode fiber core, the size of a multimode fiber core is an order of magnitude larger than the wavelength and at least comparable to that of the cladding area. Since a large number of modes are involved, we use a ray optics model to somewhat quantitatively calculate the effect of the external index on multimode fiber propagation. In this model, both the surrounding (external) index of refraction and the cladding thickness are considered. For simplicity, we assume the 2-dimensional waveguide structure shown in Figure 3-8.

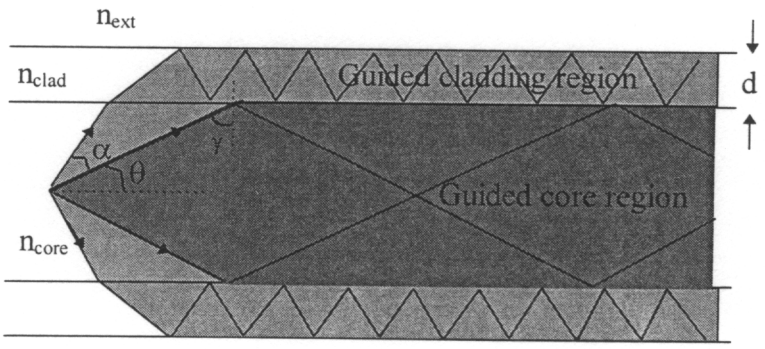

Figure 3-8. The multimode fiber taper waveguide.

The core, cladding, and external indices of refraction are n_{core}, n_{clad}, and n_{ext}, respectively. Normally, $n_{core} > n_{clad} > n_{ext}$. The angle θ gives the numerical aperture (NA)

$$NA = \sin(\theta) = \mathrm{sqrt}(n_{core}^2 - n_{clad}^2). \tag{3.29}$$

Angle α is the maximum angle for a ray undergoing total internal reflection at the cladding/external medium boundary. The cladding thickness is d. During tapering, the fiber becomes thinner and higher order modes are forced into the cladding layer and bounded by the cladding/external medium interface [22]. Hence, the total throughput power has two parts, namely

$$P = P_{core} + P_{clad}, \tag{3.30}$$

where P_{core} is the power bounded by the core/clad interface and P_{clad} is the cladding power bounded by the cladding/external medium interface. The shaded areas in Figure 3-8 include both guided core and cladding power.

Power loss of the guided cladding modes

For given n_{core} and n_{clad}, P_{clad} depends on the surrounding material (n_{ext}). The cladding mode power loss can be depicted by the angle α shown in Figure 3-4. Mathematically,

$$\alpha = \sin^{-1}\left(\frac{n_{clad}}{n_{core}}\right) - \sin^{-1}\left(\frac{n_{ext}}{n_{core}}\right). \qquad (3.31)$$

Assuming $n_{ext} < n_{clad} < n_{core}$, $n_{ext} = 1.0$ corresponds to the minimum loss, and $n_{ext} = n_{clad}$ corresponds to the complete loss of the cladding modes. In the region $1.0 < n_{ext} < n_{clad}$, the power loss of the cladding modes may be expressed in reference to the loss of $n_{ext} = 1.0$, which can be computed using Eq.(3.31). The result is given in Figure 3-9.

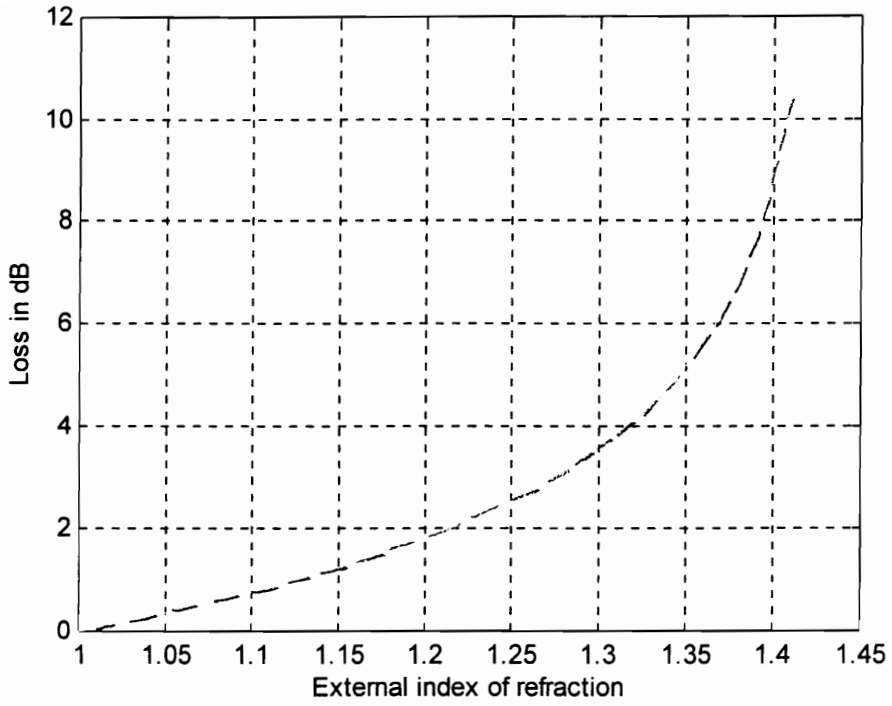

Figure 3-9. Dependence of the cladding power loss on the refractive index of the surrounding material.

Power loss of the guided core modes

If $n_{ext} < n_{core}$, the guided core mode power (P_{core}) is insensitive to the properties of the external medium. However, if n_{ext} is very close to n_{core} and the cladding thickness (d) is small, P_{core} will decrease dramatically during the taper process, and the core field will penetrate into the external medium due to frustrated total internal reflection (FTIR).

Mathematically, the power loss through FTIR may be expressed by the transmission coefficient of a core-cladding-core structure [19],

$$t = 1 - \left| \frac{Z_2^{\,2} - Z_1^{\,2}}{Z_1^{\,2} + Z_2^{\,2} + 2iZ_1Z_2 \cot(k_{2z}d)} \right|^2 \qquad (3.32)$$

where Z_1, Z_2, and K_2 are defined by Equations (3.11) - (3.17). In Equation (3.32), d is the taper cladding thickness as shown in Figure 3-8. To simulate waveguide performance, one hundred rays, whose incident angles are uniformly distributed across the above range, were selected. The average transmission coefficient of the perpendicular and parallel polarization components is taken as the final transmission value, i.e. power loss. The numerical results are shown in Figure 3-10. The cladding thickness is expressed in terms of the thickness/wavelength ratio.

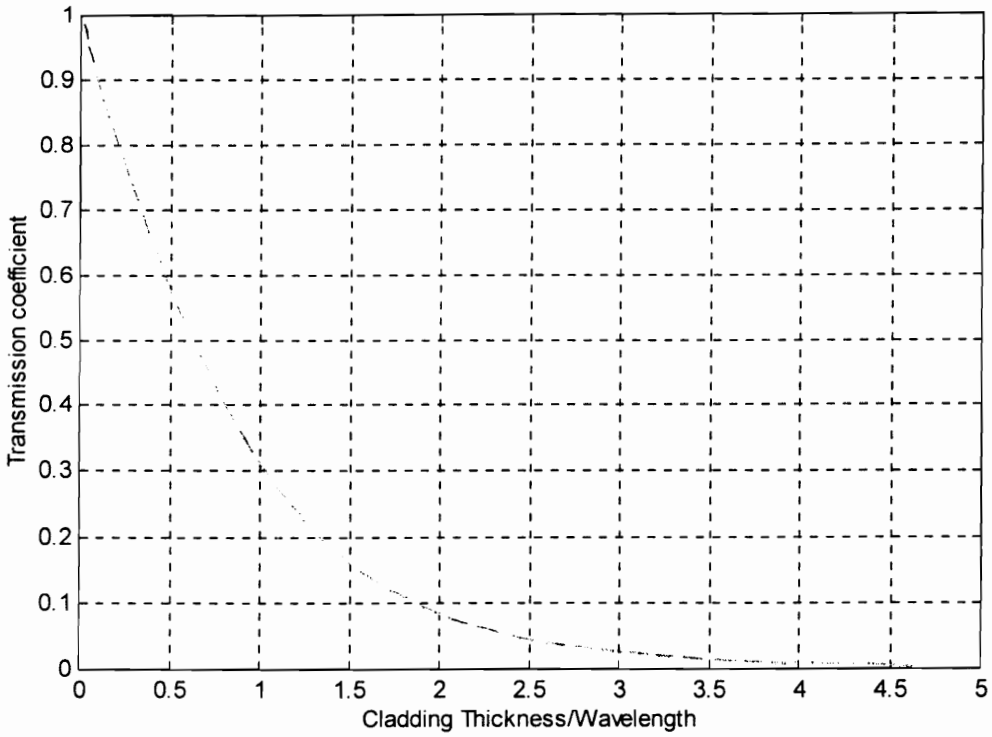

Figure 3-10. Transmission coefficient (power loss) due to FTIR.

In the case that the external medium index of refraction is near that of the fiber core, we observe that, as the overall cladding thickness approaches a few wavelengths, the core mode power loss will increase. When the cladding thickness equals one wavelength, the transmission coefficient t = 0.3, meaning that approximately 30% of the core mode power is lost. The total loss of the taper, hence the coupler, is the sum of the cladding mode loss and core mode loss as expressed in Equation (3.30).

Experiments

We have investigated experimentally the loss mechanism of multimode fiber couplers with Tapered Multimode Fiber Couplers constructed by tapering two multimode fibers together. For the purpose of discussion, we show the experimental setup in Figure 3-11.

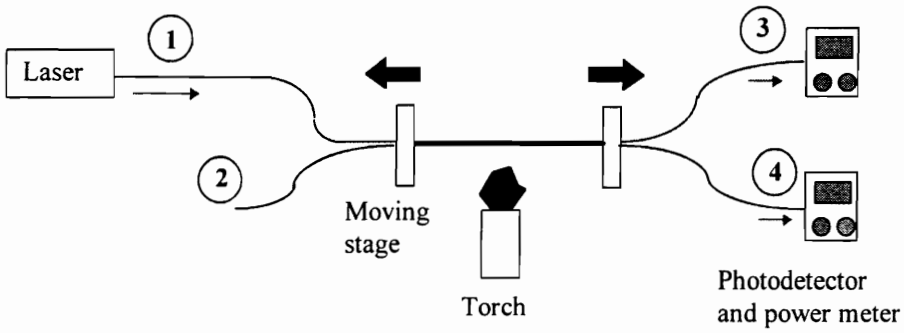

Figure 3-11. The experimental setup.

He-Ne laser light was coupled into one of the two 100 μm/140 μm graded index multimode fibers manufactured by SpecTran. The indices of the core and cladding are 1.458 and 1.429 (NA = 0.29), respectively. The ports of the coupler are labeled 1, 2, 3, and 4. The excitation port was port #1. The reason for using a He-Ne laser source is that the output light intensity pattern can be observed and the launch conditions may be easily adjusted and monitored to allow the excitation of lower order modes and ensure the far field speckle pattern is uniform. Since the performance of multimode fiber couplers is essentially wavelength independent, the outcomes of this study can be considered as general results.

External index dependence for a 3 dB coupler

The fibers were fused and stretched until the output power splitting ratio approached approximately 50/50 (actually 53/47). The combined two-fiber taper region waist section, whose cross sectional area is shown in Figure 3-12, was submerged into various liquid solutions with different indices of refraction and the corresponding excess losses were recorded.

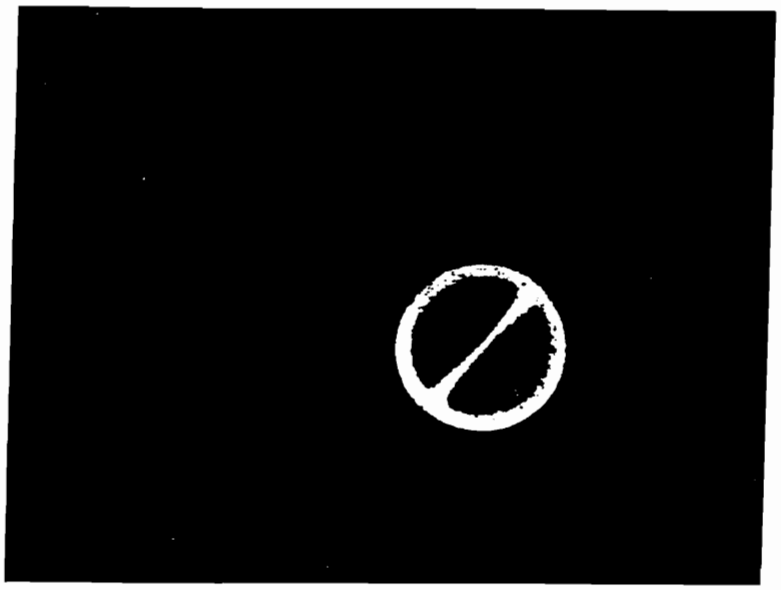

Figure 3-12. The cross sectional area of the multimode coupler taper waist.

The diameter of the taper is 47 μm. The cladding thickness is 5.1 μm and the thickness of the layer between the two cores is about 2.5 μm. Figure 3-13 shows the experimental results.

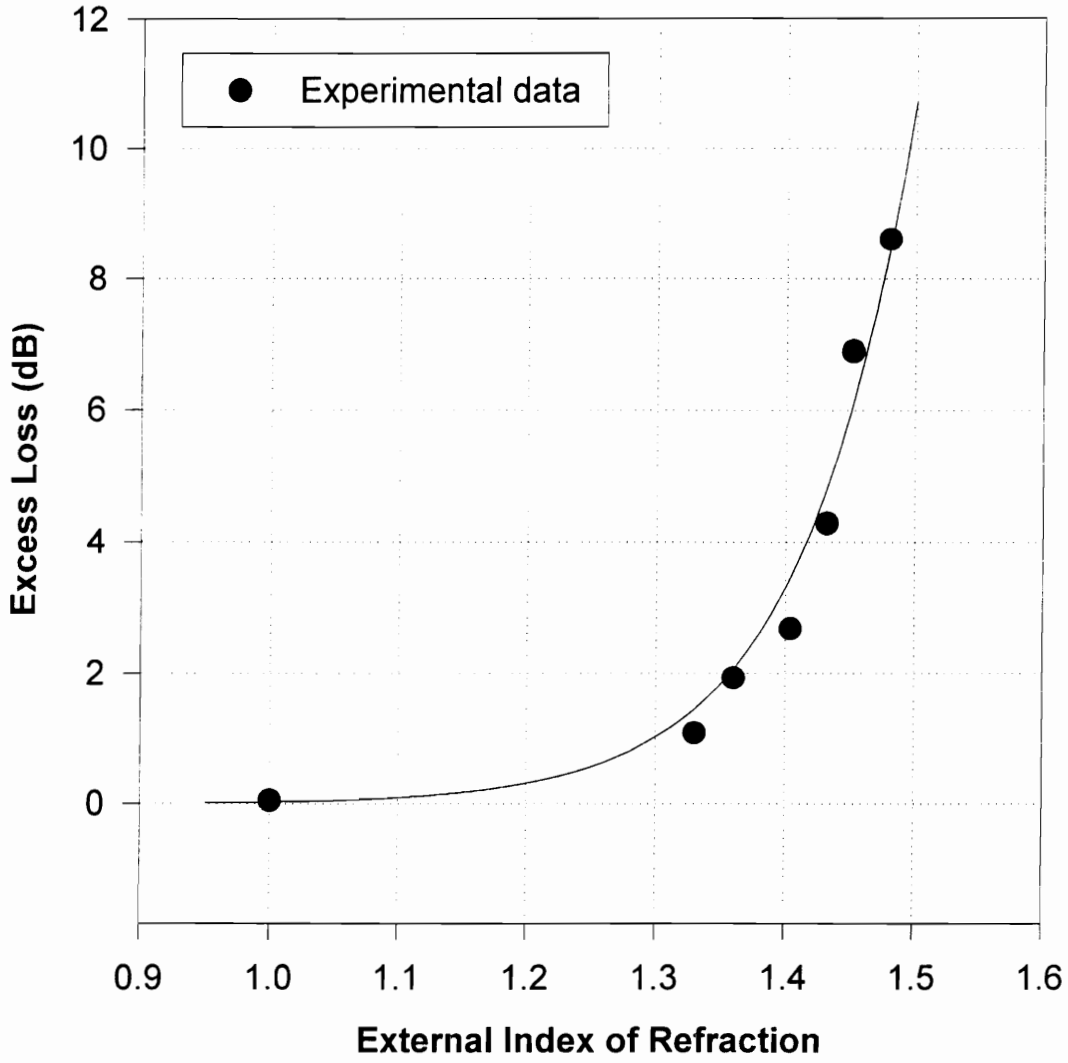

Figure 3-13. Excess loss as a function of external refractive index (at 47% power in port #4).

This experiment was performed by carefully cleaning the fiber taper section using alcohol every time a solution of a different refractive index was applied. It is evident that the excess loss of the 3 dB multimode coupler increases exponentially as the external refractive index changes from 1.0 (air) to a value equal to or greater than the fiber cladding index. Qualitatively, these data support the theoretical predication that when the external index of refraction approaches that of the fiber cladding and core, both the cladding mode and core mode power loss will increase dramatically.

External index dependence for a range of splitting power ratio of 100/0 through 50/50

To determine how the external index affects the excess loss (refer to Equation 2.0c) of a multimode coupler at different stages during a tapering process, alcohol (refractive index = 1.36) was applied to the taper waist section, and the output powers P_3 and P_4 for both air and alcohol as the surrounding materials were recorded. Alcohol was chosen in this experiment because it could be easily vaporized and the tapering process could go on until the intended splitting ratio was reached. Figure 3-14 shows the experimental data.

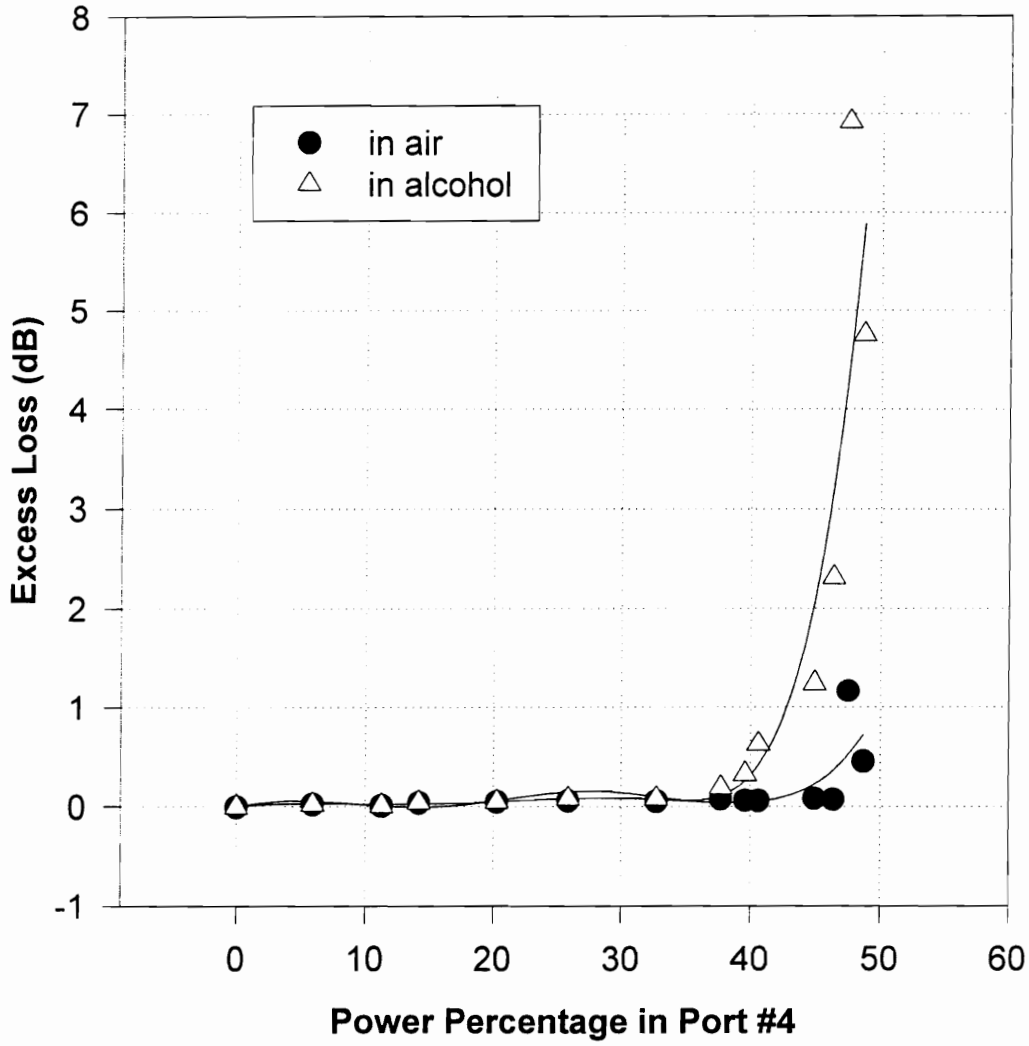

Figure 3-14. Excess loss as a function of power percentage in port #4 for different external indices of refraction.

The excess loss is less than 0.2 dB before the percentage power coupled into the secondary fiber reaches nearly 40% regardless of whether air or alcohol is used as the surrounding material. Tapering beyond this point, the coupler excess loss increases dramatically and hence becomes external index-dependent.

One direct application of the effect of external index on multimode fiber couplers is the coupler packaging. A multimode coupler with a 50/50 splitting ratio may be sensitive to the external index. Thus directly potting epoxy onto its taper region to enhance the mechanic strength as well as to isolate the fiber taper from the external environment may affect coupler outputs. However, for a multimode fiber coupler of splitting power ratios other than 50/50, it is possible that performance may not be affected by the external index of refraction.

4. Single-mode fiber wavelength-flattened coupler - the conventional method

Single-mode fibers are different from multimode fibers, and primarily single-mode fibers can support only one guided mode - the fundamental mode. The core of a single-mode fiber is no more than a few times larger than the operation wavelength. Narrow wavelength spectral width laser diodes serve as light sources for most single-mode fiber-based communication systems. Because there is no intermodal interference as in multimode fiber, single-mode fibers can carry optical signals over a long distance (more than 100 km) without regeneration or amplification. Therefore, single-mode fiber-based systems offer much larger bandwidth than multimode fiber systems. As briefly mentioned in chapters 1 and 2, single-mode fiber couplers have been deployed in communication systems as signal power splitters/combiners, wavelength-division multiplexers (WDMs), and tap-off branching devices.

The performance of a normal single mode fiber coupler is wavelength dependent. Specifically, its output power distribution is a function of wavelength. This characteristic would be a drawback in many cases, where wavelength-division multiplexing fiber communication systems demand that fiber couplers perform in the same way for all wavelength channels. In 1985, Mortimore [12] first introduced a method of fabricating wavelength-flattened (insensitive) couplers (WFCs) using a pair of dissimilar fibers. This method is often referred to as the conventional or traditional WFC fabrication technique. Although Mortimore's idea has been demonstrated to be a highly effective and successful

technique, the theoretical analysis has been proved to be not trivial [23]. To date, no theoretical model has been developed to describe the mechanism in a simple and easy-to-use manner. In this chapter, a novel analytical model is proposed to simulate the operation of the conventional wavelength-flattened fiber coupler. The basis of this model is the well-known coupled mode equations. Computer simulation is performed, and the results agree with experimental data.

4.1 Coupled mode equations

The physics of power coupling from one single-mode fiber to another indicates that when two fiber cores are sufficiently close to each other, the electric field of one fiber extends into and is received by the other fiber. Without losing generality, a 2x2 single-mode fiber coupler is analyzed. The coordinate system is shown in Figure 4-1.

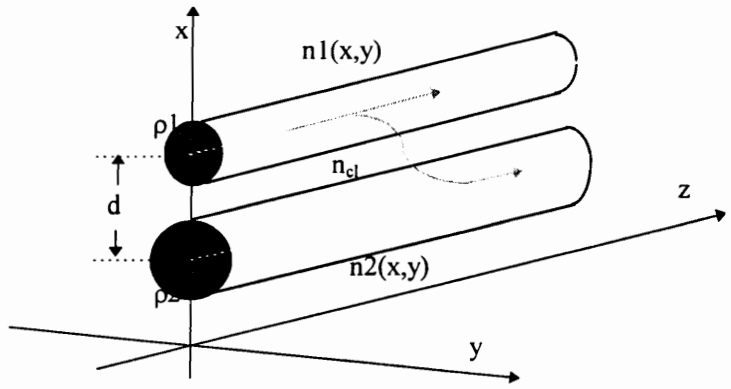

Figure 4-1. Power coupling between two parallel fibers.

Here the indexes of refraction of the first (primary) and second (secondary) fiber cores are $n_1(x,y)$ and $n_2(x,y)$, and the refractive index everywhere else (cladding) is n_{cl}. ρ_1 and ρ_2 represent the two fiber core radii, respectively, and the fiber separation is d.

To determine the electric field in each fiber, the field of the composite waveguide (two-fiber waveguide) is approximated by a linear combination of the fundamental-mode fields of each fiber in isolation, provided the two fibers are optically well separately and are not too different. Under the weakly guiding condition, Equation (4.1) gives the description [24].

$$\Psi(x,y,z) = b_1(z)\overline{\Psi_1}(x,y) / N_1^{1/2} + b_2(z)\overline{\Psi_2}(x,y) / N_2^{1/2} \quad , \qquad (4.1)$$

where Ψ is the solution of the scalar wave equation of the composite waveguide, and $\overline{\Psi}_1$ and $\overline{\Psi}_2$ are the solutions of the scalar wave equations of the first and second fibers in isolation, respectively. N_1 and N_2 are the normalization factors. The unknowns in this composite waveguide equation are the modal amplitudes $b_1(z)$ and $b_2(z)$, which are generally z-dependent and related to field coupling. To obtain these amplitudes, a perturbation theory is employed, where one fiber is viewed as the perturbation of the other fiber. For instance, the secondary fiber can be regarded as the perturbation of the first fiber, which gives

$$\frac{db_1}{dz} - i\overline{\beta}_1 b_1 = \frac{i}{4}\frac{k}{N_1^{1/2}}\left(\frac{\varepsilon_0}{\mu_0}\right)^{1/2} \int_{A_\infty} (n^2 - \overline{n_1}^2)\Psi\overline{\Psi}_1 dA \quad , \tag{4.2}$$

where n(x,y) is the index profile of the composite waveguide, i.e. $n = n_1$ corresponds to the core of the first fiber, and $n = n_2$ is for the core of the second fiber. The integral is evaluated over the cross-section of the composite waveguide. Another couple mode equation can be obtained by considering the first fiber as the perturbation of the second fiber. After simplification, the two couple mode equations can be written as

$$\frac{db_1}{dz} - i(\overline{\beta_1} + \overline{C}_{11})b_1 = i\overline{C}_{12}b_2 \quad , \tag{4.3a}$$

and

$$\frac{db_2}{dz} - i(\overline{\beta_2} + \overline{C}_{22})b_2 = i\overline{C}_{21}b_1 \quad , \tag{4.3b}$$

where $\overline{\beta}_1 and \overline{\beta}_2$ are the propagation constants for the first and second fibers in isolation, respectively, and the C_{ij} are *coupling coefficients* defined by

$$C_{ij} = \frac{1}{4}\frac{k}{(N_i N_j)^{1/2}}\left(\frac{\varepsilon_0}{\mu_0}\right)^{1/2} \int_{A_\infty} (n^2 - \overline{n_1}^2)\overline{\Psi}_1\overline{\Psi}_2 dA; i, j = 1,2 \tag{4.4}$$

Solving Equations (4.3) and (4.4) to obtain b_1 and b_2, the optical power in each fiber along the taper length can be expressed by

$$P_3(z) = |b_1(z)|^2, \tag{4.5a}$$

and

$$P_4(z) = |b_2(z)|^2. \tag{4.5b}$$

For nearly identical and non-absorbing fibers, assuming $P_1(0) = 1$ and $P_2(0) = 0$, we obtain the output power in the primary (P_3) and secondary (P_4) fibers, respectively.

$$P_3(z) = 1 - F^2 \sin^2\left(\frac{C}{F}z\right), \tag{4.6a}$$

and

$$P_4(z) = F^2 \sin^2\left(\frac{C}{F}z\right), \tag{4.6b}$$

where

$$F = \left\{1 + \frac{(\overline{\beta}_1 - \overline{\beta}_2)^2}{4C^2}\right\}^{-1/2}, \tag{4.7}$$

and

$$C = \frac{1}{4}\frac{k}{N_1}\left(\frac{\varepsilon_0}{\mu_0}\right)^{1/2} \int_{A\infty} (n^2 - \bar{n}^2)\overline{\Psi}_1\overline{\Psi}_2 dA., \tag{4.8}$$

where the 'F' and 'C' are referred to as the power transferred factor and coupling coefficient, respectively. Equations (4.6a) and (4.6b) say that the optical power in each

fiber changes periodically along the composite waveguide (taper), even though the combined power is constant (conservation of energy). The fiber coupling length for a complete cycle of power coupling between these two fibers is referred as the *beat length* (z_b), which is given by

$$z_b = \frac{2\pi F}{C}. \tag{4.9}$$

If the two fibers are identical, Equations (4.6)-(4.9) can be further simplified. For a 2x2 symmetric single-mode fiber coupler using two identical fibers, the power transfer factor Equation (4.7) and the coupling coefficient Equation (4.8) can be simplified to [25]:

$$F = 1.0, \tag{4.10}$$

and

$$C = \frac{(2\Delta)^{1/2}}{\rho} * \frac{U^2}{V^3} * \frac{K_0\left(\frac{Wd}{\rho}\right)}{K_1^{\,2}(W)}, \tag{4.11}$$

here Δ is the usual index profile height. ρ is the fiber core radius at the taper region. d is the separation between the two cores. V, U, and W are the usual dimensionless parameters given by,

$$V^2 = U^2 + W^2 = \rho^2 k^2 \left({n_{core}}^2 - {n_{clad}}^2 \right) , \qquad (4.12)$$

$$U(V) = \frac{\left(1+\sqrt{2}\right)V}{1+\left(4+V^4\right)^{1/4}} \text{ [21]}, \qquad (4.13)$$

and the free space propagation constant k is

$$k = \frac{2\pi}{\lambda} , \qquad (4.14)$$

where λ is the wavelength. In Equation (4.11), K_0 and K_1 are the modified Bessel functions of the second kind of order 0 and 1, respectively.

4.2 A simulation model

To calculate the power coupling between two identical fibers during the fiber fusing and tapering process, a fiber deformation model needs to be developed, in which the fiber

dimension and core separation are inversely proportional to the taper length. Figure 4-2 shows the geometry.

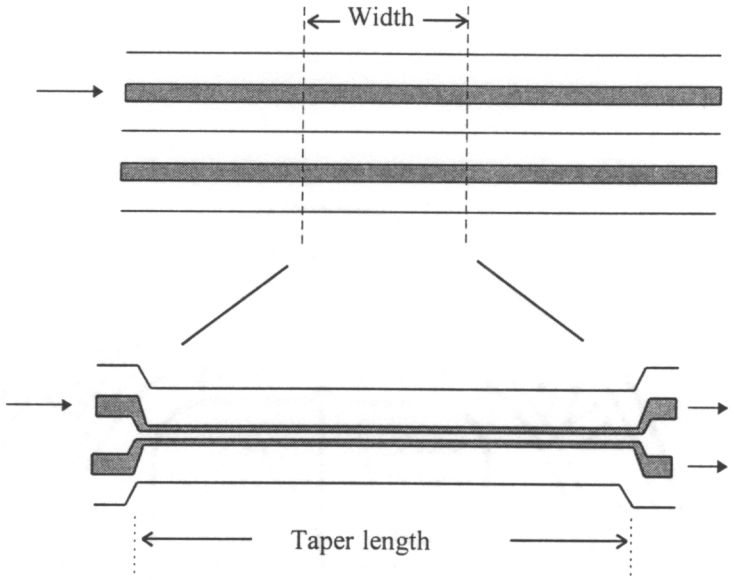

Figure 4-2. Single mode fiber taper.

The cross-sectional areas of the taper waveguide for three different stages may appear as shown in the following figures.

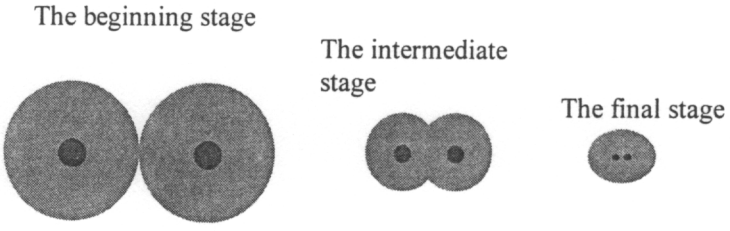

Figure 4-3. Fiber cross-sectional areas for different stages.

Notice the two fiber cores are distinct and well isolated in the taper region. This is the essential theme of the coupled mode theory. Assuming the single mode fiber has a = 4 μm (core radius), b = 62.5 μm (cladding radius), and n_{core} = 1.46, and n_{clad} = 1.455 (NA = 0.12), and using Equations (4.6) and (4.11) - (4.14), the following power transferring graphs are obtained using the computer program listed in Appendix C.

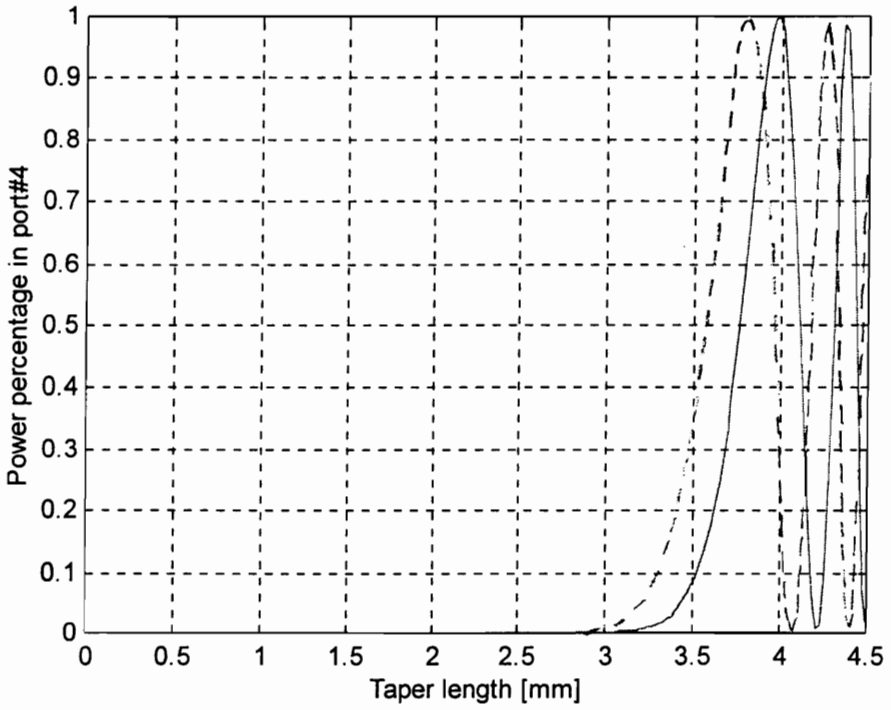

Figure 4-4. Power coupling in a symmetric 2x2 single-mode fiber coupler.

The curve on the left corresponds to the power coupling for λ = 1.5 μm, and the one on the right is for λ = 1.3 μm. In this model, the fiber core radius (ρ) and core-to-core separation (d) are expressed by,

$$\rho = \gamma a, \tag{4.15}$$

and

$$d = 2b * \exp\left[\alpha\left(1 - \frac{1}{\gamma^2}\right)\right], \tag{4.16}$$

where α is a positive constant which can be determined empirically ($\alpha = 6.0$ in the simulation). From the conservation of mass, we have

$$\gamma = \sqrt{\frac{width}{width + z}}. \tag{4.17}$$

Here the 'width' is the fused section length (approximately the heating source length), and z is the coupler taper length. Notice that in Figure 4-4 the optical power of $\lambda = 1.5$ μm is coupled into the secondary fiber before that of $\lambda = 1.3$ μm. This is due to the fact that the electric field of a longer wavelength extends more into the cladding than that of a shorter wavelength for a given single-mode waveguide [26]. Fiber coupler power coupling is strongly wavelength dependent. Using the same set of equations, the wavelength output spectrum of a coupler can be obtained. Figure 4-5 illustrates the spectrum for a 50/50 single-mode coupler at 1.5 μm (the first 3 dB point) [the computer program is listed in Appendix D].

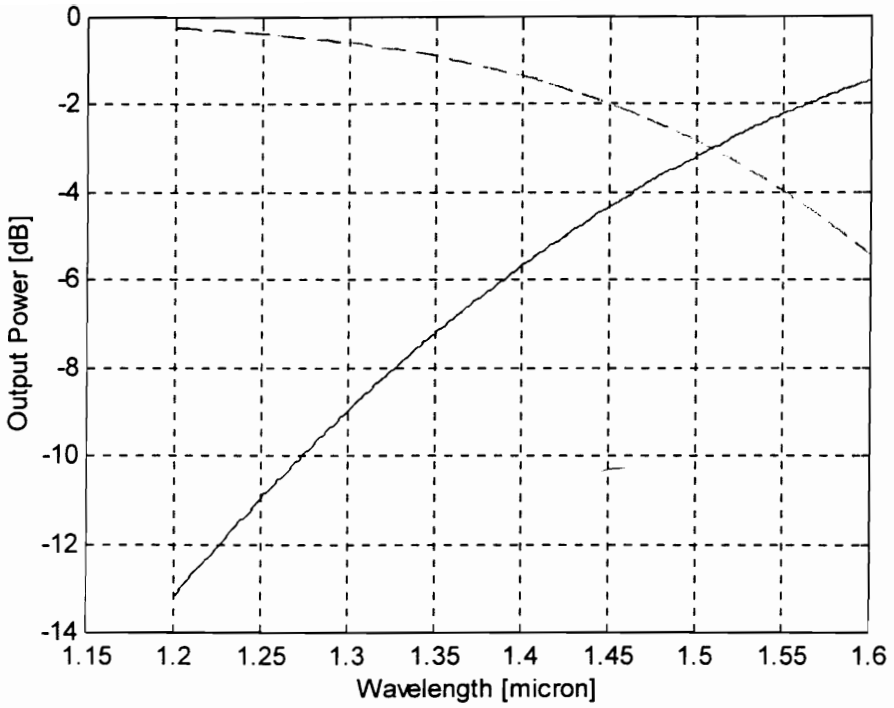

Figure 4-5. The coupler output power wavelength spectrum.

The top and bottom curves correspond to the power in port#3 and port#4, respectively. Note that at λ=1.5 μm, both output spectrum profiles intersect at 3 dB, corresponding to 50/50 splitting ratio. At λ=1.3 μm, the splitting ratio is 90/10. In general, a coupler could be made for any pre-determined output splitting ratio such as 50/50, 60/40, 90/10, and others at one specified wavelength. The output spectra of regular single-mode couplers are not flat (varied).

4.3 Wavelength-flattened couplers

Having obtained all the necessary equations based on coupled mode theory, we are now in the position to analyze the Mortimore wavelength-flattened coupler. This

conventional technique relies on the fact that a dissimilarity between the primary and secondary fibers creates a partial power coupling. For an ideal 2x2 single mode wavelength-flattened coupler, one of the fibers should be deformed by pre-tapering or etching prior to fusion in a way that the maximum power transfer is about 50%. Since this 50% turning point is stable, a wide range of wavelength components might have their first turning points nearby, and they might also have a 50/50 splitting ratio.

Theoretically, the wavelength compensation can be explained using the power transfer factor F of the coupled mode theory. Unlike the case of two identical fibers, because the fiber is slightly deformed relative to the other fiber, the F factor is no longer equivalent to 1.0, and its expression can be derived from Equation (4.7) to be

$$F^2 = \frac{1}{1 + \frac{WV^4}{2\pi} * K_0^4(W) * \frac{d}{\rho} * \exp\left(2W\frac{d}{\rho}\right) * \left(\frac{\delta\rho}{\rho}\right)^2}, \qquad (4.18)$$

where $\delta\rho$ is the fiber core diameter difference between the primary and secondary fibers, and all other parameters have the same meaning as in Section 4.2. Figure 4-6 shows the power coupling in the asymmetric single-mode coupler [Appendix E shows the program].

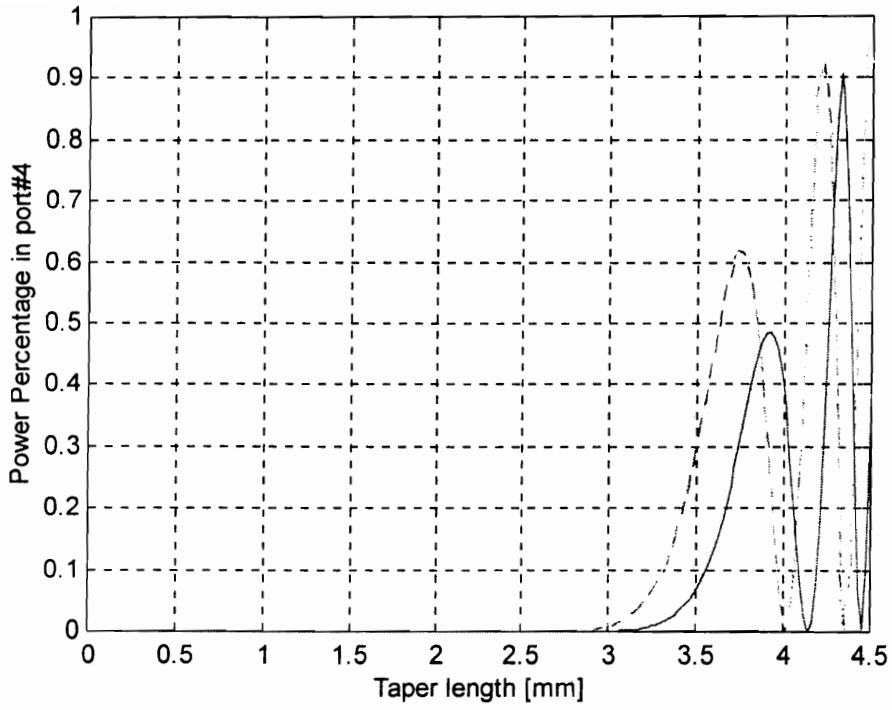

Figure 4-6. Power coupling in the output port #4 for an asymmetric fiber coupler.

The left curve is for $\lambda = 1.5$ μm, and the other one is for $\lambda = 1.3$ μm. The fiber is 8/125 μm/μm and has the refractive indices of n_{core}=1.460 and n_{clad}=1.455. The fiber core difference $\delta\rho$ is modeled by

$$\delta\rho = a\gamma\sqrt{\frac{width}{width + L}}, \tag{4.19}$$

where L is the pre-tapered length, i.e. one of the fibers is pre-tapered before combining and fusing with the other fiber. In this example, L = 0.9 mm. Again, the longer

wavelength (1.5 μm) component couples its power into the secondary fiber before that of the shorter wavelength (1.3 μm) component. The fiber coupler made this way has the wavelength output spectra shown in Figure 4-7 [Appendix F shows the program].

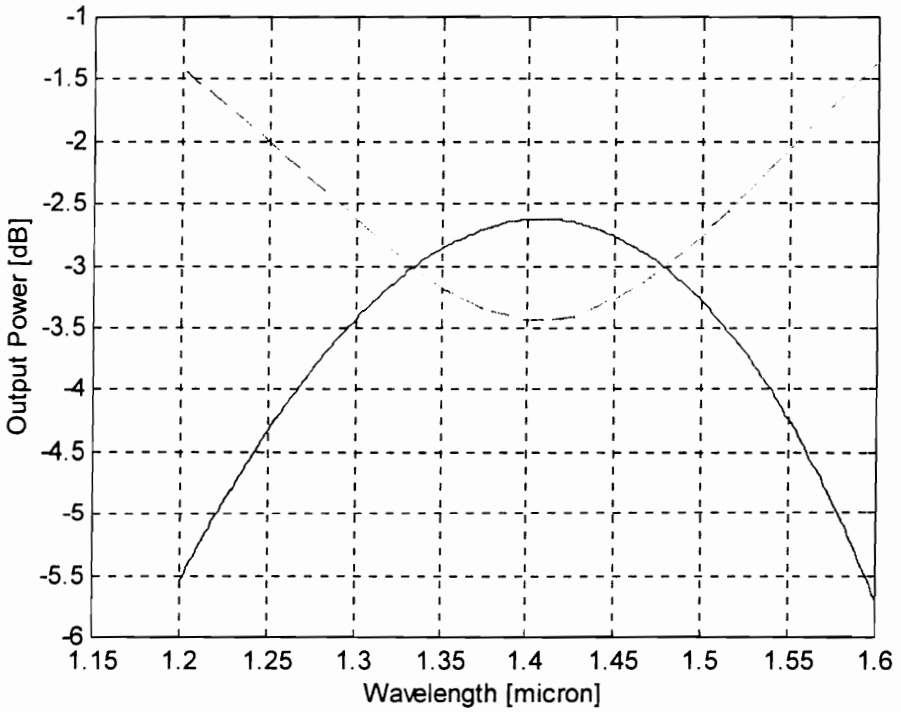

Figure 4-7. The output spectrum of the wavelength-flattened coupler.

The top and bottom curves represent the spectra of port#3 and port#4, respectively. The taper length we chose is 3.90 mm, where both the 1.5 μm and 1.3 μm components are

near their first turning points as indicated in Figure 4-6. It is observed that the spectra are reasonably flat between 1.3 μm and 1.5 μm (3 dB +/- 0.5 dB).

In a corresponding experiment, the aforementioned pre-tapering technique was used and the fiber was made by Corning for single-mode operation at both 1.3 μm and 1.55 μm. Figure 4-8 shows the output spectra.

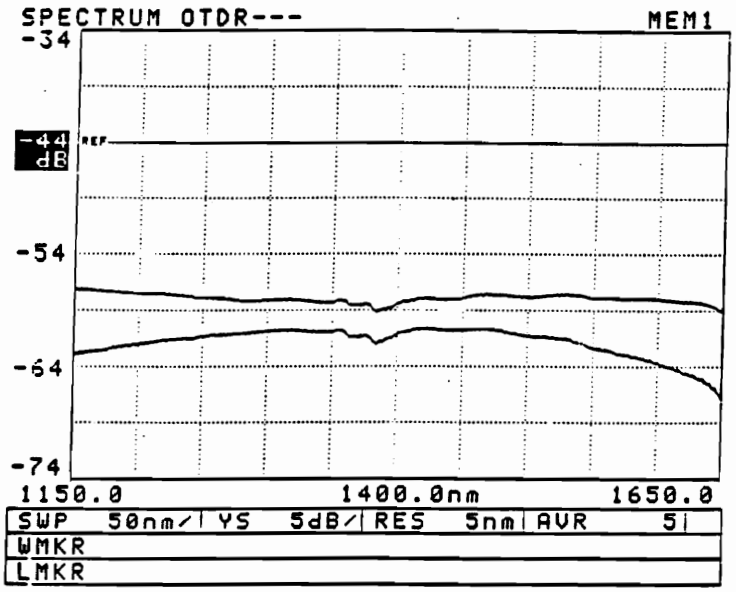

Figure 4-8. Output wavelength spectra of a WFC (experimental result)

Wavelength-flattened couplers are essential devices in fiber optic communication systems in which wavelength-division multiplexing is employed, and signals would be split evenly among output ports regardless of what wavelengths are used.

There is a significant difference between the theoretical simulation (Figure 4-7) and experimental observation (Figure 4-8), even though the general trend is the same - flat wavelength output. This is the limitation of the coupled mode equations, where two distinct waveguides are considered in the coupler taper region. The coupled mode theory can provide only a qualitative description of the power coupling in WFCs. The major reason for its popularity is that it gives a sound physical insight concerning the optical interaction in fiber couplers. In the next chapter, a different method is employed to construct wavelength-flattened couplers, where a composite waveguide model is used to simulate the power coupling in the taper region.

5. Wavelength spectral compensation using regular 2x2 fiber couplers

The conventional method of fabricating wavelength-flattened couplers (WFCs) described in Chapter 4 is effective, however it requires pre-tapering or etching one of the fibers to create a phase mismatch such that the first turning point is at around 50%. Practically, the precise amount of pre-tapering or etching could be a difficult task, and it is often determined from experience. In this chapter, a new technique is proposed and developed to fabricate wavelength-flattened couplers (WFCs) using regular 2x2 single-mode couplers. As will be demonstrated in this chapter and the next chapter, this method is quite general and could be used to construct $1x2^N$ wavelength-flattened trees and other star WFCs.

The building block of the technique is a regular single-mode 2x2 coupler. Hence, the spectral characteristic of this coupler is first studied. Secondly, a 2x2 wavelength-flattened coupler (WFC) is constructed using two regular couplers. Thirdly, the wavelength compensation concept can be extended to construct a 1x3 WFC using three regular 2x2 couplers. The final section of this chapter deals with coherence properties of these couplers aiming to stabilize the coupler outputs. For convenience and without losing any generality, we assume there is no loss in a regular single-mode 2x2 fused fiber coupler.

5.1 Regular (standard) 2x2 single-mode fiber couplers

Figure 5-1 shows a typical 2x2 single-mode fiber coupler.

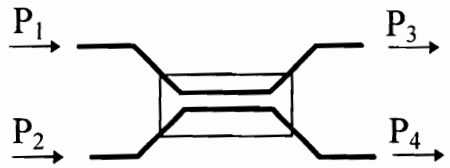

Figure 5-1. A regular 2x2 fiber coupler.

The labeling of each port is illustrated in the figure. P_1, P_2, P_3, and P_4 are the optical powers in the corresponding fiber ports. Normally, port#1 and port#3 are associated with one fiber, and port#2 and port#4 are associated with the other fiber. If light is launched into one input port, say port#1 (P_1 is not zero and $P_2 = 0$), that fiber is considered as the primary fiber. The other fiber is the secondary fiber. It is important to make a distinction between the primary and secondary fibers.

As described in Chapter 4, the power coupling between the two fibers is due to the modal field interference in the coupling region. The output power splitting ratio is a function of wavelength, because wavelength alters the propagation constant and hence the waveguiding properties. For a regular 2x2 single-mode fiber coupler, the spectra of the two outputs are functions of wavelength. However, these two output spectra are complementary to one another, i.e. the sum of the two equals the input power

spectrum. This symmetric property would make a regular 2x2 coupler an ideal spectrum compensator.

Theoretically, the power coupling could be described more accurately using composite waveguide approaches than the coupled mode equations [27-29]. The operation of the coupler with two inputs originated from the same source can be written in terms of a product transfer matrix [30]

$$\begin{pmatrix} E_3 \\ E_4 \end{pmatrix} = \begin{pmatrix} \cos(\theta) & \sin(\theta) \\ \sin(\theta) & -\cos(\theta) \end{pmatrix} * \begin{pmatrix} 1 & 0 \\ 0 & e^{j\Delta\phi} \end{pmatrix} * \begin{pmatrix} E_1 \\ E_2 \end{pmatrix}, \tag{5.1}$$

where $E_i = P_i^{1/2}$ (i =1,2,3,and 4) is the corresponding electric field amplitude, $\Delta\phi$ is the phase difference between the two input fields, and θ is given by

$$\Theta = \int_0^L C * dx. \tag{5.2}$$

Here C is the coupling coefficient and the integration is evaluated along the coupling length. From Equation (5.1), we obtain

$$\begin{pmatrix} E_3 \\ E_4 \end{pmatrix} = \begin{pmatrix} \cos(\theta) & \sin(\theta) * e^{j\Delta\phi} \\ \sin(\theta) & -\cos(\theta) * e^{j\Delta\phi} \end{pmatrix} * \begin{pmatrix} E_1 \\ E_2 \end{pmatrix}. \tag{5.3}$$

The output power terms can be expressed

$$P_3 = E_3^2 = (\cos(\theta)E_1 + \sin(\theta)e^{j\Delta\phi}E_2)^* (\cos(\theta)E_1 + \sin(\theta)e^{-j\Delta\phi}E_2)$$

$$= \cos^2(\theta)E_1^2 + \sin(\theta)e^{j\Delta\phi}E_2\cos(\theta)E_1 + \cos(\theta)E_1\sin(\theta)e^{-j\Delta\phi}E_2 + \sin^2(\theta)E_2^2$$

$$= \cos^2(\theta)E_1^2 + \sin^2(\theta)E_2^2 + \sin(\theta)\cos(\theta)E_1E_2\,(e^{j\Delta\phi} + e^{-j\Delta\phi})$$

$$= \cos^2(\theta)E_1^2 + \sin^2(\theta)E_2^2 + \sin(\theta)\cos(\theta)E_1E_2(2\cos(\Delta\phi)), \qquad (5.4)$$

and similarly,

$$P_4 = E_4^2 = (\sin(\theta)E_1 - \cos(\theta)e^{j\Delta\phi}E_2)^* (\sin(\theta)E_1 - \cos(\theta)e^{-j\Delta\phi}E_2)$$

$$= \sin^2(\theta)E_1^2 + \cos^2(\theta)E_2^2 - \sin(\theta)\cos(\theta)E_1E_2(2\cos(\Delta\phi)). \qquad (5.5)$$

Using Equations (5.4) and (5.5), the power terms can be written as

$$\begin{pmatrix} P_3 \\ P_4 \end{pmatrix} = \begin{pmatrix} \cos^2(\theta) & \sin^2(\theta) \\ \sin^2(\theta) & \cos^2(\theta) \end{pmatrix} * \begin{pmatrix} P_1 \\ P_2 \end{pmatrix}, \qquad (5.6)$$

provided $\Delta\phi$ satisfies

$$\Delta\phi = \frac{\pi}{2} * (2n+1), \text{ or there is no phase correlation,} \qquad (5.7)$$

where n is an integer. Equation (5.6) implies that if Equation (5.7) is satisfied, the output power of the coupler should be the independent sum of the inputs, meaning the interference effect could be ignored.

5.2 2x2 wavelength-flattened coupler (WFC)

An easy way to fabricate a 2x2 WFC is to connect two regular 3 dB couplers back-to-back, provided the second coupler satisfies Equation (5.7). Figure 5-2 shows the configuration.

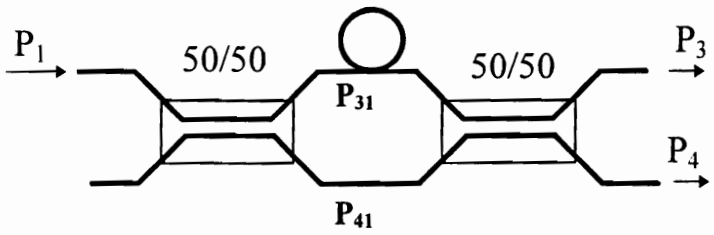

Figure 5-2. A 2x2 WFC using regular 3 dB couplers.

The fiber loop in the P_{31}-arm would be needed if a coherent light source is used to introduce a phase delay such that Mach-Zehnder interference could not take place. More about the coherent issue is discussed in the later section of this chapter. Using Equation (5.2) and assuming $P_2 = 0$, we have

$$\begin{pmatrix} P_{31} \\ P_{41} \end{pmatrix} = \begin{pmatrix} \cos^2(\theta) & \sin^2(\theta) \\ \sin^2(\theta) & \cos^2(\theta) \end{pmatrix} * \begin{pmatrix} P_1 \\ 0 \end{pmatrix} = \begin{pmatrix} \cos^2(\theta) P_1 \\ \sin^2(\theta) P_1 \end{pmatrix}, \tag{5.8}$$

and

$$\begin{pmatrix} P_3 \\ P_4 \end{pmatrix} = \begin{pmatrix} \cos^2(\theta) & \sin^2(\theta) \\ \sin^2(\theta) & \cos^2(\theta) \end{pmatrix} * \begin{pmatrix} P_{31} \\ P_{41} \end{pmatrix} = \begin{pmatrix} \cos^2(\theta) & \sin^2(\theta) \\ \sin^2(\theta) & \cos^2(\theta) \end{pmatrix} \begin{pmatrix} \cos^2(\theta) P_1 \\ \sin^2(\theta) P_1 \end{pmatrix}$$

$$= \begin{pmatrix} \cos^4(\theta) + \sin^4(\theta) \\ 2\cos^2(\theta)\sin^2(\theta) \end{pmatrix} P_1 . \tag{5.9}$$

Notice that the outputs of the first coupler ($P_{31} + P_{41} = P_1$) and the second coupler ($P_3 + P_4 = P_1$) obey the conservation of energy. Employing Equation (5.2) in which the coupling coefficient model is obtained using a rectangular composite waveguide (ax2a) [29],

$$C = \frac{3\pi\lambda}{32 n_{clad} a^2} \frac{1}{(1+1/V)^2}, \tag{5.10}$$

where 'a' the fiber core radius and V is the normalization frequency having air as the cladding material, we use computer simulation to generate the output spectra for both fiber couplers. A laser diode operating at $\lambda = 1.3$ μm is assumed as the light source. Figure 5-3 is the first coupler output spectra [the computer program is listed in Appendix G].

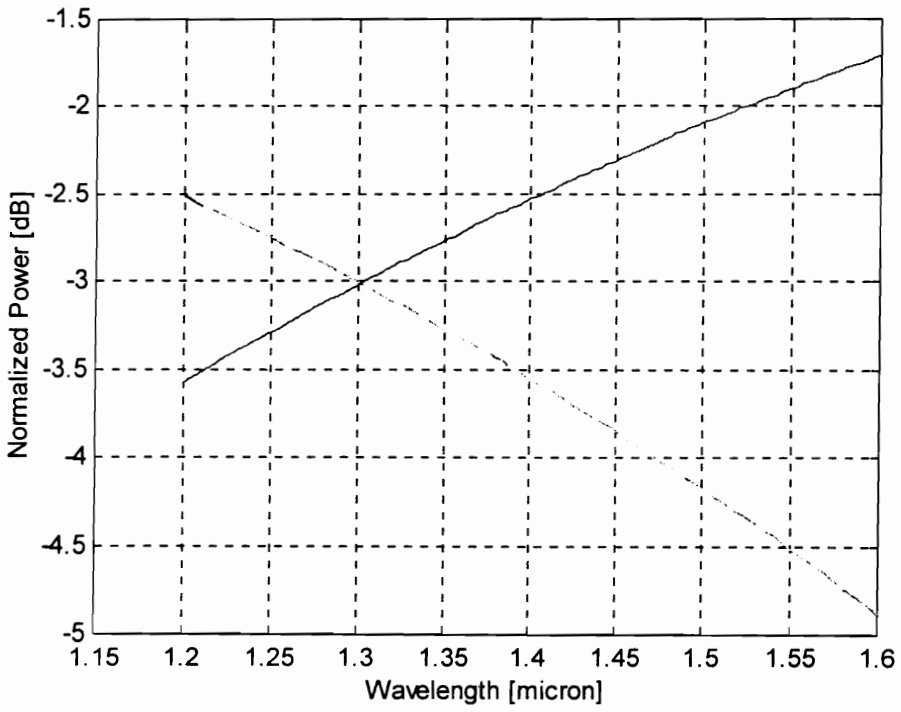

Figure 5-3. Output wavelength spectra of a regular 2x2 50/50 coupler.

The top and bottom curves on the right side correspond to P_{41} and P_{31}, respectively. Figure 5-4 shows the compensated (the second) coupler output spectra [Appendix G is the program].

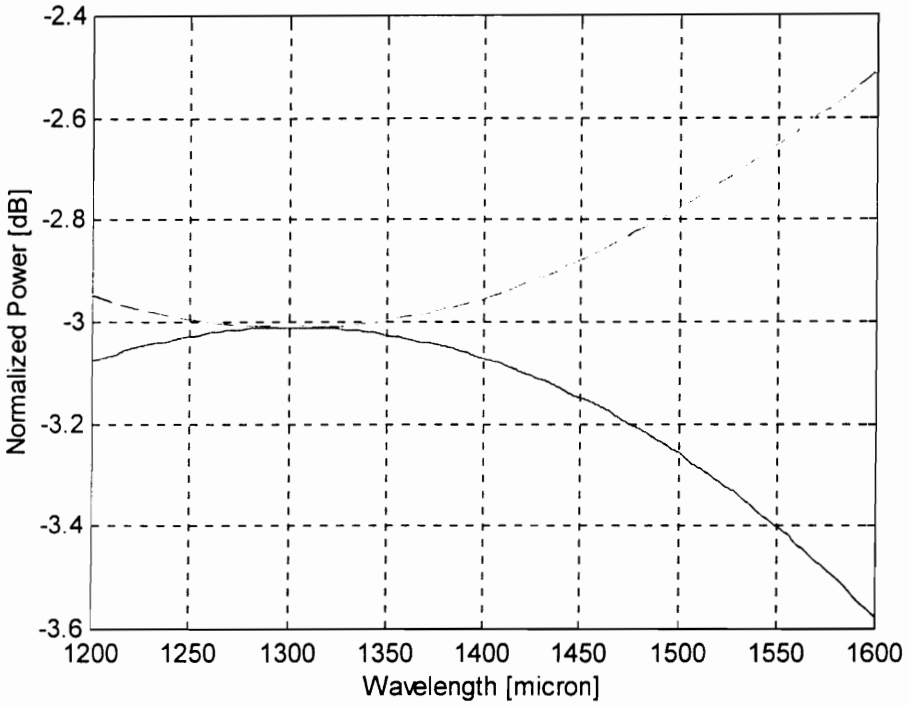

Figure 5-4. The output spectra of the two cascaded 50/50 2x2 couplers.

The top curve represents P_3 and the bottom one represents P_4. Compared with the previous spectra, these spectra are flat around 1.3 μm. Therefore, the power variation around 1.3 μm is successfully compensated for. Experimentally, this type of WFC has been obtained by connecting two 50/50 2x2 couplers. Figure 5-5 shows the output.

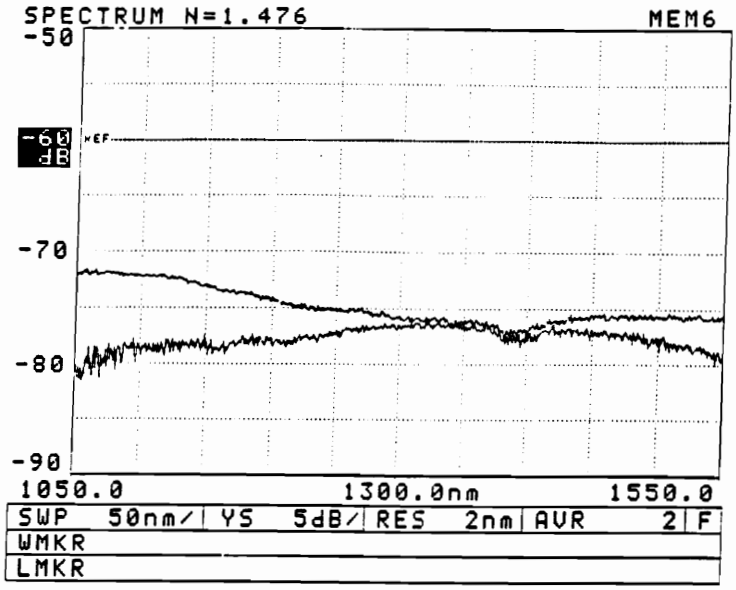

Figure 5-5. Wavelength spectrum of the 2x2 WFC.

In the experiment, white light was used in the set-up with a 5-meter long fiber delay loop and the output spectra were recorded using an ANDO Optical Spectrum Analyzer. In addition, we obtained a stable output when the laser diode was used as the source indicating this coupler could be employed for laser diode based communication systems. Another way to fabricate this type of WFCs is to use double fusing heads in the tapering process and the phase difference between the two arms should be around an odd integer times 90° as indicated in Equation 5.7.

5.3 1x3 wavelength-flattened coupler (WFC)

The concept of wavelength compensation by connecting regular 2x2 single-mode couplers can be employed to construct other types of WFCs. A new design of 1x3 WFC has been proposed using three regular 2x2 couplers. The geometry is shown in Figure 5-6.

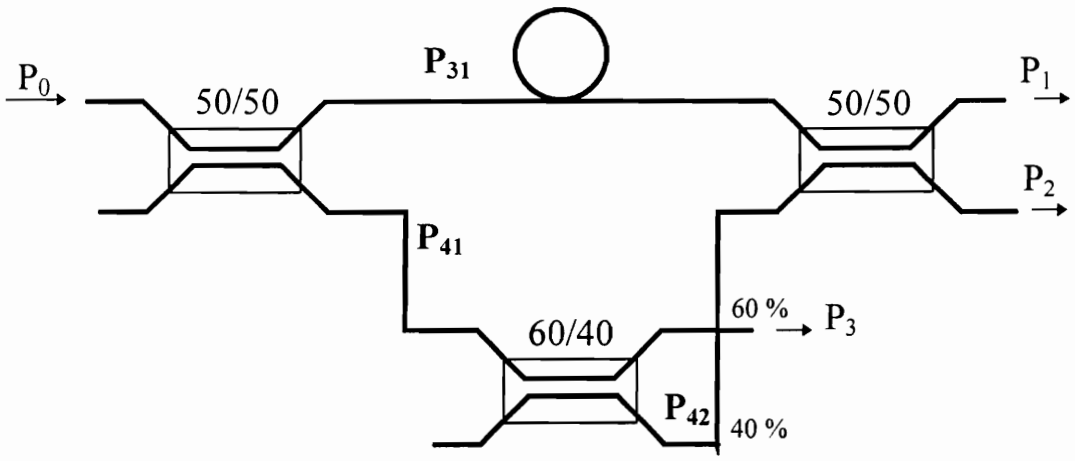

Figure 5-6. Layout of a 1x3 WFC using three regular couplers.

Similar to the previous 2x2 WFC, the wavelength spectra (transfer function) of each individual coupler are obtained, and then the output spectra of the combined structure are presented. Since two of the three couplers have the splitting ratio of 50/50, their transfer functions are the same as the one shown in Figure 5-3, and the coupling equation is given by Equation (5.6). The transfer function of the 60/40 coupler has

the coupling equation like Equation (5.6) but with a different θ, say θ'. The splitting ratio of a 2x2 single-mode fiber coupler could be varied by changing its coupling length L as indicated in the integration upper limit of Equation (5.2). Using the same C (coupling coefficient) expression, we obtain the spectra of a single 60/40 coupler at 1300 nm [Appendix G shows the program].

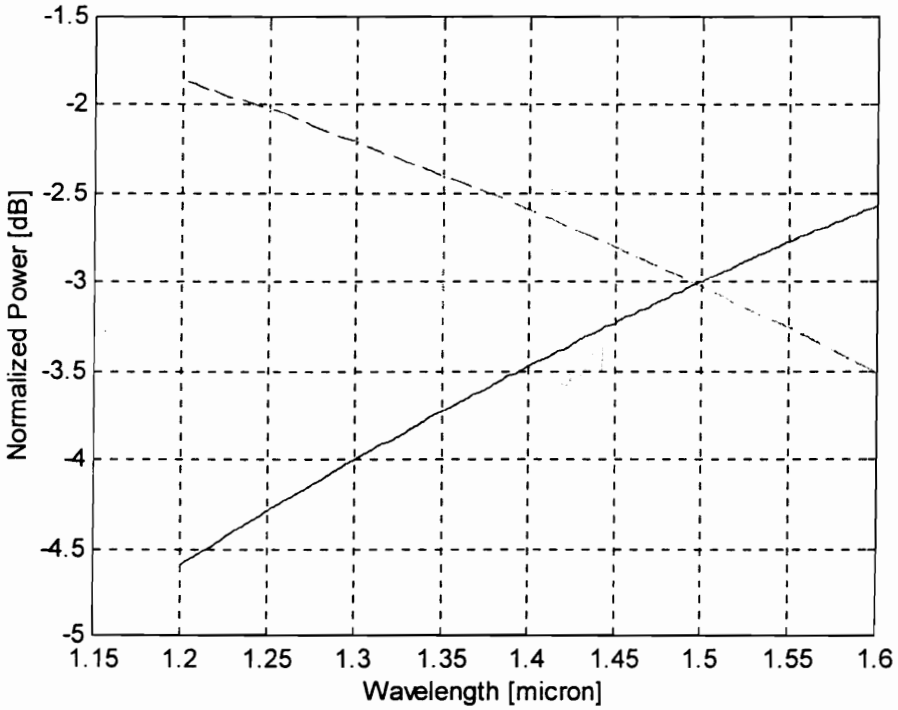

Figure 5-7. The transfer function of a 60/40 single-mode coupler.

The top curve on the left side represents the spectrum of the 60% output end, and the bottom one represents the spectrum of the 40% output end. Mathematically, we have

$$\begin{pmatrix} P_{31} \\ P_{41} \end{pmatrix} = \begin{pmatrix} \cos^2(\theta) & \sin^2(\theta) \\ \sin^2(\theta) & \cos^2(\theta) \end{pmatrix} \begin{pmatrix} 1 \\ 0 \end{pmatrix} P_0 , \tag{5.11}$$

$$\begin{pmatrix} P_3 \\ P_{43} \end{pmatrix} = \begin{pmatrix} \cos^2(\theta') & \sin^2(\theta') \\ \sin^2(\theta') & \cos^2(\theta') \end{pmatrix} \begin{pmatrix} 1 \\ 0 \end{pmatrix} P_{41} , \tag{5.12}$$

and

$$\begin{pmatrix} P_1 \\ P_2 \end{pmatrix} = \begin{pmatrix} \cos^2(\theta) & \sin^2(\theta) \\ \sin^2(\theta) & \cos^2(\theta) \end{pmatrix} \begin{pmatrix} P_{31} \\ P_{43} \end{pmatrix}. \tag{5.13}$$

Notice that Equations (5.11) and (5.13) have the same (50/50) coupling region (θ), but Equation (5.12) has a different (60/40) coupling region (θ'). The final output power terms are

$$P_1 = P_0[\cos^4(\theta)+\sin^4(\theta)\sin^2(\theta')], \tag{5.14}$$

$$P_2 = P_0\sin^2(\theta)\cos^2(\theta)[1+\sin^2(\theta')], \tag{5.15}$$

$$P_3 = P_0\sin^2(\theta)\cos^2(\theta'). \tag{5.16}$$

Computer simulation results of the 1x3 WFC is shown in Figures 5-8 and 5-9 [Appendix G is the computer program].

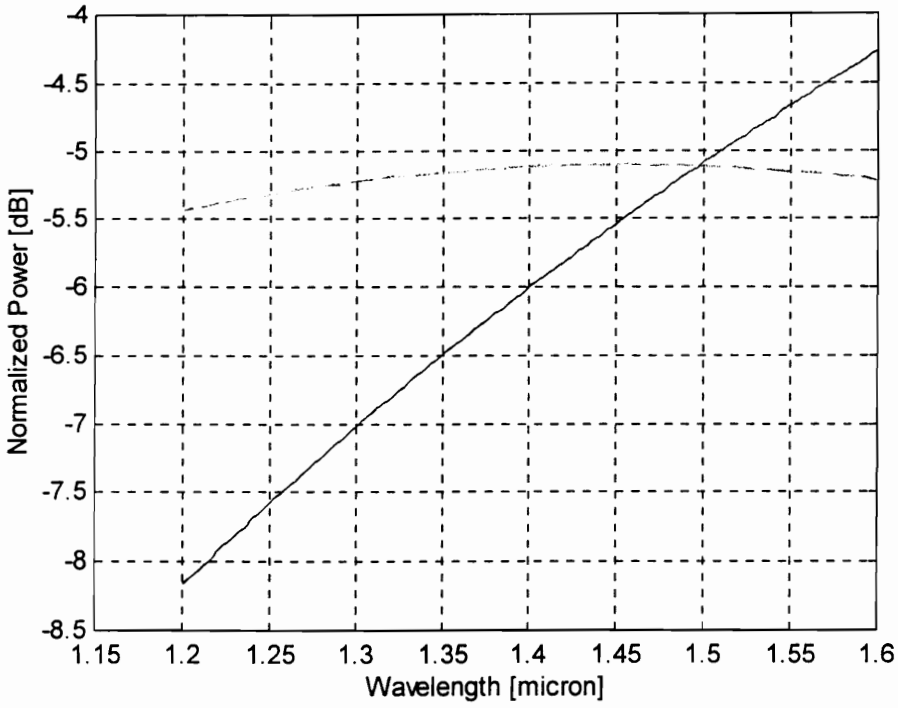

Figure 5-8. Output power spectra of the 60/40 coupler.

The top curve is P_3, and the bottom curve represents P_{42}. The final output spectra are given in Figure 5-9.

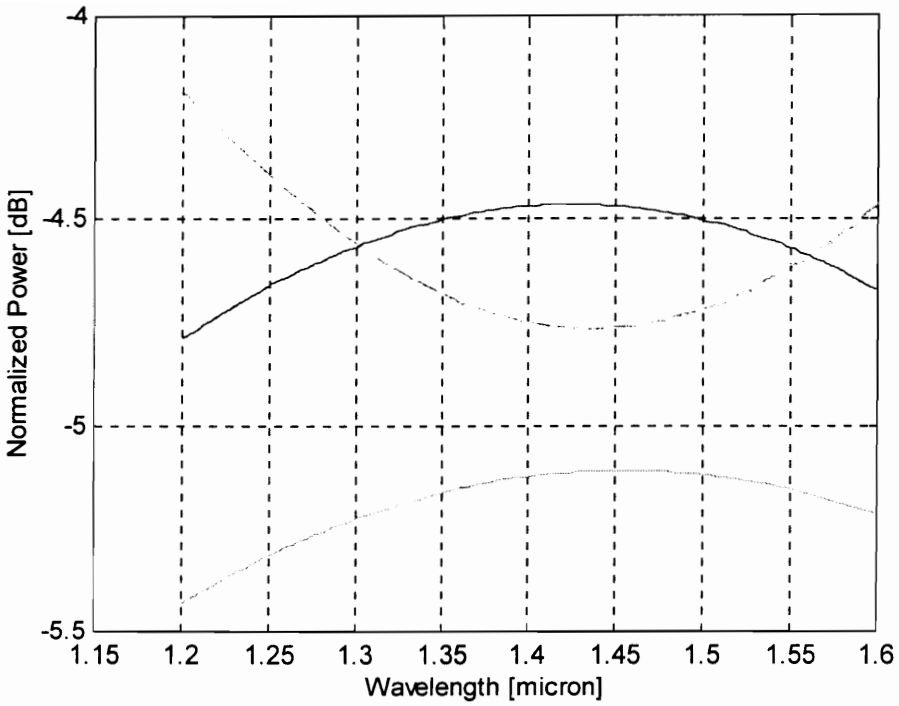

Figure 5-9. The output wavelength spectra of the 1x3 WFC.

Counting top-to-bottom, they corresponds to P_1, P_2, and P_3, respectively. The output spectra are reasonably flat between 1.2 μm and 1.6 μm, and the uniformity is within 1.0 dB.

Experimentally, we used three single-mode (λ = 1300 nm) 2x2 fused couplers, and two of them have the power splitting ratios of 50/50 and one coupler has the power splitting ratio of 62/38. The coupler arrangement is shown in Figure 5-6. A white

light source was used as the input P_0, and the three output spectra (P_1, P_2, and P_3) are recorded and given in Figure 5-10.

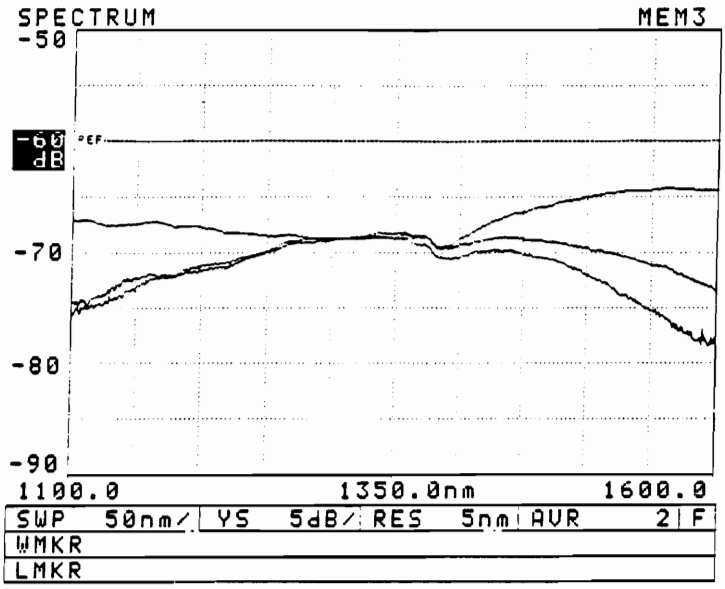

Figure 5-10. Output spectra of the 1x3 WFC.

Counting from the right-hand-side and top-down, the curves corresponds to P_1, P_3, and P_2, respectively. Notice that all output spectra are flat between 1250 nm and 1400 nm; the uniformity is within 1 dB. The fact that the P_3 spectrum is above the P_2 spectrum might be due to the 62% power coupling in P_3 instead of 60% as in the simulation. We also realize that the phase difference condition Equation (5.7) has been met in order to stabilize the output power, because the white light was an incoherent source and there was no phase relation between the two input fields of the

last coupler. If a laser diode is used as the light source, an extra fiber loop of length much greater than its coherence length may be used as a phase delay fiber.

5.4 Coherence consideration

Two-beam interference

The essential condition to achieve the wavelength flatness by connecting regular 2x2 couplers is expressed in Equation (5.7). Let us focus on how this condition should be satisfied in practice. Figure 5-11 shows a simplified Mach-Zehnder interferometer structure.

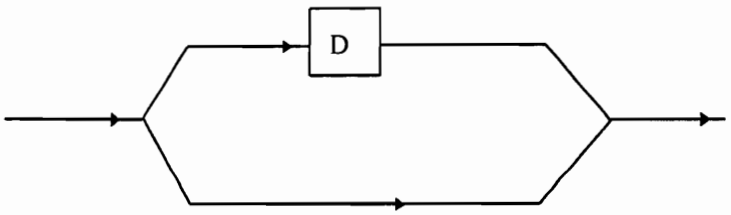

Figure 5-11. A basic Mach-Zehnder interferometer.

Here the incoming light signal is split into two parts, and they are combined into one final output. The optical phase difference between these two paths is represented by D. Normally, if a coherent light source is used, the output signal would be the result of the interference between the two optical signals. If this happens, the output signal

power level would be unstable because any disturbance on either of the arms would modulate the output signal. The exception is, as suggested in Equation (5.7), when

(1) $D = \frac{\pi}{2}(2n+1)$, where n is an integer, or

(2) D is very large compared to the light source coherence length.

Although Condition (1) might be difficult to obtain using two distinct 2x2 couplers, in practice it may be easier to achieve by fabricating two couplers together with short-length arms. Our focus is to satisfy Condition (2). The goal is to create a large phase difference in order to frustrate the phase correlation between the two signals such that the output field could be treated as the result of adding two independent sources together.

Fringe visibility

In general, the total intensity of two ideal monochromatic waves can be expressed by

$$I = I_1 + I_2 + 2\sqrt{I_1 I_2}\cos(D), \qquad (5.17)$$

where I_1 and I_2 are the intensity of the two beams, respectively. D is the phase difference between the two fields. The *fringe visibility* (FV) is defined as

$$FV = \frac{I_{max} - I_{min}}{I_{max} + I_{min}}, \tag{5.18}$$

here I_{max} and I_{min} are the maximum and minimum of the total intensity. From Equation (5.1), we obtain

$$I_{max} = I_1 + I_2 + 2\sqrt{I_1 I_2}\ , \text{ when D} = 0, 2\pi, 4\pi, \ldots , \tag{5.19}$$

and

$$I_{min} = I_1 + I_2 - 2\sqrt{I_1 I_2}\ , \text{ when D} = \pi, 3\pi, \ldots . \tag{5.20}$$

Substituting Equations (5.19) and (5.20) into Equation (5.18), the FV can be obtained

$$FV = \frac{2\sqrt{I_1 I_2}}{I_1 + I_2} \leq 1. \tag{5.21}$$

Fringe visibility is a measure of the degree of two-beam correlation. It has the maximum value of one (complete correlation) and the minimum value of zero (no correlation). Anything in between corresponds to partial correlation.

In reality, the finite spectrum width of the light source must be considered in this FV calculation, and normally the two beams have the same power level. Instead of using Equation (5.17), we may write the total intensity as [31]

$$I = 2\int j(x)\left\{1+\cos\left[(\overline{k_0}+x)D\right]\right\}dx, \tag{5.22}$$

where j(x) is the source spectrum shown in Figure 5-12.

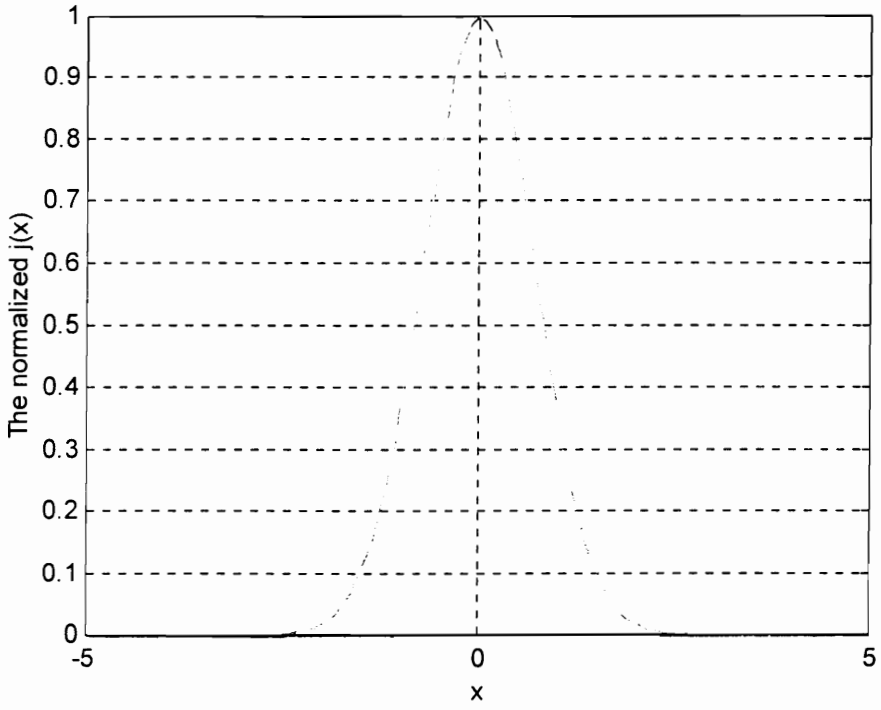

Figure 5-12. The light source spectrum.

The parameters k_0 and x are given by

$$k_0 = \frac{2\pi}{\lambda_0}, \tag{5.23}$$

where λ_0 is the wavelength, and

$$x = k_0 - \bar{k}_0, \tag{5.24}$$

respectively. Here $\bar{k}_0$ is the central wave propagation constant. Using Equation (5.22) and then substituting it into Equation (5.18), we obtain the *fringe visibility* expression [31],

$$FV = \frac{\left|\int j(x)\cos(xD)dx\right|}{\int j(x)dx}. \tag{5.25}$$

Evaluating Equation (5.25), we obtain the normalized fringe visibility as

$$FV = e^{-\left(\frac{D}{2\alpha}\right)^2}, \tag{5.26}$$

where

$$\propto = \frac{1}{\frac{\pi}{\bar{\lambda}^2}|\Delta\lambda|}, \tag{5.27}$$

here $\bar{\lambda}$ is the central wavelength and $\Delta\lambda$ is the wavelength spectrum width of the light source. Therefore, for a given light source, the two-beam interference fringe visibility could be determined using Equations (5.26) and (5.27). Figures 5-13 and 5-14 show fringe visibility curves.

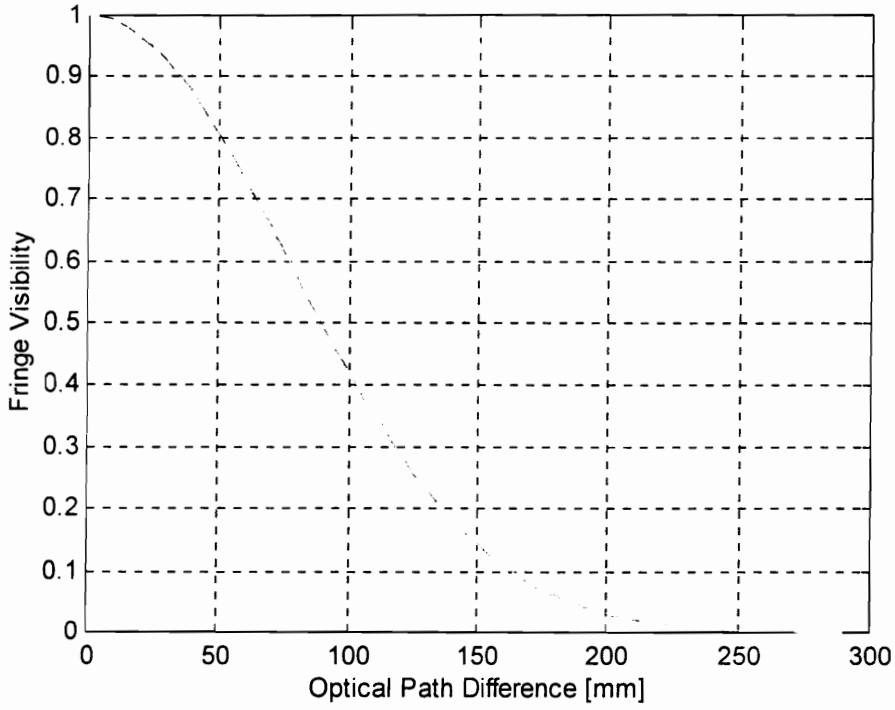

Figure 5-13. The central wavelength is 1.3 μm and $\Delta\lambda$=0.01 nm.

This is the fringe visibility profile for a typical fiber optic communication laser diode. For a laser diode with wider wavelength spectrum (lower in cost), the fringe visibility could be calculated and plotted as shown in Figure 5-14.

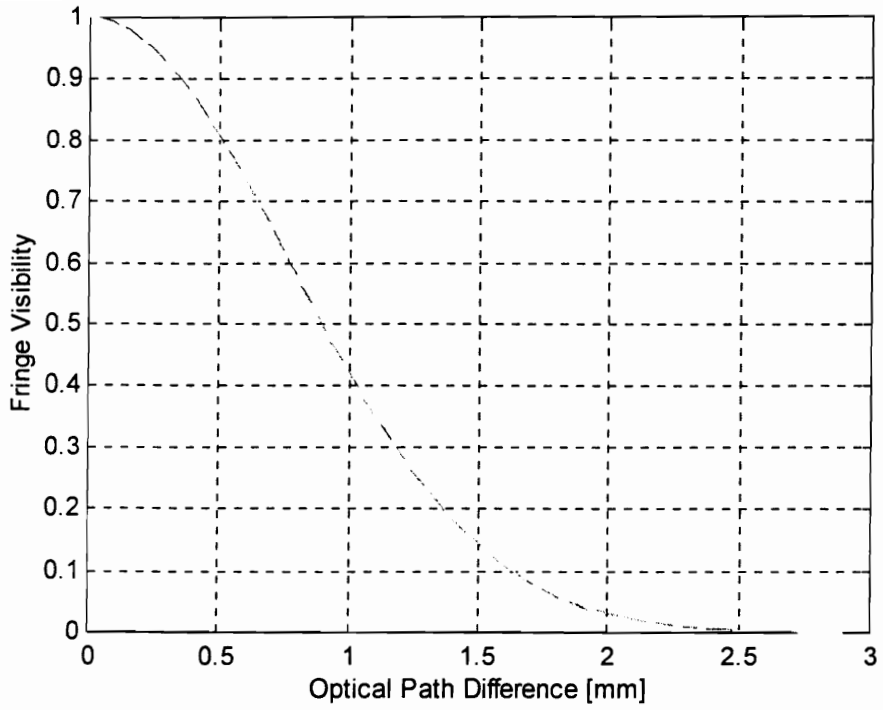

Figure 5-14. The central wavelength is 1.3 μm and $\Delta\lambda$=1 nm.

Studying Figures (5-13) and (5-14), the fringe visibility for a Mach-Zehnder interferometer can be decreased to practically zero if the optical path difference of the two arms is larger than 300 mm for a typical communication laser diode. In the case of two cascaded 2x2 single-mode 3 dB couplers shown in Figure 5-2, the introduction of an extra fiber length in one arm could eliminate the interference effect at the last stage coupler output ports. Hence, the phase condition Equation (5.7) (the second part) is satisfied.

6. Wavelength-flattened tree and star couplers using regular couplers

In recent years, the fabrication of large tree (1xN) wavelength-flattened couplers have been developed by Mortimore based on the conventional method (see Chapter 4) [32,33]. However, it involves extremely delicate fiber arrangement processes, and it would take much longer time to fabricate, say a 1x4 WFC, than a 2x2 WFC. For couplers larger than 1x16, the fabrication process is even more difficult if not possible. In addition, the direct fabrication of *star* wavelength-flattened couplers such as 4x4's has not been developed. Because star couplers require operation in both directions, i.e. from the right to the left and from the left to the right, it may be an impossible task to fabricate WFC stars using the conventional method.

The concept of fabricating wavelength-flattened couplers by cascading regular single-mode fiber couplers can be extended to construct more complex WFCs such as tree and star couplers without much difficulty and complication. In this chapter, the theoretical formulation in constructing $1x2^N$ and 4x4 WFCs is discussed. Computer simulations are performed based on the symmetrical property of 3 dB couplers and the analysis presented in Chapter 5. The results of corresponding experimental work is also presented.

6.1 $1x2^N$ WFCs

The essential property of an ideal 2x2 3 dB or 50/50 single-mode coupler is that it splits an input signal such that both output wavelength profiles are complimentary to one another, and at the central wavelength both output ports give 50% power distribution. It is natural that 3 dB couplers may be added as wavelength spectral compensators to regular $1x2^N$ tree couplers to achieve the wavelength-flattening effect.

1x4 WFC

Figure 6-1 shows a 1x4 WFC using four regular single-mode 2x2 fiber couplers. The objective is to make the output power insensitive to wavelength around the central wavelength of the light source.

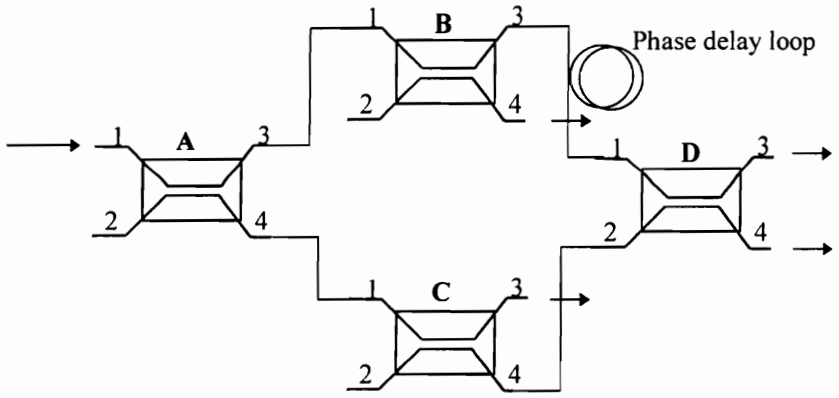

Figure 6-1. 1x4 WFC layout.

As the case in Chapter 5, it is important to label each port of a 2x2 coupler. The convention is that port #1 and #3 belong to the same fiber before the coupler is made.

Port #2 and #4 associate with the other fiber. If light is launched into port #1, then the fiber associated with ports #1 and #3 is the primary fiber, and the other fiber is the secondary fiber. Four couplers A, B, C, and D are all 3 dB couplers at the central wavelength (say 1.3 μm). For the convenience of discussion, any one port of a coupler could be identified with a letter (A, B, C, or D) followed by a number (1, 2, 3, or 4). For example, the input port of the coupler in Figure 6-1 is A1.

Assuming a broadband light with a normalized amplitude is launched at A1, the wavelength spectra could be described using Equation (5.6). Hence, any other output ports could be determined.

$$\begin{pmatrix} P_{A3} \\ P_{A4} \end{pmatrix} = \begin{pmatrix} \cos^2(\theta) & \sin^2(\theta) \\ \sin^2(\theta) & \cos^2(\theta) \end{pmatrix} \begin{pmatrix} 1 \\ 0 \end{pmatrix}. \tag{6.1}$$

$$\begin{pmatrix} P_{B3} \\ P_{B4} \end{pmatrix} = \begin{pmatrix} \cos^2(\theta) & \sin^2(\theta) \\ \sin^2(\theta) & \cos^2(\theta) \end{pmatrix} \begin{pmatrix} P_{A3} \\ 0 \end{pmatrix}. \tag{6.2}$$

$$\begin{pmatrix} P_{C3} \\ P_{C4} \end{pmatrix} = \begin{pmatrix} \cos^2(\theta) & \sin^2(\theta) \\ \sin^2(\theta) & \cos^2(\theta) \end{pmatrix} \begin{pmatrix} P_{A4} \\ 0 \end{pmatrix}. \tag{6.3}$$

$$\begin{pmatrix} P_{D3} \\ P_{D4} \end{pmatrix} = \begin{pmatrix} \cos^2(\theta) & \sin^2(\theta) \\ \sin^2(\theta) & \cos^2(\theta) \end{pmatrix} \begin{pmatrix} P_{B3} \\ P_{C4} \end{pmatrix}. \tag{6.4}$$

Substituting Equation (6.1) into Equations (6.2) and (6.3), we obtain the outputs of the coupler B and C. Using these results, the output of D can be determined. The θ parameter can be evaluated employing Equations (5.2) and (5.10). Figures (6-2), (6-3), and (6-4) shows the output spectra at each stage.

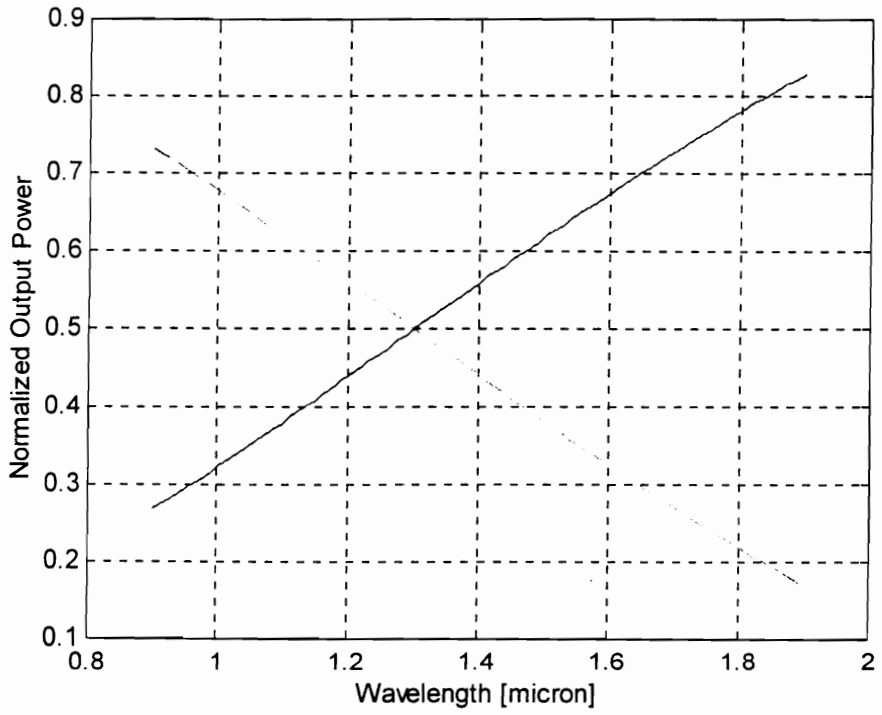

Figure 6-2. Output spectra of Coupler A. The top curve at the left is P_{A3} and the bottom curve is P_{A4}.

The split power percentage at 1.3 μm is 50% for both output ports, and the power percentage at any other wavelength is not 50%. These spectra are typical for a regular single-mode fiber coupler.

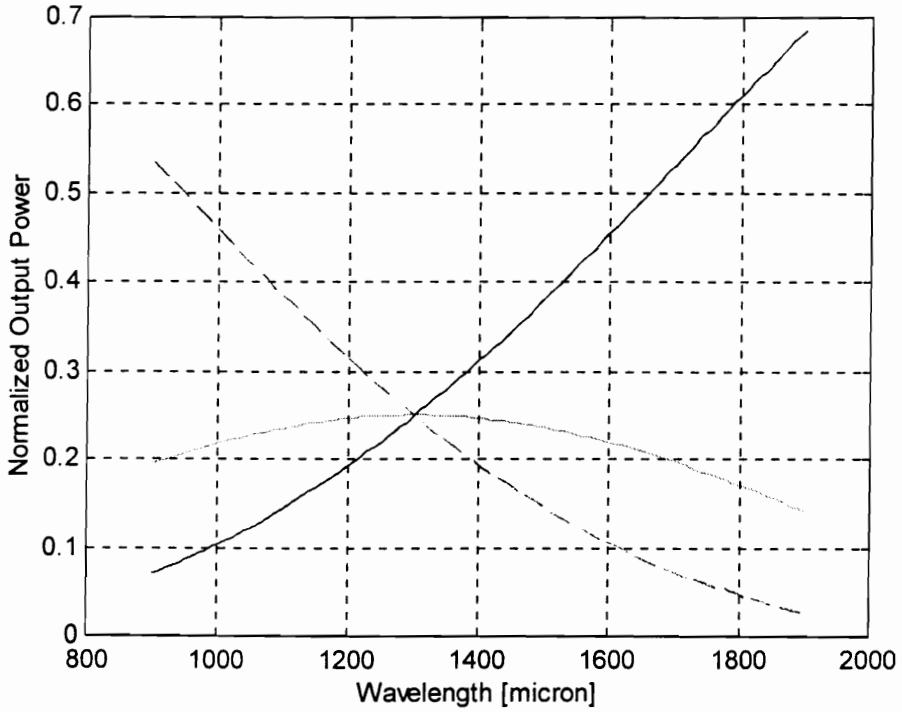

Figure 6-3. Output spectra of Couplers B and C. The top curve at the left is P_{B3} and the bottom curve at the left is P_{C4}. The middle curves are both P_{B4} and P_{C3}.

Let us focus on the output spectra of Coupler B. P_{B3}, the top curve on the left, has an even sharper profile than Coupler A. On the other hand, P_{B4} is already flat at about the 25% level around the central wavelength (1.3μm). Similarly for Coupler C, P_{C3} is flat but P_{C4} becomes steeper. For ideal 2x2 single-mode couplers, the spectra of P_{B4} and P_{C3}

coincide with each other. Therefore, the spectra of P_{B4} and P_{C3} no longer need to be compensated for, and would be used directly as two outputs. P_{B3} and P_{C4} are fed into another ideal 2x2 50/50 single-mode coupler, and the output spectra are shown in Figure 6-4.

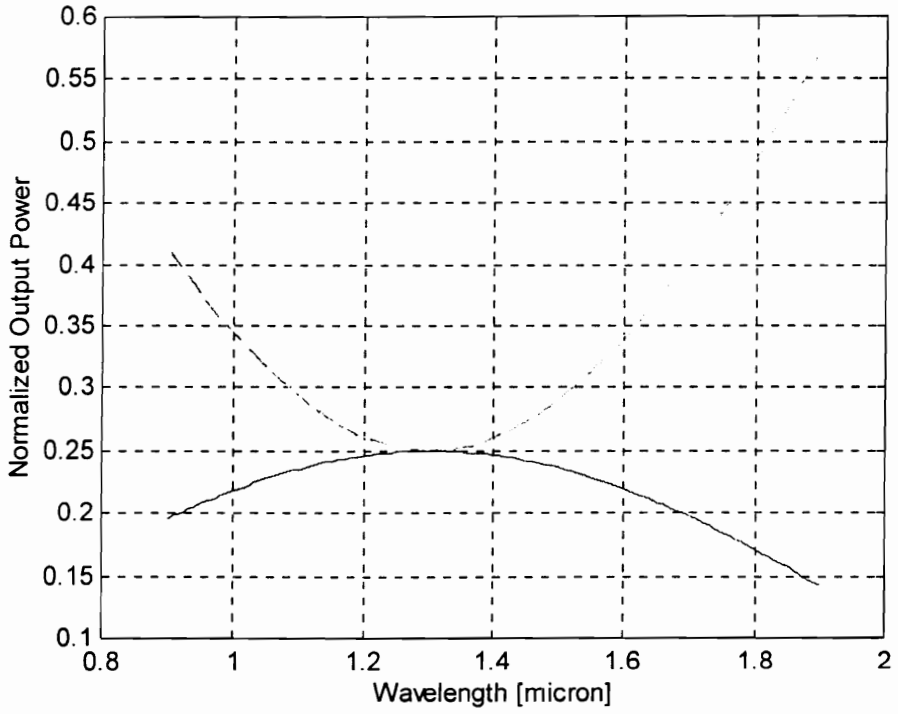

Figure 6-4. The output spectra of Coupler D. The top and bottom curves represent P_{D3} and P_{D4}, respectively.

It is evident that the output wavelength spectral variations are effectively compensated for. The final output ports are P_{B4}, P_{D3}, P_{D4}, and P_{C3}, respectively.

Experimentally, four single-mode 2x2 3 dB couplers were used to construct a 1x4 WFC shown in Figure 6-1. A 5-meter long fiber phase delay loop was inserted to stabilize the output. To observe the spectra, white light was employed and the result is shown in Figure 6-5.

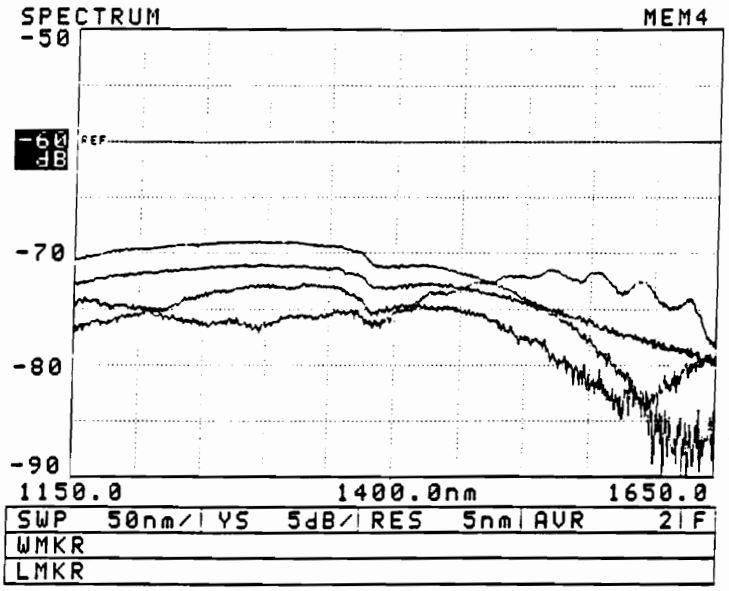

Figure 6-5. The output spectra of the 1x4 WFC (experimental data).

1x8 WFC

Larger tree wavelength-flattened couplers can be implemented using regular 2x2 single-mode couplers. Figure 6-6 illustrates a 1x8 WFC structure.

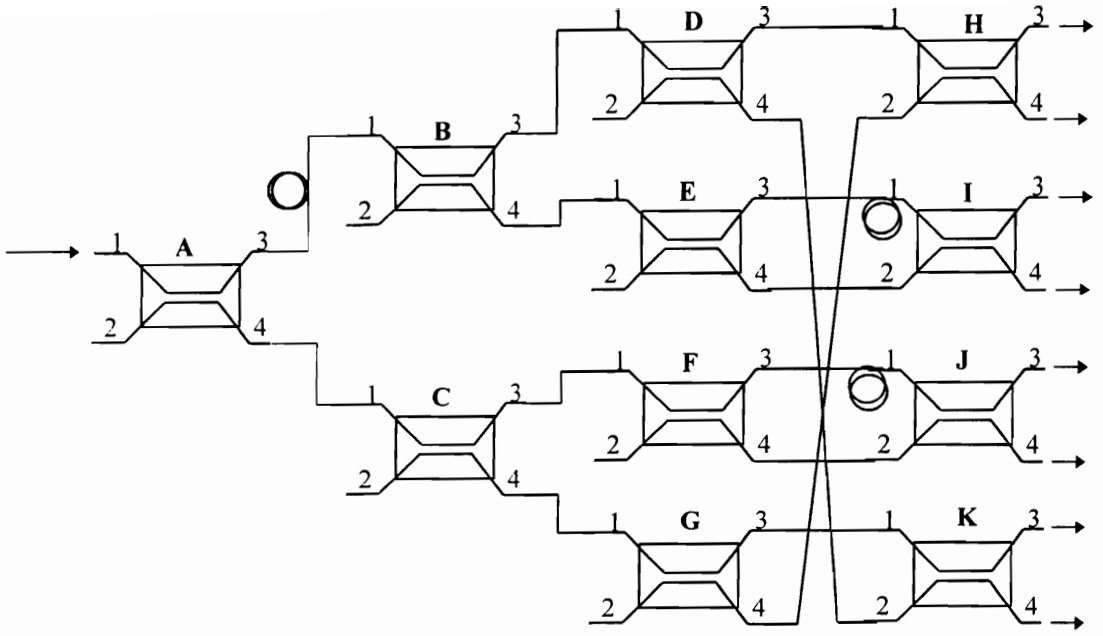

Figure 6-6. The structure of 1x8 WFC using regular 2x2 single-mode couplers.

Notice that the total number of regular couplers used is 11. Couplers A-G represent the geometry of the regular 1x8 coupler. The four couplers H-K serve as the compensation couplers to flatten the output spectra. Similar to the study of the 1x4 WFC, we would like to monitor the spectral variation at different stages. The emphasis is the output spectra of Couplers D-G and H-K. Following the same formalism as Equations (6.1)-(6.4), we obtain Figures 6-7 and 6-8.

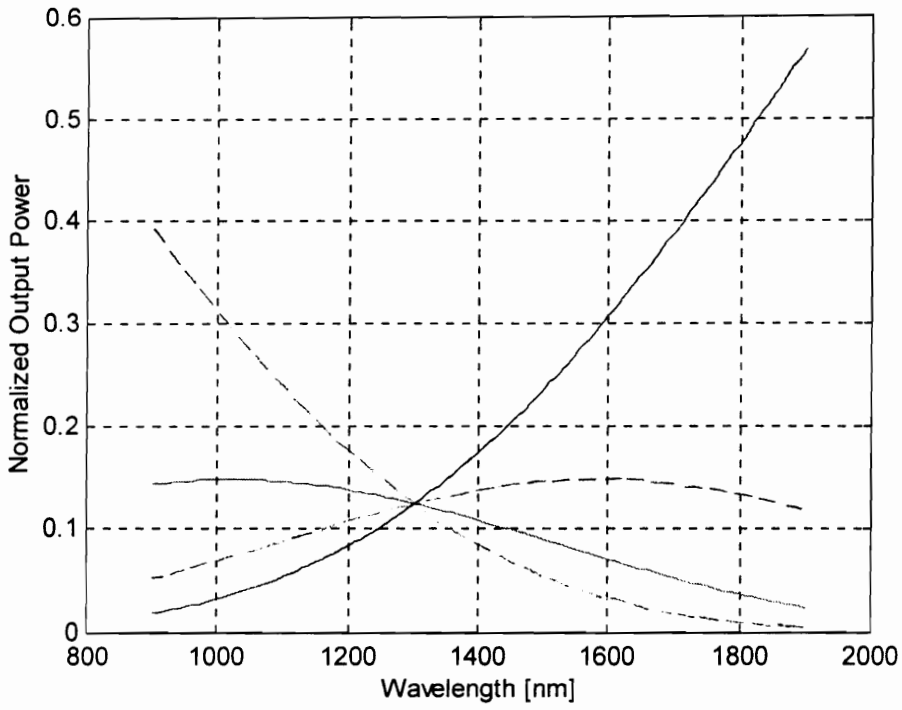

Figure 6-7. The output spectra of Couplers D-G.

Counting from the left hand-side, the top curve corresponds to D3, the second curve corresponds to D4, E3, and F3, the third curve corresponds to G3, E4, and F4, and finally, the bottom curve corresponds to G4. Although the spectra of all output ports intersect at 1300 nm with a normalized power of 12.5% (1/8 of the input power), they vary significantly for wavelength apart from 1300 nm.

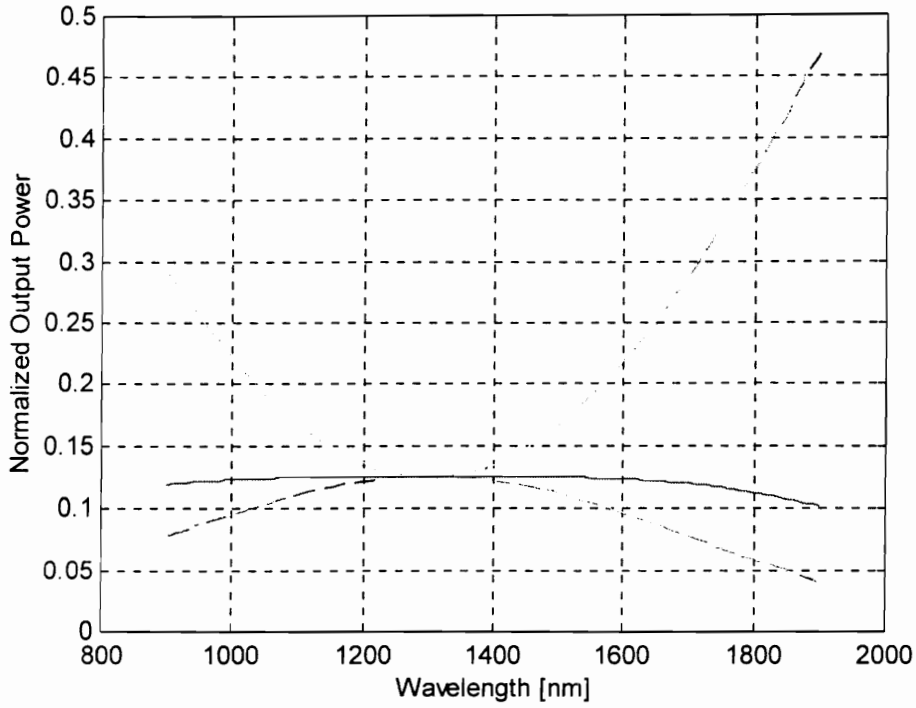

Figure 6-8. The output spectra of Couplers H-K.

After the compensation, the flatness of the output has been improved dramatically. The top curve corresponds to H3, the middle curve corresponds to H4, I3, J3, and K4, and the bottom curve corresponds to I4, J4, and K3. Noticeably, the spectra around 1300 nm are flat and have the output value of 12.5%. The operation of this 1x8 coupler would be insensitive to wavelength variation around 1300 nm.

6.2 4x4 WFC star

To construct WFC stars using regular couplers is much more difficult than to construct tree couplers due to the fact that star couplers require symmetric (bi-directional) performance, i.e. any port could be considered as an input port as well as output port, and the output port signals should have the same value. After much consideration, a 4x4 WFC has been developed. The structure is shown in Figure 6-9.

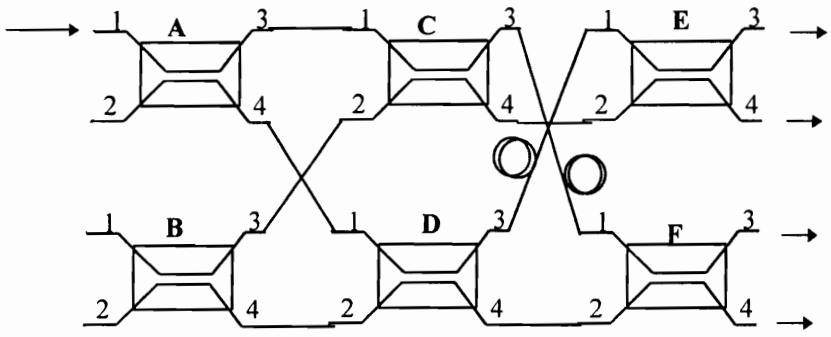

Figure 6-9. The structure of the 4x4 WFC star.

Couplers A-F are all 2x2 single-mode 3 dB (50/50) regular couplers. To see whether the combination is indeed a star, we should launch light from each port at both the left-side and the right-side, respectively. Because of the symmetric nature, we choose several representative cases listed below:

Case I, the input port is A1, the output ports are E3, E4, F3, and F4.

Case II, the input port is A2, the output ports are E3, E4, F3, and F4.

Case III, the input port is E3, the output ports are A1, A2, B1, and B2.

Case IV, the input port is E4, the output ports are A1, A2, B1, and B2.

Based on the theoretical analysis outlined in Chapter 5, computer simulation of each case is performed, and the spectra are shown in Figure 6-10.

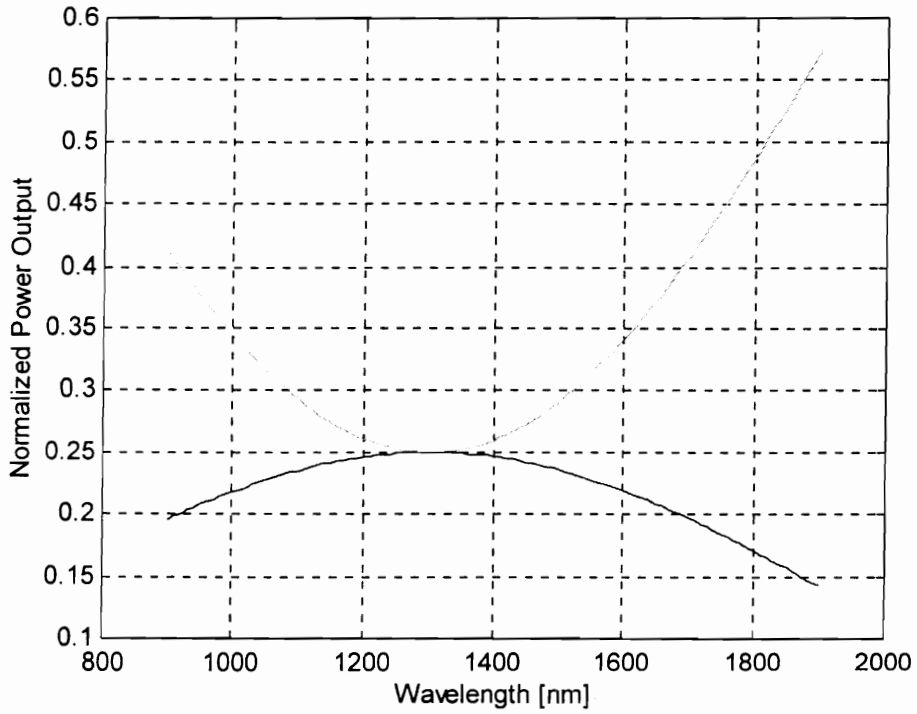

Figure 6-10. The output spectra of the 4x4 WFC.

For Case I, the top curve represents F3, and the bottom curve corresponds to E3, E4, and F4. For Case II, the top curve represents E3, and the bottom curve corresponds to E4, F3, and F4. For Case III, the top curve represents A2, and the bottom curve corresponds to A1, B1, and B2. For Case IV, the top curve represents B1, and the bottom curve

corresponds to A1, A2, and B2. Notice that these spectra are flat around 1300 nm with 1/4 (25%) of the input power.

7. Conclusions

The function of fiber couplers is to redistribute optical signals in fiber optic communication systems. Their applications include tapping off main-bus-line signals for the purpose of monitoring, power dividing/combining, and multiplexing signals. Like fiber optic connectors, fiber couplers are essential passive components in any fiber optic system. Based on specific operations, most common fiber couplers include regular (standard) 2x2 couplers, wavelength-division multiplexers (WDMs), and wavelength-flattened couplers (WFCs). Depending upon the complexity in construction, fiber couplers could also be grouped into one of the following classifications: 2x2 couplers, tree couplers (1xN), and star couplers (NxM). Although there are many different ways to manufacture fiber couplers of various types, the fused biconical tapered (FBT) method remains the most popular.

Wavelength-flattened couplers (WFCs) are fiber couplers whose performance are insensitive to wavelength. In a regular coupler operation, a WFC produces a stabilized output power distribution. In wavelength-division multiplexing applications, WFCs are essential devices to divide/combine many signals evenly. The core content of this dissertation concerns wavelength compensation techniques in fused biconical taper (FBT) couplers, which could be employed to effectively fabricate wavelength-flattened couplers.

Multimode fiber couplers are made of multimode fibers, which can support up to thousands of guided modes. Because there are a large number of modes involved, it is difficult to analyze multimode fiber coupler operation. In this dissertation, using the frustrated total internal reflection (FTIR) principle, the following two areas are studied : (1) multimode fiber power coupling and (2) the external index refraction effect on multimode fiber couplers. A novel two-dimensional ray optics model has been developed based on the establishment of a static ray interaction pattern in coupler taper region. This model successfully describes both symmetric and asymmetric multimode fiber coupler operations. The dependence of external index of refraction on multimode couplers is investigated both theoretically and experimentally. It has been found that coupler power loss is strongly dependent on the index of refraction surrounding the taper region only when the fiber taper is stretched to a certain length. This loss mechanism could be explained by analyzing both the fiber cladding and core modes. The experimental data support the ray optics model. The wavelength dependence of multimode fiber coupler operation has been studied in effect by varying the number of modes. It has been found that since there are so many modes, on the average, multimode fiber coupler performance is wavelength independent (insensitive).

Single-mode fiber couplers, particularly wavelength-flattened couplers (WFCs), are studied in great detail. First, we use the coupled mode equations to model a WFC made by employing the conventional method. The wavelength-flattened effect could be predicted by suitably modeling the fiber core diameter and fiber-to-fiber separation in the

taper region, and their contribution to the power transfer factor F. Secondly, a new and more generalized method of fabricating wavelength-flattened couplers (WFCs) has been developed by connecting many regular 2x2 couplers. The basic principle is the symmetric properties of a 2x2 coupler, i.e. its output wavelength spectra are complementary to each other such that the sum of the two always equals the input. WFCs such as 2x2, 1x3, 1x4, 1x8 and 4x4 can be fabricated using this method. In order to stabilize coupler outputs, additional phase delay fibers are used to eliminate the interference among any two paths at the output. Experimental results agree with the theoretical modeling. One concern about these WFCs constructed by connecting many couplers is the extra phase delay fiber which may cause signal distortion. Even though the delay fiber is short (in the order of one meter), depending upon source coherence length, it may create a propagation delay in high speed systems. Optimum design should be done in practical implementations.

Looking ahead, there might be some challenges that face the fused biconical taper (FBT) coupler technology in the future. One of the major challenges may be the realization of high density and high isolation wavelength-division multiplexers (WDMs). This is due to the fact that the WDM operation depends on the field interference in the taper section, and for high density WDMs, FBT coupler fabrication requires much longer taper length. This often increases the degree of complication and difficulty in manufacturing process. In high density WDM, good channel isolation is much harder to obtain, although the

direct implementation of fiber in-line gratings at the output ports could help to a certain extent.

Another major challenge for FBT technology is in the area of mass-production. As more and more fiber systems are deployed in local area networks in the future, a much larger quantity of fiber couplers would be consumed. The cost of fiber couplers must come down significantly like the trend of fiber connector prices. Therefore, mass-production of fiber couplers is an important issue. Already, fiber couplers based on integrated optics have been fabricated in a mass-production fashion, and there have been products competing with FBT couplers in the market, especially in the area of large and complicated fiber couplers. The bottleneck for integrated optics technology may be its compatibility with fibers, i.e. extra waveguide-to-fiber splices are required for the final packaging. On another front, manufacturers of FBT technology have striven to make their fabrication process automatic or semi-automatic. Every year new improvements are made to make the FBT technology more automatic and to require less human intervention. To date, the FBT technology still gives better quality/price ratio than the other technologies in most applications. The future of the FBT technology relies partially on which direction the market (applications) will move. Considering the technology advancement in other areas including electronics, microprocessors (microcontrollers), and integrated optics, it is uncertain at this point which fiber coupler fabrication technology will dominate in the future market. Perhaps, different technologies will coexist for a long time.

References

1. Gerd Keiser, **Optical Fiber Communications**, 2nd edition, Chap. 1, 10-12, 1991, McGraw-Hill.

2. Gerd Keiser, **Optical Fiber Communications**, 2nd edition, Chap. 3, 104-106, 1991, McGraw-Hill.

3. Govind P. Agrawal, **Fiber-Optic Communication Systems**, Chap.2, 42-46, 1992, John Wiley & Sons, Inc.

4. Chinlon Lin, "High-capacity fiber-optic networks to transpot diverse multimedia services," LIGHTLWAVE, Special report on technology forecast, 28-34, December 1995, Penn Well.

5. K. Nosu et al., "Slab waveguide star coupler for multimode optical fibres," *Electronics Letters*, vol. 16, no. 15, 608-609, 1980.

6. Kent A. Murphy, Michael F. Gunther, and Richard O. Claus, U.S. patents no. 5,339,374 and 5,216,731 in "Fused Biconical Taper Fiber Optic Coupler Station and Fabrication Techniques."

7. Michel Digonnet and H. J. Shaw, "Wavelength multiplexing in single-mode fiber couplers," *Applied Optics*, vol. 22, no. 3, 484-491, 1983.

8. K. Kobayashi et al. ,"Micro-optic devices for branching, coupling, multiplexing and demultiplexing," *Technical Digest of the First Integrated Optics and Optical Fiber Communication Conference*, Toyko, 367-370, 1980.

9. W. J. Tomlinson, "Wavelength multiplexing in multimode optical fibers," *Applied Optics*, vol. 16, no. 8, 2180-2194, 1977.

10. Bahaa E. A. Saleh and Malvin C. Teich, **Fundamentals of Photonics**, Chap. 7, 1991, John Wiley & Sons, Inc.

11. Frederick C. Allard, **Fiber Optics Handbook for Engineers and Scientists**, Chap. 3, 376-378, 1990, McGraw-Hill.

12. David B. Mortimore, "Wavelength-flattened fused couplers," *Electronics Letters*, vol. 12, no. 17, 742-743, August, 1985.

13. M. Kawachi, B. S. Kawasaki, K. O. Hill, "Fabrication of single-polarisation single-mode-fibre couplers," *Electronics Letters*, vol. 18, no. 22, October, 1982.

14. Allan W. Synder and John D. Love, **Optical Waveguide Theory**, Chap. 36, 1983, Chapman and Hall.

15. Allan W. Synder and John D. Love, **Optical Waveguide Theory**, Chap. 11, 1983, Chapman and Hall.

16. A. W. Synder and P. McIntyre, "Crosstalk between light pipes," *J. Opt. Soc. Am.*, vol. 66, no. 9, 877-882, 1976.

17. Yi-Fan Li and John W. Y. Lit, " Coupling efficiency of a multimode biconical taper coupler," J. Opt. Soc. Am. A, vol. 2, no. 8, 1301-1306, August, 1985.

18. George Z. Wang, Kent A. Murphy, and Richard O. Claus, "Effect of external index of refraction on multimode fiber couplers," *Applied Optics*, to be published early 1996.

19. L. M. Brekhovskikh, **Waves In Layered Media**, t2nd edition, Chap. 3 and 4, 1980, Academic Press.

20. R. Griffin, J.D. Love, P.R.A. Lyons, D. A. Thorncraft, and S. C. Rashleigh, "Asymmetric multimode couplers," *J. Lightwave Technology*, vol. 9, no. 11, 508-517, November, 1991.

21. D. Gloge, "Weakly guiding fibers," *Applied Optics*, vol. 10, no. 10, 2252-2258, October, 1971.

22. D. Marcuse, **Theory of Dielectric Optical Waveguides**, Chap. 1 and 2, 2nd edition, Academic Press, 1991.

23. Katsunari Okamoto, "Theoretical investigation of light coupling phenomena in wavelength-flattened couplers," *IEEE J. Lightwave Technology*, vol. 8, no. 5, 678-683, May, 1990.

24. Allan W. Synder and John D. Love, **Optical Waveguide Theory**, Chap. 29, 1983, Chapman and Hall.

25. Allan W. Synder and John D. Love, **Optical Waveguide Theory**, Chap. 18, 1983, Chapman and Hall.

26. Allan W. Synder and John D. Love, **Optical Waveguide Theory**, Chap. 14, 1983, Chapman and Hall.

27. J. Bures, S. Lacroix, and J. Lapierre, "Analyse d'un coupleur bidirectionel a fibres optiques monomodes fusionnees," *Applied Optics*, 22, 1918-1921 (1983).

28. Suzanne Lacroix, Francois Gonthier, and Jacques Bures, "Modeling of symmetric 2x2 fused-fiber couplers," *Applied Optics*, vol. 33, no. 36, 8361-8369, December, 1994.

29. F. P. Payne, C. D. Hussey, and M. S. Yataki, "Modeling fused single-mode fibre couplers," *Electronics Letters*, vol. 21, no. 11, 461-462, May, 1985.

30. Richard G. Friest, "Analysis of fiber interferometer utilizing 3x3 fiber coupler," *IEEE J. of Quantum Electronics*, vol. QE-18, no. 10, 1601-1603, October, 1982.

31. Max Born and Emil Wolf, **Principles of Optics**, *Electromagnetic theory of propagation interference and diffraction of light*, 6th Edition, Chap. VII, Pergamon Press (reprint of 1993).

32. David B. Mortimore and John W. Arkwright, "Theory and fabrication of wavelength flattened 1xN single-mode couplers," *Applied Optics*, vol. 29, no. 12, 1814-1818, April, 1990.

33. D. B. Mortimore, J. W. Arkwright, and R. M. Adnams, "Monolithic wavelength-flattened 1x4 singlemode fused fibre coupler," *Electronics Letters*, vol. 27, no. 24, 2252-2253, November, 1991.

Appendix A

```
function[taper_length,fiber1,fiber2]=crstlk(theta1,theta2,theta_num,length1,length2,l_num)
%This program calculates the power in both primary and secondary fibers
%accumulating angles from theta1 to theta2.
%Sub-functions used: layer_1.m and sing_1.m(t,theta,taper_length).
%george wang
%1/25/95
%
%input parameters ----------------------------------------------------
%theta1              -       starting angle (the critical)in degree
%theta2              -       ending angle (90 degree)
%theta_num    -      number of rays within the two angles
%taper_length  -     coupler taper length in micron

%setup the necessary variables ----------------------------------------
n1=1.458;            %core index
n2=1.429;            %cladding index (NA=0.29)
a0= 100;             %initial one fiber core diameter (mircon)
d0= 140;             %initial one fiber cladding diameter (micron)
w= 10000;            %fusion length (micron)
wavelength= 0.633;   %micron
theta_step=(theta2-theta1)/theta_num;          %incremental step in angle
theta=theta1:theta_step:theta2;                %angle vector

%fiber dimension changes due to tapering
length_step=(length2-length1)/l_num;          %step for taper length
taper_length=length1:length_step:length2;     %taper length vector
p_ones=ones(1,l_num+1);                              %ones for vector div
d= d0*w*p_ones./taper_length; %final one fiber cladding diam vec
a= a0*w*p_ones./taper_length; %final one fiber core diam vec
thick= (d0-a0)*w*p_ones./taper_length; %the middle layer thickness

%the loops ------------------------------------------------------------
for k=1:l_num+1
for i=1:theta_num+1
        t(k)=layer_1(thick(k),theta(i),n1,n2,wavelength);        %transmission coeff
        [prim(i),secn(i)]=sing_1(t(k),theta(i),taper_length(k),a(k));      %get the power
end
fiber1(k)=sum(prim)/size(prim,2);              %the power in the primary fiber
fiber2(k)=sum(secn)/size(secn,2);              %the power in the secondary fiber
end

plot(taper_length,fiber1,taper_length,fiber2); grid;

%the end of the program -----------------------------------------------
```

```
function t=la
yer_1(d,theta1,n1,n2,wavelength)
% This program calculates the transmission and reflection coeffs when
% a plane wave passes through a three-layer waveguide structure undergoing
% TIR and FTIR. To simplify the mathematics, a n1-n2-n1 structure is assumed
% The model is based on WAVES IN LAYERED MEDIA by Brekhovskikh.
%Programmer:  George Wang
%data:          1/20/95
%name:                  layer_ft.m
%
%input/output parameters
%d      -       thickness of the middle layer in micron
%theta1         -       the incident angle in degree, must be larger than the critical angle
%
%definition of the parameters used ----------------------------------------------
%wavelength = 0.633;            %wavelength in micron
%n2=1.429;                      %middle layer
%n1=1.458;                      %top and bottom layers
theta1=theta1*pi/180;           %convert theta3 from degree to radian
cos1=cos(theta1);               %cosine of the incident angle
cos2=sqrt(n1*n1/n2/n2*sin(theta1)*sin(theta1)-1)*i;%pure imag for TIR
z1=1/cos1/n1;           % impedance in top and bottom layers (real)
z2=1/cos2/n2;           % impedance in the middle layer (imaginary)
k2z=2*pi/wavelength*cos2;       %z comp prop vector
%reflection and transmission coeffs ---------------------------------------------
r_pd=(z2*z2-z1*z1)/(z1*z1+z2*z2+2*i*z1*z2*cot(k2z*d));      %perpendicular
z1=cos1/n1;             %imped for parallel in the top and bott layer
z2=cos2/n2;             %imped for parallel in the mid layer
r_pl=(z2*z2-z1*z1)/(z1*z1+z2*z2+2*i*z1*z2*cot(k2z*d));      %parallel
r=0.5*(r_pd*conj(r_pd) + r_pl*conj(r_pl));      %overall reflect coeff
t=1-r;                  %transmission coeff
%disp(r); disp(t);
%end of the program ------------------------------------------------------------


function [upper,lower]=sing_1(t,theta,taper_length,a)
%This program calculates the upper power and lower power in 2-d waveguide
%simulating a multimode coupler's coupling activity, symmetrical case
%George Wang
%1/15/95
%
%input parameters: --------------------------------------------------
%t              -       transmission coeff (layer thickness)
%theta          -       angle respect to the fiber axis
%taper_length   -       coupler taper length in micron

%set up the waveguide -----------------------------------------------
%a=25;                  %fiber diameter at taper waist (micron)
```

```
theta= theta*pi/180;      %propagation angle respect to the fiber axis (rad)
l=taper_length;           %coupler taper length (micron)
m=floor( l/2/a/tan(theta));       %number of reflection in fiber pipe
%disp(m);                 %print the number reflections

%body of action ------------------------------------------------------
r=1-t;                    %reflection coefficient
upper0=r;                 %the first upper (the primary fiber)
lower0=t;                 %the first lower (the secondary fiber)
%loop of reflection along the fiber
for i=2:m
        upper=r*upper0+t*lower0;      %the next upper
        lower=t*upper0+r*lower0;      %the next lower
        upper0= upper;                %transfer value
        lower0= lower;
end
%disp('upper='); disp(upper);
%disp('lower='); disp(lower);
%end of the program
```

Appendix B

```
function [fiber1,fiber2,taper_length]=crstlk_2(theta1,theta2,theta_num,length1,length2,l_num)
%This program calculates the power in both primary and secondary fibers
%accumulating angles from theta1 to theta2. the diam of the primary fiber is
%double that of the secondary fiber (hence asymmetrical coupler).
%Sub-functions used: layer_1.m and asym_1.m(t,theta,taper_length).
%george wang, 1/27/95

%input parameters ----------------------------------------------------
%theta1          -       starting angle (the critical)in degree
%theta2          -       ending angle (90 degree)
%theta_num   -       number of rays within the two angles
%length1      -       starting taper length in micron (larger than w)
%length2      -       final taper length (miron)
%l_num          -       number of data points in length vector

%setup the necessary variables ---------------------------------------
n1=1.458;               %core index
n2=1.429;               %cladding index (NA=0.29)
a01= 100;               %initial fiber core diam of the prim fiber (mircon)
d01= 140;               %initial one fiber cladding diameter (micron)
a02= 50;                %initial fiber core diam of the secd fiber (micron)
d02= 125;               %initial fiber clad diam of the secd fiber (micron)
w= 10000;               %fusion length (micron)
wavelength= 0.633;      %micron
theta_step=(theta2-theta1)/theta_num;           %incremental step in angle
theta=theta1:theta_step:theta2;                 %angle vector

%fiber dimension changes due to tapering
length_step=(length2-length1)/l_num;           %step for taper length
taper_length=length1:length_step:length2;      %taper length vector
p_ones=ones(1,l_num+1);                                 %ones for vector div
d1= d01*w*p_ones./taper_length;        %final fiber cladding diam vec (prim)
a1= a01*w*p_ones./taper_length;        %final fiber core diam vec (prim)
d2= d02*w*p_ones./taper_length;        %final fiber cladding diam vec (secd)
a2= a02*w*p_ones./taper_length;        %final fiber core diam vec (secd)
thick= 0.5*(d1+d2-a1-a2);       %the middle layer thickness

%the loops ------------------------------------------------------------
for k=1:l_num+1
for i=1:theta_num+1
        t(k)=layer_1(thick(k),theta(i),n1,n2,wavelength); %transmission coeff
        [prim(i),secn(i)]=asym_1(t(k),theta(i),taper_length(k),a1(k));     %get the power
end
fiber1(k)=sum(prim)/size(prim,2);       %the power in the primary fiber
fiber2(k)=sum(secn)/size(secn,2);       %the power in the secondary fiber
```

```
end
plot(taper_length,fiber1,taper_length,fiber2); grid;

%the end of the program ----------------------------------------------


function [p3,p4]=asym_1(t,theta,taper_length,a)
%This program computes the optical power in the primary and secondary
%fibers of a asymmetrical multimode coupler. the primary fiber diameter
%is double the secondary fiber diameter.
%George Wang, 1/26/95
%
%input parameters: ----------------------------------------------------
%t              -       transmission coeff (layer thickness)
%theta          -       angle respect to the fiber axis
%taper_length   -       coupler taper length in micron
%a              -       the primary fiber diameter (micron)

%set up the waveguide -------------------------------------------------
%a=25;                  %fiber diameter at taper waist (micron)
theta= theta*pi/180;    %propagation angle respect to the fiber axis (rad)
l=taper_length;         %coupler taper length (micron)
m=floor( l/2/a/tan(theta));     %number of reflection in fiber pipe

%body of action ------------------------------------------------------
r=1-t;                  %reflection coefficient
b1=t*t;                 %the first initial incoming beam
b2=t*t*r+r*r;           %the second initial incoming beam
b3=t*r*r+r*t;           %the third initial incoming beam

%loop of reflection along the fiber
for i=2:m
        a1= b1*r+b3*t;          %the first emerging beam
        a2= b2*r+b3*r*t+b1*t*t;     %the second emerging beam
        a3= b2*t+b3*r*r+b1*t*r;     %the third emerging beam

        b1=a1; b2= a2; b3=a3;  %feedback for the next run
end
p3= a1+a2;      %power in the primary fiber
p4= a3;         %power in the secondary fiber
%disp(p3); disp(p4);
%end of the program
```

Appendix C

```
function        [z,p4]=syml(z1,z2,width,wavelength)
%this function computes the secondary fiber power (p4) of a single mode
%2x2 (symetric) fiber coupler using the coupled mode theory (Synder's formula).
%program is developed using vector capability
%date: 2/10/95, george wang
%inputs ----------------------------------------------------------------------
%z1    -       starting taper length in mm, z1 >= 0
%z2    -       ending taper length in mm
%width -       fuse length (heating section) in mm
%outputs---------------------------------------------------------------------
%z     -       the taper length in mm
%p4    -       power in the secondary output port

%set up the problem ----------------------------------------------------------
n1=1.460;       %core index
n2=1.455;       %cladding index (na= 0.12)
del_n=(n1*n1-n2*n2)/(2*n1*n1);          %index profile height
a=8/2;          %initial core radius in micron
b=125/2;        %initial cladding radius in micron
k=2*pi/wavelength;      %propagation constant
%vectors ---------------------------------------------------------------------
z_num=200;                      %total number of data points
z_step= (z2-z1)/z_num;          %step of the vector (taper length)
z=z1:z_step:z2;                 %the taper length vector
z_ones= ones(1,size(z,2));      %ones for later calculation
%calculation procedure -------------------------------------------------------
para=   6;                              %parameter used in d
red_fac=sqrt(width*z_ones./(width+z)); %reducing diameter factor
row=    red_fac*a;                      %taper fiber radius
d=      2*b*exp(para)*exp(-para*z_ones./(red_fac.^2));%fiber separation
v=      row*k*sqrt(n1*n1-n2*n2);        %norm freq
u=      (1+sqrt(2))*v./(1+(4+v.^4).^0.25);      %the u parameter
w=      sqrt(v.*v-u.*u);        %the w parameter
k0=     besselk(0,(w.*d)./row);         %bessel of K0
k1=     besselk(1,w);                   %bessel of K1
c=      sqrt(2*del_n)*((u.*u).*k0)./((row.*(v.^3)).*(k1.*k1));   %coupling coeff
p4=     (sin(c.*z*1000)).^2;            %power in port#4

%output ----------------------------------------------------------------------
plot(z,p4);
grid;
```

Appendix D

```
function        [wavelength,p4]=sym2_wav(wave1,wave2,width,z)
%this function computes the secondary fiber power (p4) of a single mode
%2x2 (symetric) fiber coupler using the coupled mode theory (Synder's formula).
%program is developed using vector capability. output is displaced vs. wavelength
%date: 2/13/95, george wang
%inputs ----------
%wave1          -       starting wavelength in micron
%wave2          -       ending wavelength in micron
%z      -       taper length, z >= 0
%outputs----------
%wavelength-  the wavelength vector in micron
%p4     -       the power spectrum vector

%set up the problem ----------
n1=1.460;       %core index
n2=1.455;       %cladding index (na= 0.12)
del_n=(n1*n1-n2*n2)/(2*n1*n1);          %index profile height
a=8/2;          %initial core radius in micron
b=125/2;        %initial cladding radius in micron
%vectors ----------
wav_num=200;                    %total number of data points
wav_step= (wave2-wave1)/wav_num;%step of the vector (taper length)
wavelength=wave1:wav_step:wave2;%the wavelength vector
wav_ones= ones(1,size(wavelength,2)); %ones for later calculation
k=2*pi*wav_ones./wavelength;            %propagation constant vector
%calculation procedure ----------
para=   6;                              %parameter used in d
red_fac=sqrt(width/(width+z));          %reducing diameter factor
row=    red_fac*a;                      %taper fiber radius
d=      2*b*exp(para)*exp(-para/(red_fac^2));%fiber separation
v=      row*k*sqrt(n1*n1-n2*n2);        %norm freq vector
u=      (1+sqrt(2))*v./(1+(4+v.^4).^0.25 );%the u parameter vector
w=      sqrt(v.*v-u.*u);            %the w parameter vector
k0=     besselk(0,(w*d)/row);           %bessel of K0 vector
k1=     besselk(1,w);                   %bessel of K1 vector
c=      sqrt(2*del_n)*((u.*u).*k0)./(row*(v.^3).*(k1.*k1));%coupling coeff
p4=     (sin(c*z*1000)).^2;             %power in port#4
p3=     1-p4;                           %the port#3
%output ----------
p3=10*log10(p3); p4=10*log10(p4);       %convert to dB
%plot(wavelength,u.^2,wavelength,v.^3);
%plot(wavelength,k0,wavelength,k1.*k1);
plot(wavelength,p3,wavelength,p4);
%plot(wavelength,c);
grid;
```

Appendix E

```
function        [z,p4]=asym1(z1,z2,width,wid_pre,wavelength)
%this function computes the secondary fiber power (p4) of an asymetric
%single mode 2x2 fiber coupler using the coupled mode theory (Synder's formula).
%program is developed using vector capability
%date: 3/10/95, george wang
%inputs ----------------------------------------------------------------------
%z1     -       starting taper length in mm, z1 >= 0
%z2     -       ending taper length in mm
%width  -       fuse length (heating section) in mm
%wid_pre-       pre-fuse taper length in mm, wid_pre >= 0
%wavelength     wavelength in micron
%outputs---------------------------------------------------------------------
%z      -       the taper length in mm
%p4     -       power in the secondary output port

%set up the problem ----------------------------------------------------------
n1=1.460;       %core index
n2=1.455;       %cladding index (na= 0.12)
del_n=(n1*n1-n2*n2)/(2*n1*n1);          %index profile height
a=8/2;          %initial core radius in micron
b=125/2;        %initial cladding radius in micron
k=2*pi/wavelength;      %propagation constant
%vectors ---------------------------------------------------------------------
z_num=200;                      %total number of data points
z_step= (z2-z1)/z_num;          %step of the vector (taper length)
z=z1:z_step:z2;                 %the taper length vector
z_ones= ones(1,size(z,2));      %ones for later calculation
%calculation procedure -------------------------------------------------------
red_fac=sqrt(width*z_ones./(width+z)); %the reducing diameter factor
row=    red_fac*a;                      %taper fiber radius
para=   6;                              %parameter for exp
d=      exp(para)*exp(-para*z_ones./(red_fac.^2)); %exp
d=      d*(sqrt(width/(width+wid_pre))+1)*b;%fiber core separation
del_row=red_fac*(1-sqrt(width/(width+wid_pre)))*a;%fiber core diff
v=      row*k*sqrt(n1*n1-n2*n2);        %norm freq
u=      (1+sqrt(2))*v./(1+(4+v.^4).^0.25);      %the u parameter
w=      sqrt(v.*v-u.*u);            %the w parameter
k0=     besselk(0,(w.*d)./row);         %bessel of K0
k1=     besselk(1,w);                   %bessel of K1
k0w=    besselk(0,w);                   %bessel of k0 with w
c=      sqrt(2*del_n)*((u.*u).*k0)./((row.*(v.^3)).*(k1.*k1));    %coupling coeff
temp1= ((w.*(v.^4)/(2*pi)).*((k0w.^4)).*(d./row));
temp2= exp(2*(w.*d)./row);
f2=     z_ones./(1+(temp1.*temp2).*( (del_row./row).^2 ));%f squared
f=      sqrt(f2);                                       %f itself
```

```
p4=      f2.*((sin((c.*z*1000)./f)).^2);                    %power in port#4
%output ---------------------------------------------------------------------
plot(z,p4);
grid;
xlabel('p4 vs. z');
```

Appendix F

```
function        [wavelength,p4]=asym3(width,z,wid_pre,wave1,wave2)
%this function computes the secondary fiber power (p4) of an asymetric
%single mode 2x2 fiber coupler using the coupled mode theory (Synder's formula).
%analysis on the wavelength dependance is investigated.
%date: 4/12/95, george wang
%inputs ----------------------------------------------------------------------
%z      -        taper length in mm, z1 >= 0
%width -        fuse length (heating section) in mm
%wid_pre-       the pre-tapered length
%wave1          -       initial wavelength in micron
%wave2          -       final wavelength in micron
%outputs---------------------------------------------------------------------
%wavelength -  the wavelength vector
%p4     -       power in the secondary output port

%set up the problem ----------------------------------------------------------
n1=1.460;       %core index
n2=1.455;       %cladding index (na= 0.12)
del_n=(n1*n1-n2*n2)/(2*n1*n1);          %index profile height
a=8/2;          %initial core radius in micron
b=125/2;        %initial cladding radius in micron
%vectors ---------------------------------------------------------------------
wav_num=200;                    %total number of data points
wav_step= (wave2-wave1)/wav_num;%step of the vector (taper length)
wavelength=wave1:wav_step:wave2;%the taper length vector
wav_ones= ones(1,size(wavelength,2)); %ones for later calculation
k=2*pi*wav_ones./wavelength;            %propagation constant
%calculation procedure -------------------------------------------------------
red_fac=sqrt(width/(width+z)); %the reducing diameter
row=    red_fac*a;      %taper fiber radius
para=   6;              %parameter for exp
d=      exp(para)*exp(-para/(red_fac.^2));              %fiber separa
d=      d*(sqrt(width/(width+wid_pre))+1)*b;%fiber core separation
del_row=red_fac*(1-sqrt(width/(width+wid_pre)))*a;    %fiber core diff
v=      row*k*sqrt(n1*n1-n2*n2);        %norm freq
u=      (1+sqrt(2))*v./(1+(4+v.^4).^0.25);      %the u parameter
w=      abs(sqrt(v.*v-u.*u));           %the w parameter
k0=     besselk(0,w*d/row);             %bessel of K0
k1=     besselk(1,w);                   %bessel of K1
k0w=    besselk(0,w);                   %bessel of k0 with w
c=      sqrt(2*del_n)*((u.*u).*k0)./((row*(v.^3)).*(k1.*k1));    %coupling coeff
temp1= ((w.*(v.^4)/(2*pi)).*(k0w.^4))*(d/row);
temp2= exp(2*w*d/row);
f2=     wav_ones./(1+(temp1.*temp2)*(del_row/row)^2 );      %f squared
f=      sqrt(f2);                                           %f itself
```

```
p4=     f2.*((sin((c*z*1000)./f)).^2);                    %power in port#4
p3=     1-p4;                                             %the primary fiber
%output ---------------------------------------------------------------------
p3=10*log10(p3); p4=10*log10(p4);     %convert to dB
plot(wavelength,p3,wavelength,p4);
grid;
xlabel('Wavelength [micron]');
ylabel('Output Power [dB]');
```

Appendix G

```
function [wave,p3,p4]=p4_wav2(wave1,wave2,num,p1,p2,a0,width,length)

%this program computes the power coupling of a symmetrical single mode 2x2
%fiber coupler using Panye's model (rectangular), considering amplitudes
%sub-routine used: c_pany.m
%george wang, 4/15/95

%input parameters ----------------------------------------------------------
%wave1              -       left end wavelength in nanometer
%wave2              -       right end wavelength in nanometer
%num        -       number of element of vector
%p1         -       input power amplitude vector at p1
%p2         -       input power amplitude vector at p2
%width      -       fusion width (torch length) in mm
%a0         -       originial fiber diameter in micron
%length             -       beginning taper length (>= width) in mm

%setting up ----------------------------------------------------------------
step= (wave2-wave1)/num;        %density of data points
wave= wave1:step:wave2;                 %taper length vector

%calculation ---------------------------------------------------------------
for i=1: num+1
        c(i)= c_pany(wave(i),width,a0,length);   %the coupling coeff
end
c= c*1000;      %convert to 1/mm
%power in the secn fiber
p4= p1.*sin(c*length).*sin(c*length) + p2.*cos(c*length).*cos(c*length);
p3= p1+p2-p4;           %power in the primary fiber
%p3=10*log10(p3); p4=10*log10(p4);%%%%%%%dB
plot(wave/1000,p3,wave/1000,p4); grid;
%xlabel('Wavelength [micron]');
%ylabel('Normalized Power [dB]');

%the end -------------------------------------------------------------------


function coef=c_pany(wave,w,a0,length)

%this routine gives the coupling coefficient of a symmetrical 2x2 sm fiber
%coupler. the model is Panye's (rectangular). the reduced fiber diameter
%is calculated based on conservation of mass

%input parameters ----------------------------------------------------------
%wave           -       wavelength in nanometer
```

```
%w              -       fusion width in mm
%a0             -       original fiber diameter
%length                 -       taper length

%action ----------------------------------------------------------------
n2= 1.458;              %index of refraction of the fiber cladding
n3= 1.000;              %external index of refraction (air)
a= a0*sqrt(w/length);   %reduced taper width
k= 2*pi/wave;           %wave number in free space
v= a*k*1000*sqrt(n2*n2-n3*n3);          %norm frequency, 1000 is for micron to nm
coef= 3*pi/32/n2*wave/1000/a/a/((1+1/v)^2);    %coupling coeff

%the end ----------------------------------------------------------------
```

Vita

The author was born on February 5, 1963, in Wuhan, China. He received an associate degree in computer science from Zhongshan University in 1982. After working as a computer programmer for two years in the Microelectronics Research Institute of the same university, he came to the United States studying at Southern University in Baton Rouge, Louisiana and obtained his B.S. degree (magna cum laude) in physics in 1988. In 1989, he received a M.A. degree in physics from Washington University in St. Louis, Missouri. He came to Virginia Tech to study electrical engineering and received his M.S. degree in 1992. He has been employed as a graduate research assistant and later a research associate at the Fiber & Electro-Optics Research Center in the department of electrical engineering. In February 1996, he successfully defended his Ph.D dissertation. Mr. Wang was a recipient of Paul Torgerson Research Award in the College of Engineering (Virginia Tech) in 1992.